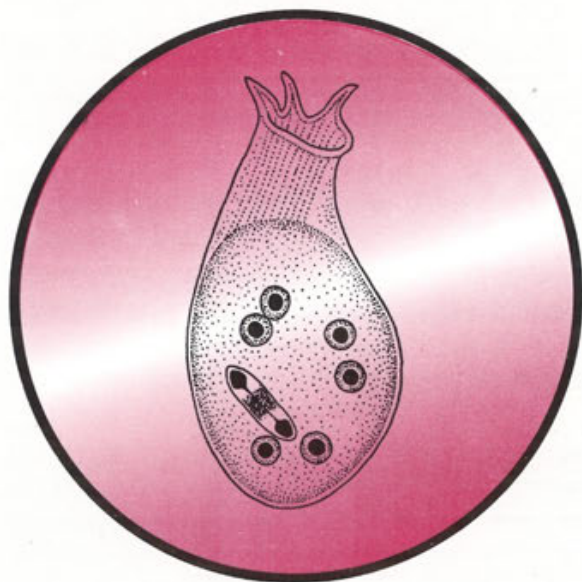


ACTA

PROTOZOOLOGICA



NENCKI INSTITUTE OF EXPERIMENTAL BIOLOGY
WARSAW, POLAND

1996

VOLUME 35 NUMBER 3
ISSN 0065-1583

Polish Academy of Sciences
Nencki Institute of Experimental Biology

ACTA PROTOZOLOGICA

International Journal on Protistology

Editor in Chief Jerzy SIKORA

Editors Hanna FABCZAK and Anna WASIK

Managing Editor Małgorzata WORONOWICZ

Editorial Board

Andre ADOUTTE, Paris	Leszek KUŹNICKI, Warszawa, <i>Chairman</i>
Christian F. BARDELE, Tübingen	J. I. Ronny LARSSON, Lund
Magdolna Cs. BERCZKY, Göd	John J. LEE, New York
Y.-Z. CHEN, Beijing	Jiři LOM, České Budějovice
Jean COHEN, Gif-Sur-Yvette	Pierangelo LUPORINI, Camerino
John O. CORLISS, Albuquerque	Hans MACHEMER, Bochum
Gyorgy CSABA, Budapest	Jean-Pierre MIGNOT, Aubière
Isabelle DESPORTES-LIVAGE, Paris	Yutaka NAITOH, Tsukuba
Tom FENCHEL, Helsingør	Jytte R. NILSSON, Copenhagen
Wilhelm FOISSNER, Salzburg	Eduardo ORIAS, Santa Barbara
Vassil GOLEMANSKY, Sofia	Dimitrii V. OSSIPOV, St. Petersburg
Andrzej GRĘBECKI, Warszawa, <i>Vice-Chairman</i>	Igor B. RAIKOV, St. Petersburg
Lucyna GRĘBECKA, Warszawa	Leif RASMUSSEN, Odense
Donat-Peter HÄDER, Erlangen	Michael SLEIGH, Southampton
Janina KACZANOWSKA, Warszawa	Ksenia M. SUKHANOVA, St. Petersburg
Witold KASPRZAK, Poznań	Jiři VÁVRA, Praha
Stanisław L. KAZUBSKI, Warszawa	Patricia L. WALNE, Knoxville

ACTA PROTOZOLOGICA appears quarterly.

The price (including Air Mail postage) of subscription to ACTA PROTOZOLOGICA at 1997 is: US \$ 180.- by institutions and US \$ 120.- by individual subscribers. Limited number of back volumes at reduced rate are available. TERMS OF PAYMENT: Cheque, money order or payment to be made to the Nencki Institute of Experimental Biology. Account Number: 370044-3522-2700-1-73 at Państwowy Bank Kredytowy XIII Oddz. Warszawa, Poland. WITH NOTE: ACTA PROTOZOLOGICA ! For matters regarding ACTA PROTOZOLOGICA, contact Managing Editor, Nencki Institute of Experimental Biology, ul. Pasteura 3, 02-093 Warszawa, Poland; Fax: 48-22 225342; E-mail: Jurek@ameba.nencki.gov.pl

Front cover: *Stephanopogon colpoda*. In: I. B. Raikov - Kariologiya prosteishikh. Izd. Nauka, Leningrad 1967

©Nencki Institute of Experimental Biology, Polish Academy of Sciences Printed at the MARBIS, ul. Kombatantów 60, 05-070 Sulejówek, Poland

Cytoplasmic Calcium Transients in *Amoeba proteus* during Induction of Pinocytotic and Non-pinocytotic Rosettes*

Wanda KŁOPOCKA and Paweł POMORSKI

Department of Cell Biology, Nencki Institute of Experimental Biology, Warszawa, Poland

Summary. Dynamics of the total level and intracellular distribution of cytosolic free Ca^{2+} was studied in *Amoeba proteus* stimulated to form pinocytotic rosettes in 125 mM NaCl or 125 mM KCl and non-pinocytotic rosettes in 125 mM acetylcholine chloride or 125 mM choline chloride. In both cases a sharp increase in total $[Ca^{2+}]_i$ was observed a few seconds after external application of a solution from a micropipette. Since the Ca^{2+} signal precedes the loss of locomotion and rosette formation independently of the presence or absence of pinocytosis, it is considered to trigger only the motor reaction resulting in changing the cell shape from locomotory form to a rosette. The formation of pinocytotic channels seems to be related rather to the residual increased level of cytoplasmic Ca^{2+} observed only in NaCl and KCl solutions. Differences were demonstrated in the spatial distribution of increased $[Ca^{2+}]_i$ and the direction of calcium wave propagation depending on the kind of inducer. Differences between the pinocytotic induction by NaCl and KCl correspond to the morphological changes observed at the beginning of Na^+ and K^+ pinocytosis. During Na^+ induced pinocytosis the Ca^{2+} signal and the first channels appear in the uroidal cell region before suppression of the tail-front differentiation. In the presence of 125 mM KCl, $[Ca^{2+}]_i$ raises simultaneously in the whole amoeba, and pinocytotic channels appear in any place after the cell deformation. The $[Ca^{2+}]_i$ increase starts from the frontal cell region in acetylcholine and choline chlorides which produce only non-pinocytotic rosettes.

Key words: *Amoeba proteus*, calcium, Fura-2, pinocytosis, signal transduction.

INTRODUCTION

Calcium ions act as intracellular messenger in the majority of living systems. They initiate muscle contraction and regulate various responses of non-muscle cells (Ebashi and Endo 1968, Williams 1974, Carafoli et al. 1975, Hitchcock 1977, Wassermann et al. 1977). In amoebae, besides other functions, Ca^{2+} is involved in the control of specialized movement phenomena such as locomotion (Nuccitelli et al. 1977, Hellewell and

Taylor 1979, Taylor et al. 1980, Taylor and Fechheimer 1982, Kuroda et al. 1988), pinocytosis (Allison 1973, Josefsson 1975, Johansson and Josefsson 1978, Klein and Stockem 1979, Taylor et al. 1980, Stockem and Klein 1988), phagocytosis (Prusch and Minck 1985) and cytokinesis (Satterwhite and Pollard 1992).

All investigators agree on the significance of intracellular Ca^{2+} for actomyosin network activation and motive force generation, not only for locomotion but also for formation of the channels during pinocytosis (Klein and Stockem 1979, Gollnick et al. 1991). It should be, however, kept in mind that pinocytotic channels of *Amoeba proteus* do not develop by a simple and immediate invagination of cell periphery, but arise at the tips of specialized pinocytotic pseudopodia, which radially grow out after cessation of lo-

*Preliminary results were presented during the IX International Congress of Protozoology in Berlin (1993)

Address for correspondence: Wanda Kłopocka, Nencki Institute of Experimental Biology, Department of Cell Biology, ul. Pasteura 3, 02-093 Warszawa, Poland; Fax (0-48)(0-22)225342; E-mail: pp@nencki.gov.pl

comotion and spherulation of the cell. This form of amoeba is called pinocytotic rosette (Chapman-Andresen 1962, Holter 1965). Some inducers produce non-pinocytotic rosettes, similar in shape but without channels.

The aim of the present study was to check whether Ca^{2+} signals, which are usually generated when external stimuli activate surface receptors, are responsible for formation of pinocytotic channels or they rather trigger the first motor reaction, i. e. cell transformation from the locomotory form to the rosette stage. Changes in free $[\text{Ca}^{2+}]_i$ were studied in the cytoplasm of *Amoeba proteus* treated with two pinocytotic inducers: NaCl and KCl, and two agents known as inducers of non-pinocytotic rosettes: acetylcholine and choline chlorides.

MATERIALS AND METHODS

Amoeba proteus was cultured in standard Pringsheim medium (Chapman-Andresen 1968) and fed on *Tetrahymena pyriformis*. During experiments, amoebae were adhering to round coverslip, mounted in a 1 ml stainless steel experimental chamber. They were microinjected with 100 μM Fura-2 (Molecular Probes, Eugene; USA) pentapotassium salt dissolved in half concentrated Pringsheim medium. For microinjections, glass micropipettes pulled by Medipan micropuller were used. Micropipettes were mounted on de Fonbrune pneumatic micromanipulator.

All inducers: Na^+ , K^+ , acetylcholine and choline chlorides were dissolved to 1.25M concentration in Pringsheim medium ($\text{Ca}(\text{NO}_3)_2 \cdot 4\text{H}_2\text{O}$ 200 $\mu\text{g ml}^{-1}$, $\text{MgSO}_4 \cdot 7\text{H}_2\text{O}$ 20 $\mu\text{g ml}^{-1}$, $\text{Na}_2\text{HPO}_4 \cdot 2\text{H}_2\text{O}$ 20 $\mu\text{g ml}^{-1}$, KCl 26 $\mu\text{g ml}^{-1}$, $\text{FeSO}_4 \cdot 7\text{H}_2\text{O}$ 2 $\mu\text{g ml}^{-1}$). Such solution has been injected into the experimental chamber. The final concentration of inducer in culture medium was 125 mM.

The loaded cells were observed in phase contrast before application of the inducers and just after recording Ca^{2+} transients. In each one of the five types of experiments 6-10 amoebae were monitored. It produced the total of 31 tested amoebae. Nevertheless, we do not have enough data for statistical analysis of calcium distribution in the cell and averaging shapes of cell response curves. Therefore the graphs most typical for a given experimental situation are shown in Figures. All graphs present average calcium concentration measured over the whole cell area.

Loaded cells were visualized by a MagiCal image processing system (Joyce Loebel) connected by a Photonic Science Extended Isis intensified CCD video camera to a Nikon Diaphot inverted epifluorescence microscope equipped with 10X objective. Calculations of calcium concentration maps were done by Tardis v. 7.2 program (Applied Imaging) based on Grynkiewicz et al. (1985) equation. For calibration of the system a modified whole cell calibration method was used (Carew et al. 1994).

RESULTS

Immediately after microinjection of fura-2 into normal migrating amoebae, they stop locomotion and loose motor polarity. However 1-3 min. later the injected cells start

to migrate again. All experiments were run after the fura-2 loaded amoebae have returned to normal locomotor activity.

Changes in the level of cytoplasmic calcium were provoked as well by pinocytotic inducers: NaCl (Fig. 1a) and KCl (Fig. 1b), as by acetylcholine chloride (Fig. 2a) and choline chloride (Fig. 2b) which produce rosettes without pinocytotic channels, under present experimental conditions, that is in presence of 0.85 mM CaCl_2 . Independently of the kind of the substance used, a few seconds after its application, a sharp increase in $[\text{Ca}^{2+}]_i$ from the level characteristic for migrating cells (10-20 nM) to about 80 nM was observed (Figs. 1, 2). In all experiments Ca^{2+} signals appeared about 20 s after application of a stimulus and reached the peak during the following 40 s when the maximal Ca^{2+} concentration increase spread over the whole cytoplasm (compare Fig. 1 with Figs. 3, 4 and, respectively, Fig. 2 with Figs. 5, 6). Within the next minute it fell down again to the initial level when non-pinocytotic agents have been applied (Fig. 2). After induction of pinocytosis the residual increase in $[\text{Ca}^{2+}]_i$ - about twice the original concentration (Fig. 1a) was observed.

Application of the culture medium from the micropipette, as a form of mechanical stimulus, usually does not change $[\text{Ca}^{2+}]_i$ (Fig. 2a - P). Sometimes only, a small increase in $[\text{Ca}^{2+}]_i$, correlated with a transient reversal of endoplasmic streaming in frontal pseudopodia, was observed.

Rapid intracellular calcium transients preceded loss of locomotion and cellular polarity, as well under the influence of Na^+ and K^+ as in acetylcholine and choline chloride. Calcium signals obtained in NaCl and KCl solutions were correlated in time rather with the motor reaction resulting in the formation of rosettes than with the development of pinocytotic channels (Figs. 3-6).

Figures 3 and 4 show also differences between pinocytotic induction provoked by Na^+ and K^+ . In amoebae, stimulated by 125 mM NaCl, transient increase of $[\text{Ca}^{2+}]_i$ is at the beginning limited to the uroidal region (Fig. 3c). During the following 20s high $[\text{Ca}^{2+}]_i$ moves as a wave from this part of the cell via intermediate region to the former fronts (Fig. 3d). This corresponds to the first peak in Fig. 1a. The second one may correlated in time with the retraction of motor pseudopodia and formation of the first pinocytotic pseudopodia in the uroid (Klein and Stockem 1979, Grębecka and Kłopočka 1986). A polarity in the distribution of cytosolic free calcium and in the formation of channels has never been observed when pinocytosis was induced by K^+ . After application of 125 mM KCl $[\text{Ca}^{2+}]_i$ raises simultaneously in the whole amoeba

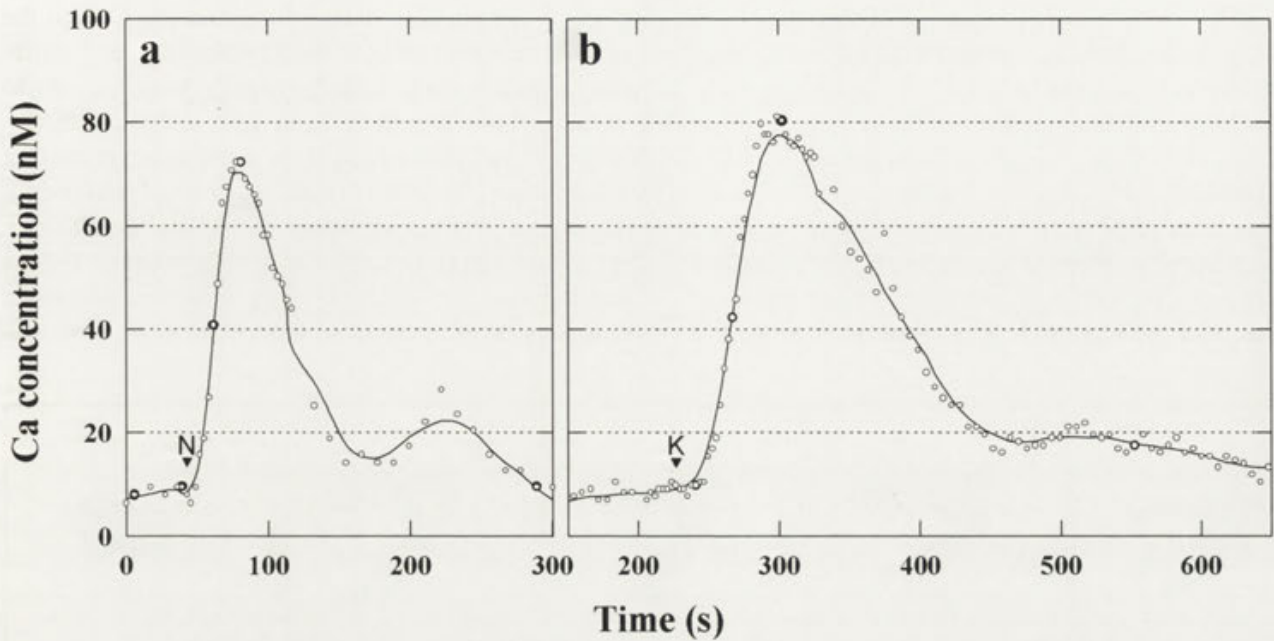


Fig. 1. Curves illustrating transient average increase of cytoplasmic Ca²⁺ induced by external application of 125mM NaCl (a) or 125mM KCl (b). N - NaCl, K - KCl. Black dots indicate the stages displayed as images in Figs. 3-6

(Figs. 4c, d), and pinocytotic channels appear in any place after the cell deformation.

The initial morphological changes that follow the application of acetylcholine or choline chloride are similar to those observed during the first steps of pinocytotic induction. All these substances provoke rapid inhibition of migration, loss of cellular polarity, and development of

rosettes. In each case the described reactions are correlated in time with transient increase of the internal calcium concentration. The final result however, it is the formation of rosettes, is achieved independently of the direction of propagation of the transient increase of cytosolic Ca²⁺. Immediately after the application of acetylcholine or choline chloride, the [Ca²⁺]_i rapidly increases in the former

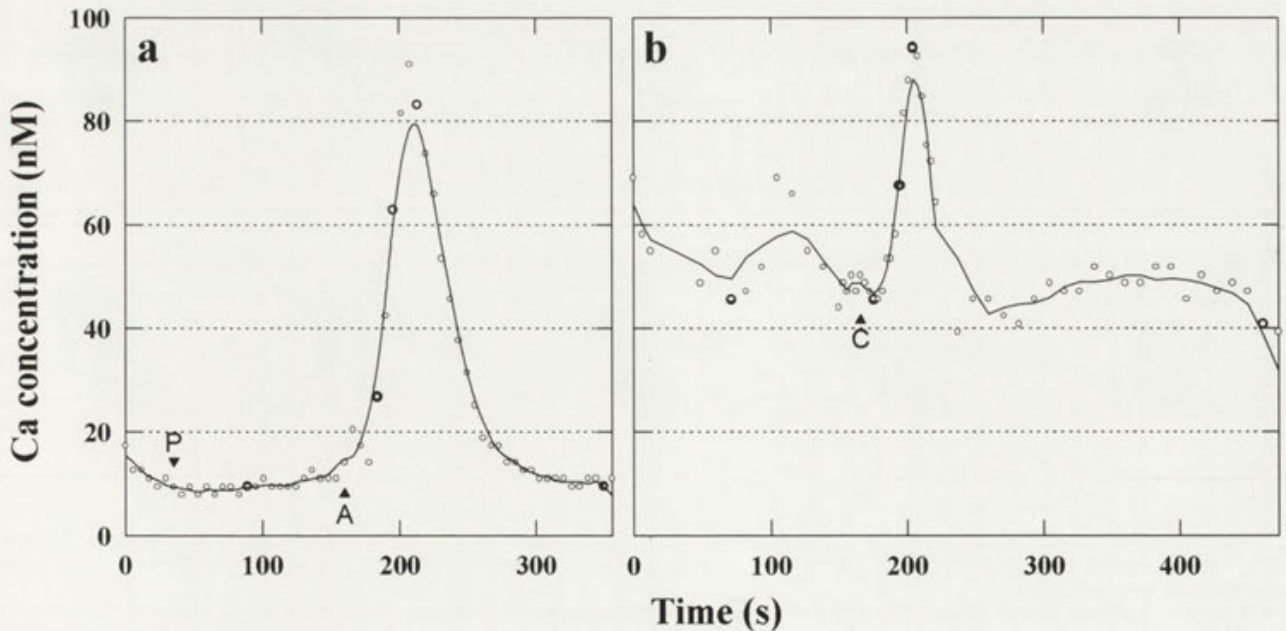


Fig. 2. Calibrated curves demonstrating the time course of average [Ca²⁺]_i changes in amoebae treated with 125mM acetylcholine chloride (a) or 125mM choline chloride (b). A - acetylcholine chloride, C - choline chloride. Notice that control application of culture medium (marked as P in Fig. 3a) does not influence the level of cytoplasmic calcium. Black dots indicate the stages displayed as images in Figs. 3-6

fronts, and then Ca^{2+} wave propagates toward the posterior region (Figs. 5, 6), in contrast to the cases of NaCl or KCl application (Figs. 3, 4).

DISCUSSION

It is generally accepted that calcium is an essential factor in the complicated movement phenomena in amoebae, by controlling sol-gel-sol transformations and

triggering contraction. In migrating *Amoeba proteus* the spatial distribution of increased localized $[\text{Ca}^{2+}]_i$ corresponds to places where the actomyosin system is known to generate motive force (Stockem and Kłopocka 1988). $[\text{Ca}^{2+}]_i$ is higher than 10^{-7} M at the uroid and in retracting pseudopodia. In the frontal regions of extending pseudopodia it does not attain 10^{-8} M (Gollnick et al. 1991). So, the intracellular $[\text{Ca}^{2+}]_i$ gradients always correspond to the direction of cytoplasmic streaming and characteristic pattern of amoeboid movement. An

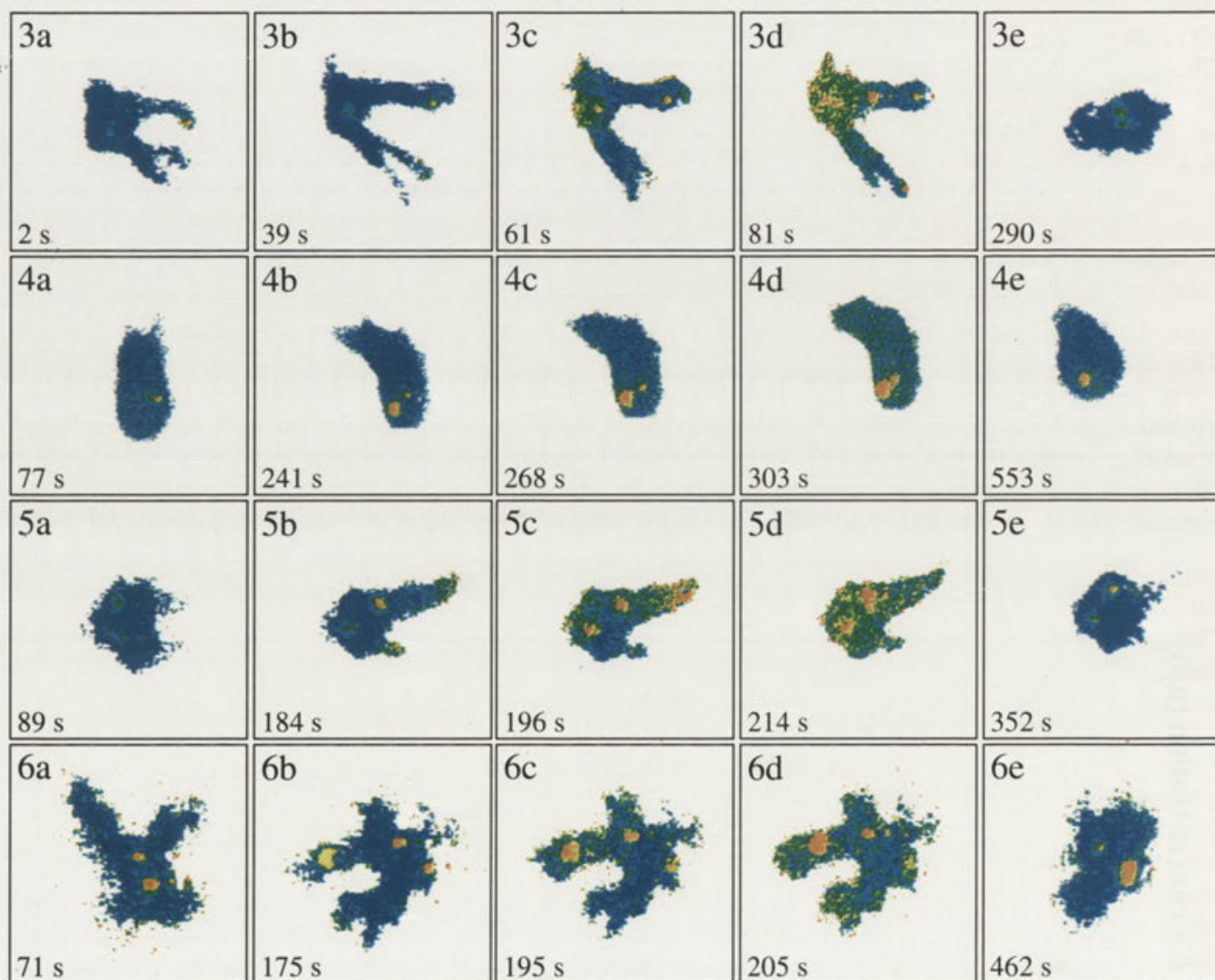


Fig. 3. Six stages selected from a series of images at the time points indicated as black dots in Fig. 1a. The successive pictures show changes in the level and distribution of cytoplasmic calcium. Notice the propagation of a Ca^{2+} wave from the uroidal region (U) to the former fronts (F) of the experimentally treated cell (c-d)

Fig. 4. Six stages (indicated as black dots in Fig. 1b) demonstrating the KCl induced Ca^{2+} transients. Increase of $[\text{Ca}^{2+}]_i$ occurs simultaneously in the whole cell (c-d)

Fig. 5. Propagation of the cytoplasmic calcium wave induced by acetylcholine. The Ca^{2+} wave propagates from the former front of the amoeba (b) towards the uroidal region (b-d)

Fig. 6. The stages of choline induced Ca^{2+} transients selected from the experiment graphically illustrated in Fig. 2b. Notice the similar direction of wave propagation as in acetylcholine (Fig. 5)

internal concentration of Ca²⁺ above 10⁻⁷ M induces contraction and transformation of ectoplasmic gel into endoplasmic sol that flows toward fronts where in [Ca²⁺]_i below 10⁻⁸ M the reconstruction of the rigid gel occurs (Taylor 1977, Hellewell and Taylor 1979, Taylor et al. 1980, Kuroda and Sonobe 1981, Taylor and Fehheimer 1982). In large amoebae, calcium ions are involved in controlling the reversible equilibrium between G- and F-actin via profilin and cytoplasmic kinase (Sonobe et al. 1985, 1986). Phosphorylation of the profilin/G-actin complex by kinase occurs under high concentration of Ca²⁺, which promotes destruction of F-actin network.

External application of different stimuli alters the former intracellular Ca²⁺ gradients and in consequence influences the motor behaviour of amoeba. The stimulation usually leads to a transient increase in cytoplasmic calcium level which triggers different responses of amoebae. For example, the calcium signal generated by local irradiation with UV-light is followed by reversal of endoplasmic streaming from the stimulated area. The reaction lasts until the normal physiological conditions are restored, i.e. about 1 min. (Gollnick et al. 1991). 30 mM KCl generates a Ca²⁺ wave which leads to a uniform distribution of increased [Ca²⁺]_i in cytoplasm. This is correlated in time with the inhibition of locomotion and loss of cell polarity (Gollnick et al. 1991).

The participation of calcium ions in signal transduction and motive force generation during pinocytosis, by changing the permeability of the plasma membrane and consecutive activating the contractile microfilament system, has been demonstrated in many studies (Allison 1973, Josefsson 1975, Josefsson et al. 1975, Prusch and Hannafin 1979, Gawlitta et al. 1980, Kukulis et al. 1986, Prusch 1986, Stockem and Klein 1988). The pinocytotic inducers such as Na⁺ and K⁺ probably substitute for the externally bound Ca²⁺, which results in a shift of membrane potential, related to the conformational changes of membrane components, which could influence the ionic concentration and distribution between the cell inside and outside (Brandt and Freeman 1967, Josefsson 1975, Stockem 1977). The external Ca²⁺ can influence the induction of pinocytosis in amoebae (Cooper 1968; Josefsson 1968, 1975; Gawlitta et al. 1980), owing to the stabilizing effect of this ion on plasma membrane. Therefore, the concentration of inducers necessary for the initiation of the phenomenon depends on [Ca²⁺]_e (Kłopotcka and Grębecka 1985).

According to present results, application of 125 mM NaCl or KCl, in presence of 0.85 mM CaCl₂ causes a sharp increase of the cytoplasmic calcium level in *Amoeba*

proteus. In consequence, the cells lose after such treatment the locomotor activity and polarity, undergo spherulation, probably by general contraction of the microfilament layer and finally produce numerous hyaline pseudopodia with channels and assume the shape of pinocytotic rosettes. However, similar Ca²⁺ signals appear also as a result of surface receptor activation by acetylcholine chloride and choline chloride, which in the same rather high [Ca²⁺]_e fail to induce pinocytosis, but lead only to the formation of non-pinocytotic rosettes. This suggests that calcium signals, which were visualized in the present experiments, trigger the cell shape changes rather than the formation of pinocytotic channels.

In contrast to acetylcholine and choline chlorides, introduction of pinocytotic inducers (Na⁺ or K⁺) leads to a transient increase in free [Ca²⁺]_i which is most often followed by a sustained level somewhat above the basal concentration observed in migrating amoebae. This phenomenon is more clear in K⁺ than in Na⁺, but this corresponds to the duration and intensity of pinocytotic reaction which is much higher in K⁺ (Kłopotcka and Grębecka 1986). This residual increased level of cytoplasmic calcium might be responsible for channel formation. As it is known, channels are invaginated due to active contraction of the microfilament system within discrete cortical regions (Klein and Stockem 1979, Stockem et al. 1983, Grębecki 1991). Temporal fluctuations of [Ca²⁺]_i during pinocytosis were earlier demonstrated with aequorin (Taylor et al. 1980).

Rapid elevations in [Ca²⁺]_i either arise from Ca²⁺ discharge from internal stores or from entry into the cytoplasm via Ca²⁺ channels in the cell membrane or both simultaneously (Tsien 1990). The results of experiments with very low [Ca²⁺]_e or Ca²⁺-influx antagonists imply that external Ca²⁺ is of minor importance for the regulation of [Ca²⁺]_i in *Amoeba proteus* (Josefsson 1968, 1975; Johansson and Josefsson 1978; Stockem and Klein 1979, 1988; Kłopotcka and Grębecka 1985;). Calcium released from accumulating systems, i.e. smooth ER and membrane-attached Ca²⁺-binding sites, may be sufficient to induce actomyosin contraction (Reinold and Stockem 1972, Stockem and Klein 1979). On the other hand, depletion of intracellular stores activates calcium influx across the plasma membrane resulting amplification of calcium signal duration (Putney 1993). It was demonstrated that intracellular Ca²⁺ signals that last more than a few minutes depend on influx of extracellular calcium (Randriamampita and Tsien 1993). If so, the influx of external Ca²⁺ may be not necessary for initiation of general contraction of the cortical layer and the first

channels formation but can influence the intensity of a long lasting phenomenon, such as pinocytosis.

The results show also differences in the spatial distribution of increased $[Ca^{2+}]_i$ and the direction of calcium wave propagation between the experimentally treated cells. Differences in Ca^{2+} transients between the induction of pinocytosis by NaCl and KCl correspond to the morphological changes observed at the initial stages of Na^+ or K^+ induced pinocytosis (Grębecka and Kłopocka 1986). In amoebae treated with 125mM NaCl the Ca^{2+} signal appears in the uroidal region before suppression of the tail-front differentiation and then moves *via* intermediate region to the former front. Such a propagation of Ca^{2+} wave may be correlated with distinct polar distribution of the arising pinocytotic channels. First of them develop in the rear part of amoeba after the locomotion ceases, but before the usual tail-front morphological differentiation is completely effaced (Klein and Stockem 1979, Grębecka and Kłopocka 1986). So, both phenomena start in this part of the cell where during migration the permanent pinocytosis occurs (Wohlfarth-Bottermann and Stockem 1966). However after application of 125mM KCl, $[Ca^{2+}]_i$ raises simultaneously in the whole amoeba and pinocytotic channels appear in any place after the cell deformation.

Reverse Ca^{2+} waves were observed in subthreshold concentrations of inducers. In our experiments Ca^{2+} waves, generated by acetylcholine and choline chlorides, start from the front regions. Morphological changes are thus limited at the beginning to the anterior cell part. Also in a lower concentration of KCl (30mM in the presence of 1mM $CaCl_2$) a rapid increase of $[Ca^{2+}]_i$ appears at the front of amoeba and moves to the uroid (Gollnick et al. 1991). Such a signal transiently effaces cell polarity, but is not followed by pinocytotic channels formation, although 30mM KCl is sufficient to depolarize the plasma membrane of amoeba (Bruce and Marshall 1965, Prusch and Dunham 1972). According to Gollnick et al. (1991), NaCl in the same concentration does not induce any calcium signal.

In general, it may be suggested that a short rapid increase of $[Ca^{2+}]_i$ precedes the cell shape alteration in all solutions. If the pinocytosis is not eventually induced, the Ca^{2+} wave is propagated from the front backwards. Above the pinocytotic threshold either the Ca^{2+} increase is propagated from the uroid forwards (NaCl) or it occurs simultaneously everywhere (KCl), which corresponds to the order in which pinocytotic channels are developed.

Acknowledgements. We are grateful to Professor A. Grębecki for his helpful suggestions and discussion.

REFERENCES

- Allison A. C. (1973) The role of microfilaments and microtubules in cell movement, endocytosis and exocytosis. In: Locomotion of tissue cells, 14th Ciba Found. Symp., (Eds. R. Porter and D. W. Fitzsimons). Elsevier, Amsterdam London New York, 109-143
- Brandt P. W., Freeman A. R. (1967) Plasma membrane: Substructural changes correlated with electrical resistance and pinocytosis. *Science* **155**: 582-585
- Bruce D. L., Marshall J. M. (1965) Some ionic and bioelectric properties of the amoeba *Chaos chaos*. *J. Gen. Physiol.* **49**: 151-178
- Carafoli E., Clementi F., Drabikowski W., Margreth A. (1975) Calcium transport in contraction and secretion. North-Holland Publ. Comp. Amsterdam
- Carew M. A., Wu M., Law G. J., Tseng Y., Mason W. T. (1994) Extracellular ATP activates calcium entry and mobilization via P_{2U} -putinoceptors in rat lactotrophs. *Cell Calcium* **16**: 227-235
- Chapman-Andresen C. (1962) Studies on pinocytosis in Amoebae. *CR Lab. Carlsberg* **33**: 123-155
- Chapman-Andresen C. (1968) Pinocytosis of inorganic salts by *Amoeba proteus* (*Chaos oliffuens*). *CR Lab. Carlsberg* **31**: 77-92
- Cooper B. (1968) Quantitative studies of pinocytosis induced in *Amoeba proteus* by simple cations. *CR Lab. Carlsberg* **36**: 385-403
- Ebashi S., Endo M. (1968) Calcium ion and muscle contraction. *Prog. Biophys. Mol. Biol.* **18**: 123-183
- Gawlitza W., Stockem W., Wehland J., Weber K. (1980) Pinocytosis and locomotion in amoebae. XV. Visualization of Ca^{2+} -dynamics by chlorotetracycline (CTC) fluorescence during induced pinocytosis in living *Amoeba proteus*. *Cell Tiss. Res.* **213**: 9-20
- Gollnick F., Meyer R., Stockem W. (1991) Visualization and measurement of calcium transients in *Amoeba proteus* by fura-2 fluorescence. *Eur. J. Cell Biol.* **55**: 262-271
- Grębecka L., Kłopocka W. (1986) Morphological differences of pinocytosis in *Amoeba proteus* related to the nature of pinocytotic inducer. *Protistologica* **22**: 265-270
- Grębecki A. (1991) Participation of the contractile system in endocytosis demonstrated *in vivo* by video-enhancement in heat-pre-treated amoebae. *Protoplasma* **160**: 144-158
- Grynkiwicz G., Poenie M., Tsien R. Y. (1985) A new generation of Ca^{2+} indicators with greatly improved fluorescence properties. *J. Biol. Chem.* **260**: 3440-3450
- Hellewell S. B., Taylor D. L. (1979) The contractile basis of ameoboid movement. VI. The solation-contraction coupling hypothesis. *J. Cell Biol.* **83**: 633-648
- Hitchcock S. E. (1977) Regulation of motility in non-muscle cells. *J. Cell Biol.* **74**: 1-15
- Holter H. (1965) Physiologie der Pinozytose bei Amöben. In: Sekretion und Exkretion, (Ed. K. E. Wohlfarth-Bottermann). Springer, Berlin Heidelberg New York, 119-146
- Johansson P., Josefsson J.-O. (1978) Evidence for a dual effect of intracellular Ca^{2+} on pinocytosis. *Acta Physiol. Scand.* **102**: 71A-72A
- Josefsson J.-O. (1968) Induction and inhibition of pinocytosis in *Amoeba proteus*. *Acta Physiol. Scand.* **73**: 481-490
- Josefsson J.-O. (1975) Studies on the mechanism of induction of pinocytosis in *Amoeba proteus*. *Acta Physiol. Scand.* **97** (Suppl. **423**): 1-65
- Josefsson J.-O., Holmer N. G., Hansson S. E. (1975) Membrane potential and conductance during pinocytosis induced in *Amoeba proteus* with alkali metal ions. *Acta Physiol. Scand.* **94**: 278-288
- Klein H. P., Stockem W. (1979) Pinocytosis and locomotion in amoebae. XII. Dynamics and motive force generation during induced pinocytosis in *Amoeba proteus*. *Cell Tiss. Res.* **197**: 263-279

- Kłopocka W., Grębecka L. (1985) Effects of bivalent cations on the initiation of Na-induced pinocytosis in *Amoeba proteus*. *Protoplasma* **126**: 207-214
- Kłopocka W., Grębecka L. (1986) Factors limiting in time the induced pinocytotic response of *Amoeba proteus*. *Cell Biol. Int. Rep.* **10**: 109-115
- Kukulis J., Ackermann G., Stockem W. (1986) Pinocytosis and locomotion of amoebae. XIV. Demonstration of two different pinocytotic sites on the cell surface of *Amoeba proteus*. *Protoplasma* **131**: 233-243
- Kuroda K., Sonobe S. (1981) Reactivation of a glycerinated model of Amoeba. *Protoplasma* **109**: 127-142
- Kuroda K., Yoshimoto Y., Hiramoto Y. (1988) Temporal and spatial localization of Ca²⁺ in moving *Amoeba proteus* visualized with aequorin. *Protoplasma* **144**: 64-67
- Nuccitelli R., Poo M. M., Jaffe L. F. (1977) Relation between amoeboid movement and membrane-controlled electrical currents. *J. Gen. Physiol.* **69**: 743-763
- Prusch R. D. (1986) Calcium and initial surface binding phase of pinocytosis in *Amoeba proteus*. *Am. J. Physiol.* **251**: C153-C158
- Prusch R. D., Dunham P. B. (1972) Ionic distribution in *Amoeba proteus*. *J. Exp. Biol.* **56**: 551-563
- Prusch R. D., Hannafin J. (1979) Sucrose uptake by pinocytosis in *Amoeba proteus* and influence of external calcium. *J. Gen. Physiol.* **74**: 523-535
- Prusch R. D., Minck D. R. (1985) Chemical stimulation of phagocytosis in *Amoeba proteus* and the influence of external calcium. *Cell Tiss. Res.* **242**: 557-564
- Putney J. W., Jr. (1993) Excitement about calcium signaling in inexcitable cells. *Science* **262**: 676-678
- Randriamampita C., Tsien R. Y. (1993) Emptying of intracellular Ca²⁺ stores releases a novel small messenger that stimulates Ca²⁺ influx. *Nature* **364**: 809-814
- Reinold M., Stockem W. (1972) Darstellung eines ATP-sensitiven Membransystems mit Ca²⁺-transportierender Funktion bei Amöben. *Cytobiologie* **6**: 182-194
- Satterwhite L. L., Pollard T. D. (1992) Cytokinesis. *Curr. Opin. Cell Biol.* **4**: 43-52
- Sonobe S., Hatano S., Kuroda K. (1985) Cytoplasmic movement in a glycerinated model of *Amoeba proteus*. In: Cell Motility II. (Eds. H. Ishikawa, S. Hatano and H. Sato). University of Tokyo Press, Tokyo, 271-282
- Sonobe S., Takahashi S., Hatano S., Kuroda K. (1986) Phosphorylation of Amoeba G-actin and its effect on actin polymerization. *J. Biol. Chem.* **261**: 14837-14843
- Stockem W. (1977) Endocytosis. In: Mammalian cell membranes, (Eds. G. A. Jamieson and D. M. Robinson). Butterworths, London, **5**: 151-195
- Stockem W., Klein H. P. (1979) Pinocytosis and locomotion of amoebae. VI. Demonstration of Ca²⁺-binding sites during induced pinocytosis in *Amoeba proteus*. *Protoplasma* **100**: 33-43
- Stockem W., Klein H. P. (1988) Pinocytosis and locomotion of amoebae. XVII. Influence of different cations on induced pinocytosis in *Amoeba proteus*. *Europ. J. Protistol.* **23**: 317-326
- Stockem W., Kłopocka W. (1988) Ameboid movement and related phenomena. *Int. Rev. Cytol.* **112**: 137-183
- Stockem W., Naib-Majani W., Wohlfarth-Bottermann K. E., Osborn M., Weber K. (1983) Pinocytosis and locomotion in amoebae. XIX. Immunocytochemical demonstration of actin and myosin in *Amoeba proteus*. *Eur. J. Cell Biol.* **29**: 171-178
- Taylor D. L. (1977) The contractile basis of ameboid movement. IV. The visco-elasticity and contractility of *Amoeba* cytoplasm *in vivo*. *Exp. Cell Res.* **105**: 413-426
- Taylor D. L., Fechtmeier M. (1982) Cytoplasmic structure and contractility: The solution-contraction coupling hypothesis. *Phil. Trans. R. Soc. London B* **299**: 185-197
- Taylor D. L., Blinks J. R., Reynolds G. (1980) Contractile basis of ameboid movement. VII. Aequorine luminescence during ameboid movement, endocytosis and capping. *J. Cell Biol.* **86**: 599-607
- Tsien R. W. (1990) Calcium channels, stores and oscillations. *Ann. Rev. Cell Biol.* **6**: 715-760
- Wassermann R. H., Corradino R. A., Carafoli E., Kretsinger R. H., MacLennan D. H., Siegel F. L. (1977) Calcium binding proteins and calcium function. Elsevier/North-Holland Biomedical Press, Amsterdam
- Williams R. J. P. (1974) Calcium ions: Their ligands and their functions. *Biochem. Soc. Symp.* **39**: 133-138
- Wohlfarth-Bottermann K. E., Stockem W. (1966) Pinocytose und Bewegung von Amöben. II. Permanent und induzierte Pinocytose bei *Amoeba proteus*. *Z. Zellforsch.* **73**: 444-474

Received on 7th September, 1995; accepted on 14th November, 1995

Pigment Granules and Hypericin-like Fluorescence in the Marine Ciliate *Fabrea salina*

Roberto MARANGONI¹, Luigi GOBBI², Franco VERNI³, Gianni ALBERTINI² and Giuliano COLOMBETTI¹

¹Istituto di Biofisica del C.N.R., Pisa; ²Istituto di Scienze Fisiche, Facoltà di Medicina, Università di Ancona, Ancona; ³Dipartimento di Scienze dell'Ambiente e del Territorio, Pisa, Italy

Summary. *Fabrea salina* is a light-sensitive marine ciliate, which shows positive phototaxis and photophobic step-down response. It belongs to the order *Heterotrichida*, like *Blepharisma japonicum* and *Stentor coeruleus*, but, differently from those, it appears colorless when observed under the optical microscope. Living *F. salina* cells do not significantly fluoresce, but a fluorescence, similar to that observed in the fresh-water ciliate *B. japonicum*, becomes easily detectable when the cells are dead or severely damaged by chemical or physical treatments. This evidence suggests that *F. salina* might contain an endogenous pigment, probably belonging to the class of hypericins. In the case of *B. japonicum*, this pigment is localized in pigment granules preferentially located close to the cell membrane. The ultrastructural studies reported here reveal that also *F. salina* contains membranated pigment granules very similar with respect to localization, size and appearance to the pigment granules described in *B. japonicum*. An approximate evaluation shows that the relative density of these granules in *F. salina* is much lower than in *B. japonicum*, which may account for the apparent colorless of *F. salina*. Absorption and emission fluorometric measurements of sonicated samples of cells show that the fluorescence of the endogenous pigment of *F. salina* is very similar to that of a hypericin-like pigment. From these results we can draw the preliminary conclusion that *F. salina* contains a small amount of a hypericin-like pigment, organized in membranated granules. The role of such pigment in the photoreceptive processes is still an open problem.

Key words: *Blepharisma japonicum*, *Fabrea salina*, fluorescence, hypericin, pigment granules.

INTRODUCTION

Some photoresponsive ciliates belong to the order *Heterotrichida* (Corliss 1989); among them, a few are pigmented, such as *Blepharisma japonicum* and *Stentor coeruleus*; their pigment belongs to the class of hypericins, as shown by means of spectroscopic, fluorometric and microspectrofluorometric techniques (Lenci and Ghetti 1989, Kim et al. 1990, Song et al. 1990, Angelini et al. 1995). Moreover, it has been demonstrated in both ciliates that the

action spectrum of their phototile reaction is very similar to the absorption spectrum of a hypericin-like molecule (Song et al. 1980, Scevoli et al. 1987). Because of this evidence, a hypericin-like pigment has been proposed to be the molecule responsible for photoreception in these systems.

Fabrea salina Henneguy (1889) also belongs to the order *Heterotrichida* and shows phototile responses; in particular positive phototaxis and photophobic step-down reactions (Colombetti et al. 1992a, b). In the early literature (Fauré-Fremiet 1911, Ellis 1937) *F. salina* was described as red-pigmented; later Møller (1962) suggested

Address for correspondence: Roberto Marangoni, Istituto di Biofisica del C.N.R., Via S. Lorenzo 26, 56127 Pisa, Italy; Fax: (+39-50) 553501; E-mail: roberto@ib.pi.cnr.it

that the presence of a "dark" pigmentation was of a fundamental importance for the survival of *F. salina* when exposed to UV irradiations. However, our strain (and all the strains we have examined) appears colorless when observed under the optical microscope. Moreover, the action spectrum for positive phototaxis of *F. salina* (Marangoni et al. 1994a) does not resemble that of *B. japonicum*; on the contrary, it is similar to that of *Paramecium bursaria* (Nakaoka and Tokioka, 1988), another colorless photoresponsive ciliate, in which some evidences (Nakaoka et al. 1991, Tokioka et al. 1991) suggest the presence of a rhodopsin as photoreceptor pigment. In *F. salina* the presence of a rhodopsin molecule has been suggested by immunocytochemistry experiments performed with polyclonal anti-bovine rhodopsin antibodies (Podestà et al. 1994).

On the other side, it has already been reported (Marangoni et al. 1994b) that dead *F. salina* cells show a spontaneous red-orange fluorescence, indicating the presence of an endogenous pigment, which preliminary fluorometric measurements have shown to be similar to a hypericin-like molecule.

We report in this paper the results of ultrastructural studies aimed at the investigation of the possible presence in *F. salina* of pigment granules similar to those observed in *B. japonicum* and of fluorescence measurements of sonicated samples of cells. The results are compared to those reported for *B. japonicum*.

MATERIALS AND METHODS

Cell culture

Fabrea salina were grown in artificial sea water (density 1.022) at a constant temperature of 22°C in a light-dark cycle (15 h light-9 h dark). *F. salina* were fed the green marine alga *Dunaliella salina*, which was grown in the growth medium suggested by Johnson (Johnson et al. 1968) and on the same light-dark cycle. *D. salina* used to feed *F. salina* were centrifuged and washed three times in the ciliate growth medium. *F. salina* cells were starved for four days before being used for the experiments.

Scanning electron microscopy

Samples for scanning electron microscopy (SEM) were fixed in 2% (volume/volume) glutaraldehyde prepared in 0.1 M cacodylate buffer, pH 7.4 for 30 min at 4°C, washed in 0.1 M cacodylate buffer and post-fixed in 1% (weight/volume) osmium tetroxide in the same buffer, for 40 min at 4°C. The cells were placed on poly-L-lysine-coated coverslips, and then dehydrated in ethanol gradients. The samples were then coated with a gold sputter (100 nm) (5150A Sputter Coater Edwards) and observed by means of a Philips SEM 515 scanning microscope.

Transmission electron microscopy

Samples for transmission electron microscopy (TEM) were fixed in 2% (volume/volume) glutaraldehyde prepared in 0.1 M cacodylate buffer, pH 7.4 for 30 min at 4°C, washed in 0.1 M cacodylate buffer with 7% sucrose, and post-fixed in 1% (weight/volume) osmium tetroxide in the same buffer, for 40 min at 4°C. The cells were then dehydrated in ethanol gradients, washed in propylene oxide and embedded in Epon araldite. Ultrathin sections were obtained with a Ultratome LKB ultramicrotome, and stained with uranyl acetate and lead citrate. The observations were made with a Philips CM-10 transmission electron microscope operated at 80 kV.

Steady-state fluorometric measurements

Since living cells only show a hardly detectable fluorescence, fluorometric measurements were performed on sonicated samples. About 10 ml of cell suspension, kept in an ice bath, were sonicated for a total of 2 min, by means of an MSE sonicator (150 W), at a nominal amplitude of 20 µm peak to peak. Fluorometric measurements were performed by means of a Jasco FP 770 spectrofluorometer.

RESULTS

Microscopic studies

Figure 1 shows a *F. salina* cell observed under the optical microscope: no pigmentation is evident; the cytoplasm appears transparent with the exception of some

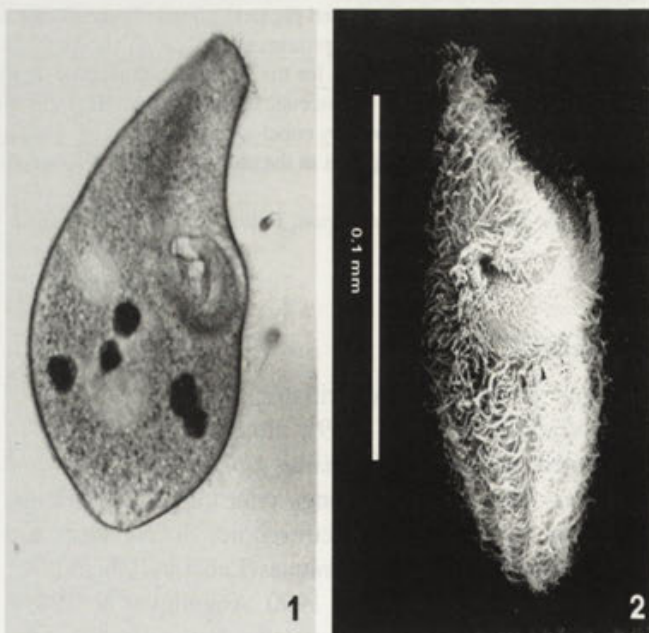


Fig. 1. *Fabrea salina* as seen under the optical microscope (x 200). The cytoplasm does not show evident pigmentation. There are some dark digestive vacuoles, filled with green residues of *Dunaliella salina* algae. Fig. 2. SEM picture of *Fabrea salina*. The arrowheads indicate the adoral zone of membranelles (AZM); a dense coat of cilia emerging from the cell's surface is clearly visible. Bar - 0.1 mm

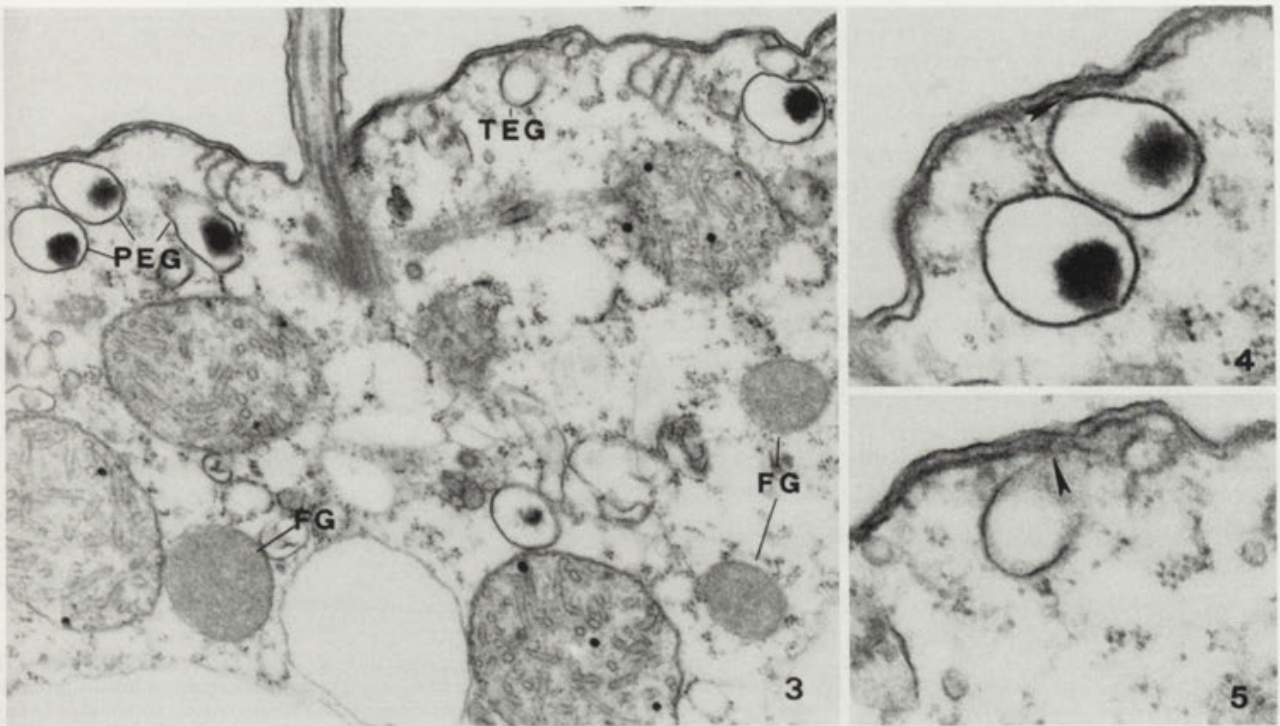


Fig. 3. A TEM section (x 36000) of a *Fabrea salina* cell. It is possible to see some granules filled of pigment (FG), some partially empty granules (PEG) and some totally empty granules (TEG)

Fig. 4. A detailed view (x 74000) of a partially empty granule located just below the cell membrane. The arrowhead indicates a probable point of junction between the membrane of the cell and of the granule

Fig. 5. A detailed view (x 79000) of a totally empty granule located just below the cell membrane. The arrowhead indicates a probable point of junction between the membrane of the cell and of the granule

food vacuoles, which appear green because of the remains of partially digested *Dunaliella salina*. Figure 2 shows an SEM picture of *F. salina*: some characteristic structures such as the adoral zone of membranelles (AZM) are clearly visible.

Figure 3 shows a TEM section taken in the AZM region: in addition to mitochondria, cilia and other structures, there are, clearly visible, many membranated granules, some of which are filled by an electron-dense pigment, while others are partially or totally empty. The diameter of these granules ranges from 0.2 up to 0.5 μm , and they are localized just below the cell membrane; in some cases, it seems that there might be a continuity between the cell membrane and the granule membranes, respectively (see Figs. 4, 5).

Figure 6 shows an enlarged view of a partially empty granule, in which two important features are detectable: (1) the granule is seemingly surrounded by two membranes, an inner and an outer membrane. These two membranes are so near that when the granule is filled by the pigment it is not possible to distinguish between them; (2) within the granule, near the edge of the inner membrane, there is an apparently stacked-lamella structure.

Fluorometric measurements

In order to rule out spectral contaminations possibly caused by impurities (or metabolites), we have run control experiments on: fresh *F. salina* growth medium, sonicated *F. salina* growth medium and *D. salina* sonicated samples. *D. salina* samples show a typical chlorophyll fluorescence spectrum. The growth medium shows (independently of sonication) a spurious fluorescence with a narrow peak in excitation at 450 nm and a corresponding emission band at around 680 nm. No emission could be found by exciting at 500 nm and this excitation wavelength also minimized the chlorophyll components due to the remains of *D. salina* cells present in *F. salina* samples. All the emission spectra reported in the following, therefore, have been obtained by exciting at 500 nm, while the excitation spectra have been measured by observing at 640 nm.

Figure 7 shows a typical emission spectrum of a sample of sonicated *F. salina* cells (concentration about 500 cells/ml): the main peak is localized at about 610 nm, and there is also a small (but meaningful) shoulder between 650 and 660 nm. Figure 8 shows the excitation spectrum for



Fig. 6. A very enlarged view (x 91000) of a partially empty granule. The arrowhead indicates a stacked-lamella structure present in the inner space of the granule. The arrows indicate the presence of two different membranes surrounding the granule.

emission at 640 nm: there is a large band between 400 and 500 nm, and two more defined peaks, the former and smaller at 560 nm, and the latter at 610 nm.

We have also determined the relative fluorescence intensities of samples obtained starting from different concentrations of *F. salina* cells (from 10 up to 1000 cells/ml). Figure 9 shows the dependence of the relative height of the emission peak at 640 nm on the cell concentration before the sonication: the fluorescence intensity is roughly proportional

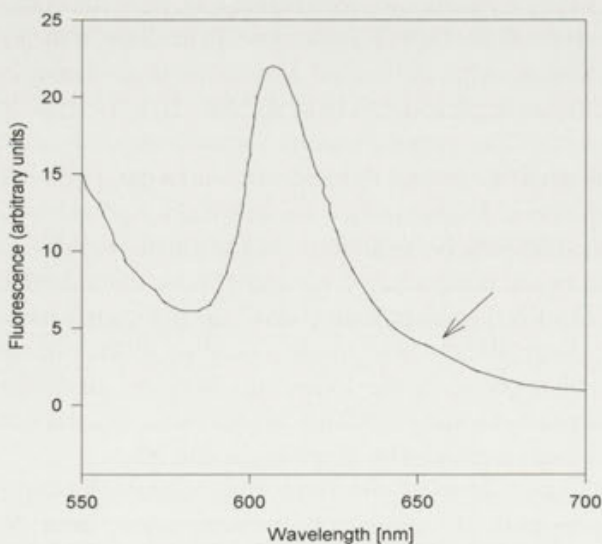


Fig. 7. Fluorescence emission spectrum for excitation at 500 nm. The abscissa shows the wavelength in nanometers; the ordinate the fluorescence intensity, in arbitrary units. The main peak is at about 610 nm; the arrow indicates the shoulder between 650 and 660 nm

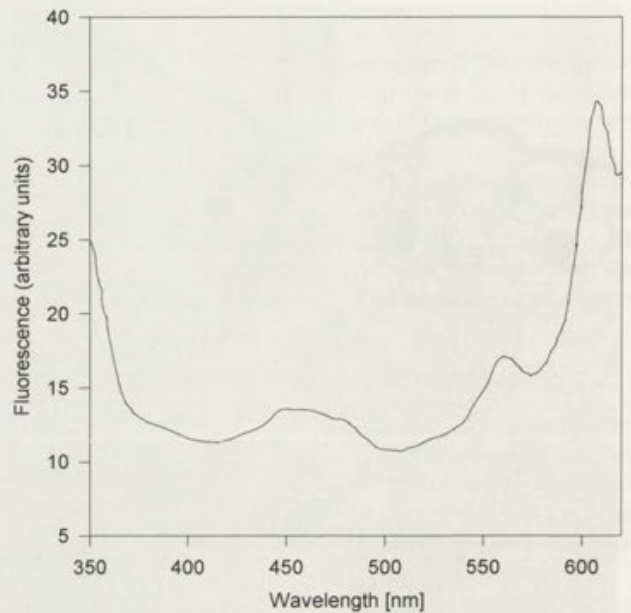


Fig. 8. Fluorescence excitation spectrum for emission at 640 nm. The abscissa shows the wavelength in nanometers; the ordinate the fluorescence intensity, in arbitrary units. The spectrum is composed of a large band between 400 and 500 nm and two peaks at 560 and 610 nm, respectively

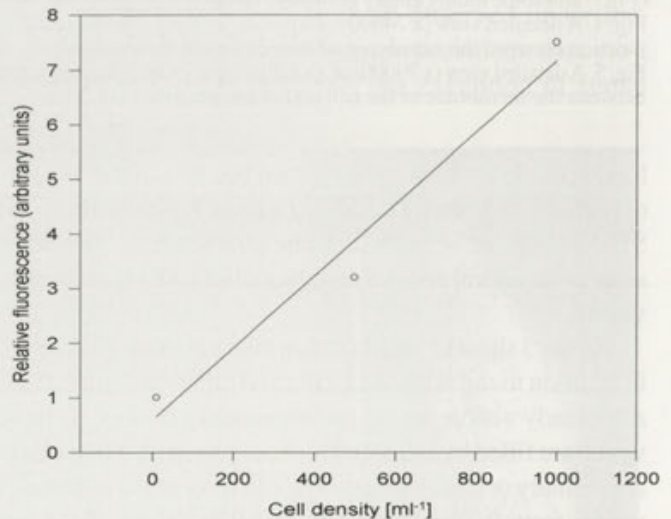


Fig. 9. Dependence of the fluorescence intensity on the cell concentration of the sample. In abscissa, the approximate cell concentration C of the sample (in cells/ml), before the sonication. In ordinate, the relative fluorescence intensity RF , in arbitrary units). The regression line represents a linear fit to the data

to the amount of sonicated cells, thus giving a direct proof that the fluorescence originates from *F. salina* cells.

DISCUSSION

The granules visible in the TEM pictures of *Fabrea salina* cells are very similar (with respect to size, localiza-

tion and membrane system) to those described in *Blepharisma japonicum* (see Giese 1973). On the other hand, both fluorescence emission and excitation spectra are very similar to those of blue *B. japonicum* (Angelini et al. 1995) and, therefore, strongly suggest the presence of a hypericin-like molecule in *F. salina*. There is no direct proof that the pigment contained in the granules is responsible for the observed fluorescence; the ultrastructural and fluorometric characteristic of *F. salina* are, however, so similar to those of other pigmented *Heterotrichida*, that it is reasonable to suggest that also in *F. salina* the hypericin-like pigment is contained in the pigment granules.

The problem of the apparent colorlessness of *F. salina* appears to be related to the relative small number of granules that this ciliate contains: preliminary observations, in fact, show that the granule density in *F. salina* is much lower than that reported for *B. japonicum*.

The TEM pictures show also two important features: the former is that, in some cases, pigment granules and cell membrane are probably joined; the latter is the presence, within the lumen of the granule, of the stacked-lamella structure. These two evidences are of a relevant importance in suggesting a photoreceptor organelle role for the pigment granule. If the hypericin-like pigment contained in the granules is the photoreceptor molecule in *F. salina*, the existence of a direct junction between the cell membrane and the granule membrane could account for a direct and rapid transmission of the signal from the photoreceptor pigment to the other molecules of the transduction chain, which are presumably membrane proteins. On the other hand, the presence of the stacked-lamella structure within the granule (perhaps generated by the inner membrane of the granule) could suggest that primary photoreceptive events take place in this region: the presence of stacked-lamella structures can, in fact, be observed in many photoreceptive structures such as chloroplasts and rod outer segments.

Our findings in *F. salina* are in agreement with some recent evidences reported by Matsuoka et al. (1994), which have described in *B. japonicum* cells the presence of junction points between the membrane of the granules and the cell membrane, and the presence of certain "honeycomb-like" membranated structures, located just below the inner membrane of the granule. Because of the large amount of evidences converging toward the assumption of a photoreceptive role for hypericin-like pigment in *B. japonicum*, Matsuoka draws the conclusion that the pigment granules are the photoreceptor organelle in *B. japonicum*.

In *F. salina* the situation is apparently more complicated. The action spectrum for the positive phototaxis reaction is not similar to the absorption spectrum of a hypericin-like molecule (Marangoni et al. 1994a), but resembles the action spectrum of *Paramecium bursaria* (Nakaoka and Tokioka 1988), in which a rhodopsin has been suggested as a photoreceptor molecule. Moreover, immunocytochemical evidences have revealed the presence on the cell membrane of *F. salina* of an opsin-like antigen (Podestà et al. 1994).

This evidence, together with that reported in this paper, shows that *F. salina* could be an intermediate system between pigmented and non pigmented ciliates, with the interesting possibility of the presence of two different photoreceptive systems active at the same time in the same cell. The relative independence and the possible interactions of these two systems are matter for further studies.

REFERENCES

- Angelini N., Cubeddu R., Ghetti F., Lenci F., Taroni P., Valentini G. (1995) In vivo spectroscopy study of *Blepharisma japonicum* photoreceptor pigments. *Biochim. Biophys. Acta* (in press).
- Colombetti G., Bräucker R., Macherer H. (1992a) Photobehavior of *Fabrea salina*: responses to directional and diffused gradient-light type. *J. Photochem. Photobiol. B* **15**: 253-257
- Colombetti G., Marangoni R., Macherer H. (1992b) Phototaxis in *Fabrea salina*. *Med. Biol. Envir.* **20**: 93-100
- Corliss J. O. (1979) The ciliated protozoa: characterisation, classification and guide to the literature. 2 ed. Pergamon Press, Oxford
- Ellis J. M. (1937) The morphology, division and conjugation of the salt marsh ciliate, *Fabrea salina* Henneguy. *Univ. Calif. Publ. Zool.* **46**: 343-388
- Fauré-Fremiet E. (1911) La structure intime de *Fabrea salina*. *C. r. Acad. Sci.* **71**: 419-420
- Giese A. C. (1973) *Blepharisma*. Stanford Univ. Press, Stanford
- Johnson M. K., Johnson E. J., MacElroy R. D., Speer H. L., Bruff B. S. (1968) Effects of salts on the halophilic alga *Dunaliella viridis*. *J. Bacteriol.* **95**: 1461-1468
- Kim I.-H., Rhee J. S., Huh J. W., Florell S., Faure B., Lee K. W., Kahsai T., Song P.-S., Tamai N., Yamazaki T., Yamazaki I. (1990) Structure and function of the photoreceptor stentorin in *Stentor coeruleus*. I. Partial characterization of the photoreceptor organelle and stentorins. *Biochim. Biophys. Acta.* **1040**: 43-57
- Lenci F., Ghetti F. (1989) Photoreceptor pigments for photomovements of microorganisms: some spectroscopic related studies. *J. Photochem. Photobiol. B (Biol.)* **3**: 1-16
- Marangoni R., Puntoni S., Favati L., Colombetti G. (1994a) Phototaxis in *Fabrea salina*. I. Action spectrum determination. *J. Photochem. Photobiol. B (Biol.)* **23**: 149-154
- Marangoni R., Cubeddu R., Taroni P., Valentini G., Sorbi R., Gioffré D., Batistini A., Colombetti G. (1994b) Fluorescence microscopy of an endogenous pigment in the marine ciliate *Fabrea salina*. *Med. Biol. Envir.* **22**: 85-89
- Matsuoka T., Tsuda T., Ishida M., Kato Y., Takayanagi M., Fujino T., Mizuta S. (1994) Presumed photoreceptor protein and ultrastructure of the photoreceptor organelle in the ciliated protozoan, *Blepharisma*. *Photochem. Photobiol.* **60**: 598-604
- Møller K. M. (1962) On the nature of stentorin. *Compt. Rend. Lab. Carlsberg* **32**: 471-498

- Nakaoka Y., Tokioka R. (1988) Photoreceptor potential causing phototaxis in *Paramecium bursaria*. *J. Exp. Biol.* **137**: 477-485
- Nakaoka Y., Tokioka R., Shinozawa T., Fujita J., Usukura J. (1991) Photoreception of *Paramecium* cilia: localization of photosensitivity and binding with anti-frog-rhodopsin IgG. *J. Cell Sci.* **99**: 67-72
- Podestà A., Marangoni R., Villani C., Colombetti G. (1994) A rhodopsin-like molecule on the plasma membrane of *Fabrea salina*. *J. Eukar. Microbiol.* **41**: 565-569
- Scevoli P., Bisi F., Colombetti G., Ghetti F., Lenci F., Passarelli V. (1987) Phototile responses of *Blepharisma japonicum*. I. Action spectrum determination and time-resolved fluorescence of photoreceptor pigments. *J. Photochem Photobiol. B (Biol.)* **1**: 75-84
- Song P.-S., Häder D.-P., Poff K. L. (1980) Step-up photophobic response in the ciliate *Stentor coeruleus*. *Arch. Microbiol.* **126**: 181-186
- Song P.-S., Kim I.-H., Florell S., Tamai N., Yamazaki T., Yamazaki I. (1990) Structure and function of the photoreceptors stentorins in *Stentor coeruleus*. II. Primary photoprocess and picosecond time-resolved fluorescence. *Biochim. Biophys. Acta* **1040**: 58-65
- Tokioka R., Matsuoka K., Nakaoka Y., Kito Y. (1991) Extraction of retinal from *Paramecium bursaria*. *Photochem Photobiol.* **53**: 149-151

Received on 5th October, 1995; accepted on 7th December, 1995

Modifications of Cortical Pattern in a Ciliate, *Dileptus margaritifer* Under the Influence of Elevated External Potassium Concentration

Krystyna GOLIŃSKA

Department of Cell Biology, Nencki Institute of Experimental Biology Warszawa, Poland

Summary. Cells of *Dileptus margaritifer* while in elevated concentration of external potassium, are depolarized and unable to carry out ciliary reversal in response to mechanical shock or injury. These cells are capable of food intake, of regeneration, of cell division initiation, although fission is rarely accomplished. In inhibited dividers, oral primordia are completely resorbed while oralized somatic kinetids persist, frequently giving rise to inverted kineties. Depolarized ciliates are often disfigured by rounding up of previously tapered cell extremities, which lead to formation of tailless, humpback, or astomous cells. The rounding up of anterior and posterior cell regions is explained as spreading of proliferation of somatic kinetids over the tapered regions where the proliferation is normally absent. The formation of astomous cells is explained as spreading of partial resorption of oral structure (in cells activated for conjugation) over the whole oral structure. The hypothesis is made that elevated external potassium may destroy borders between morphogenetically activated and inhibited cortical territories, at last in the highly labile cortex of *Dileptus*.

Key words: ciliate, *D. margaritifer*, pattern changes, potassium, proliferation-resorption pattern.

Abbreviations: a-autophagic vacuole, b-nonciliated bulge, c-cytostome, cf-cytostomal field, fl-filamentous material, ib-inner pharyngealbasket, Nd-nematodesma, o-oralized somatic kinetid, ob-outer pharyngeal basket, OF-oral fibre, ok-oral kinetid, p-proboscis, Pc-postciliary fibre, p-microtubule perpendicular microtubule, R-resorption of kinetids, s-suture, sc-sensory cilia, sk-somatic kinetids, T-transverse fibre, t-toxicyst, tl-tail, tr-transformed part of ventral band, v-tubular vesicles.

INTRODUCTION

Immediate effect of raising the concentration of potassium ions upon ciliate behaviour is ciliary reversal, while prolonged exposure to elevated concentration of potassium brings about a complete or partial inhibition of ciliary reversal during the adaptation period (de Peyer and Machemer 1977, Schusterman et al. 1978, Dryl and Hildebrand 1979, Machemer 1989). The loss of ability to carry out ciliary reversal is ascribed to depolarization of cell membrane.

The aim of this study was to investigate what possible modifications in ciliary pattern may be caused by chronic raise in external potassium concentration, in the ciliate *Dileptus margaritifer*. In ciliates other than *Dileptus*, elevated potassium concentration is known to evoke mating reaction of *Paramecium* (Miyake 1960), from degeneration of cilia over a special ventral region, up to pair formation. These changes are not different from changes observed during normal conjugation. In *Dileptus* changes in oral structure, similar to those preparatory to conjugation, were also observed under the influence of elevated potassium (Golińska and Afon'kin 1993), although pair formation was never achieved.

In this study several modifications of ciliary pattern were found to arise in *Dileptus* cells exposed to elevated

Address for correspondence: Krystyna Golińska, Department of Cell Biology, Nencki Institute of Experimental Biology, ul. Pasteura 3, 02-093 Warszawa, Poland; Fax: 48-22 225342

potassium. These abnormalities, although not specific for potassium action, are nonetheless the first described abnormalities caused by elevated potassium in a ciliate. Cell division arrest when it occurs in presence of elevated potassium, may introduce supernumerary and inverted kineties into midbody cortex of *Dileptus*. Rise of potassium concentration may also lead to rounding up of cell extremities, resulting in formation of humpback, astomous and tailless cells. An explanation is proposed and discussed, namely that depolarization of cell membrane unmakes boundaries between morphogenetically active and inactive cortical territories, leading both to cell deformations and to arrest of cytokinesis.

MATERIALS AND METHODS

Dileptus margaritifer, formerly known as *Dileptus anser* (see revision by Wirnsberger et al. 1984), was used in this study. Cells were kept in glass vessels and fed with *Colpidium* sp., twice a week. Details of culture methods are published elsewhere (Golińska and Jerka-Dziadosz 1973). Observations were carried out on cells belonging to the two different groups. The first group, further referred to as the activated cells, contained a mixture of cells belonging to the two mating types activated to conjugation. Clones belonging to two complementary mating types were cultured separately and mixed together to initiate pregamic cell division, whenever there was a need for dividing cells. At the beginning of an experiment, a complementary mating types were mixed together simultaneously with an increase of KCl concentration in surrounding medium. The second group, further on referred to as the well-fed cells, contained cells all belonging to one of the mating types. At the beginning of an experiment cells were mixed with numerous prey organisms simultaneously with an increase of KCl concentration in surrounding medium.

As a source of potassium, KCl was used. Stock solution was 100 mM KCl in distilled water, and this was diluted to the needed concentration with the culture medium of *Dileptus*. Most suitable concentration of KCl was found to be 20 mM. In this concentration cells stay depolarized (i.e. undergo adaptation) for 24 h and more. Preliminary observations have shown that the depolarized cells were able to regenerate both anterior and posterior structures. There was no difference in timing and frequency of successful regeneration in the presence and absence of elevated KCl, thus details obtained were not shown in Results. Starvation was applied to the activated cells in some experiments. Usually, the complementary mating types were mixed together one day after food exhaustion. Cells described as starved were used for experiment three days after food exhaustion.

Observations in the light microscope were made on samples impregnated with silver proteinate (protargol) after the method of Dragesco (1962) with slight modification. For electron transmission microscopy the standard procedures were applied, except for fixation. The fixative used was a mixture of 2 parts of 2% osmium tetroxide (prepared with cacodylate buffer, pH 7.2) and 1 part of 6% glutaraldehyde, freshly prepared and maintained at 0°C during fixation (30 min.). The sections were examined with JEOL transmission electron microscope.

RESULTS

Ciliary pattern on interphasal cells of *Dileptus margaritifer*

The shape of *Dileptus* is that of a cylinder, posteriorly tapered into an elongated tail (Fig. 1). Anteriorly, the ventral part of the cylinder ends at a circular cytostomal field, while the dorsal part is tapered into long anterior process, termed the proboscis. The oral apparatus consists of a circular cytostomal field with the cytostome in its centre (Figs. 1, 2), and of a long extension of the field which occupies the ventral side of proboscis and is termed the ventral band.

The somatic ciliature is represented by kineties, i.e. by rows of longitudinal somatic kinetids (Fig. 1). A kinetid, as proposed by Lynn (1988), is composed of basal body with all its fibrillar derivatives: cilium and fibrillar rootlets. The structure of a somatic kinetid is that characteristic for haptorid ciliates (Leipe et al. 1992): a single basal body anchors transverse fibres of two kinds (T fibres) in its left-anterior sector, one postciliary fibre (Pc fibre) in the right-posterior sector, and one kinetodesmal fibril in the right-anterior sector (Figs. 6, 7). All these rootlets run from the basal part of the basal body toward the cell surface. The surface is supported by microtubules of Pc and T ribbons, mostly by Pc ribbons which are especially long in *Dileptus* (Golińska 1991). Somatic kineties run parallel to each other on the cylindrical part of the cell body (Fig. 1). On the tapered parts (regions of tail and of proboscis), kineties approach each other and their kinetids become more and more scattered, until the exact arrangement of kineties becomes difficult to describe. Kineties end, however, at different distances from cell extremities since only few kinetids are found on the tips of both proboscis and tail.

Somatic kineties are arranged into a similar pattern on tail and proboscis, but on proboscis it is complicated due to the presence of the oral structure and of rows of the so-called sensory cilia (Grain and Golińska 1969). Oral structure on the ventral side of the proboscis is accompanied by oralized somatic kinetids (terminology after Foissner and Foissner 1988), which are structurally connected to oral kinetids by special filamentous rootlets (Golińska 1995). Ventral somatic kineties close to cytostomal field curve rightwards, and their bent segments parallel the row of oral kinetids (Fig. 1). Along the right margin of the ventral band a single oralized kinety parallels the oral row, along the left margin of ventral band numerous short oblique rows of oralized kinetids accompany the row of oral kinetids. In the tapered part of the

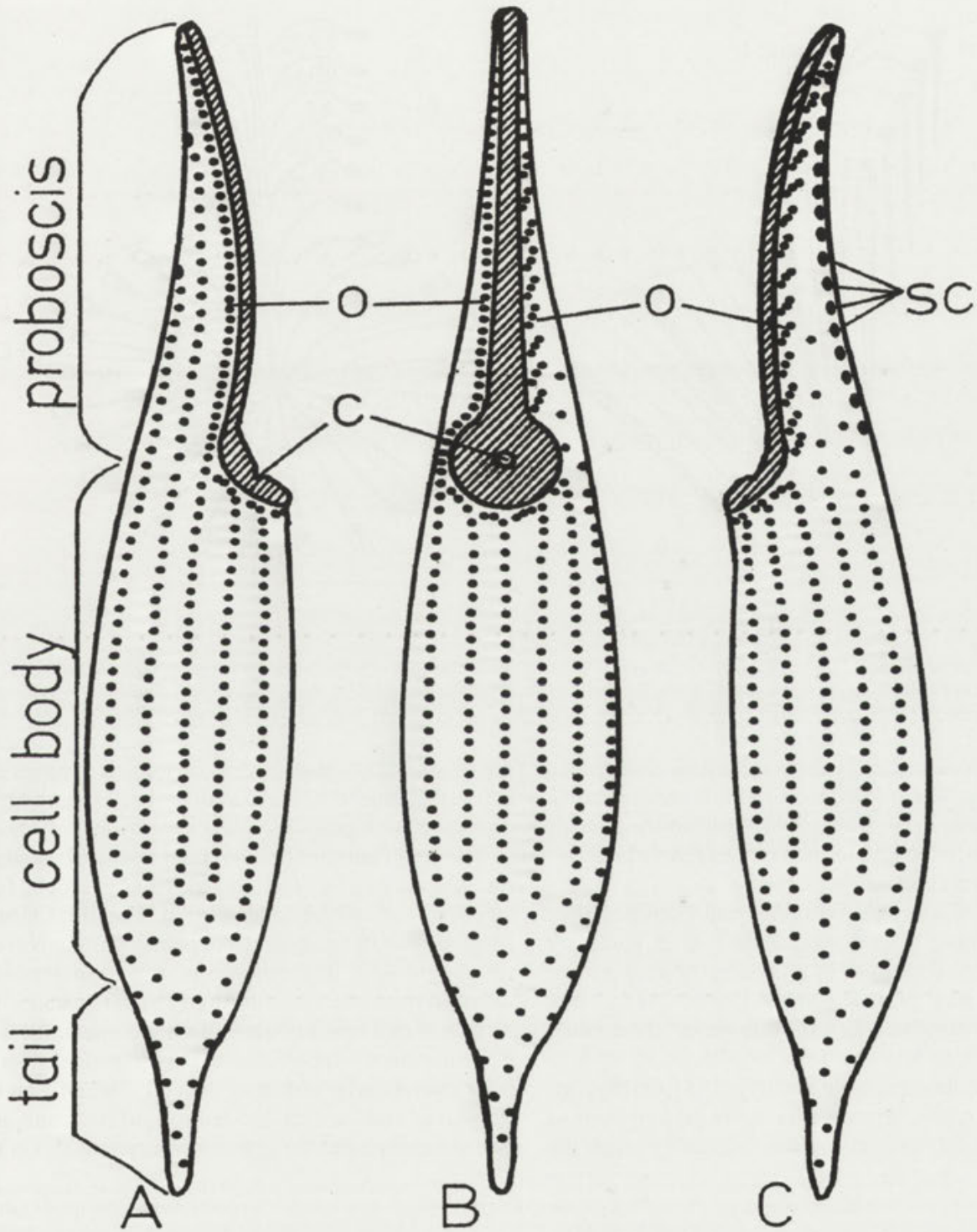


Fig. 1. Schematic representation of right **A**, ventral **B** and left **C** sides of *Dileptus margaritifer*. Oral area is hatched. c - cytostome, o - oralized somatic kinetids, sc - sensory cilia. Note the ciliary pattern on cell posterior. Dots represent somatic kinetids. Continuous line surrounding oral area represents the row of oral kinetids

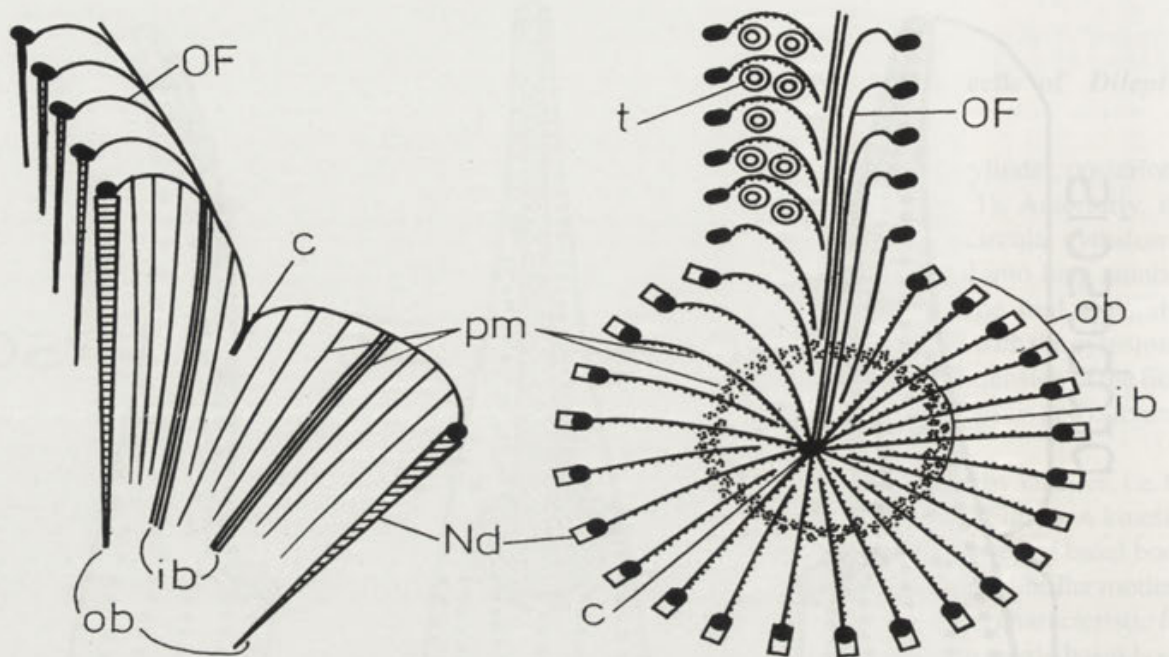


Fig. 2. Schematic representation of oral apparatus in *Dileptus margaritifer*. A - side view of oral structure, B - ventral view of oral structure. As in all the other illustrations, cell is viewed from the outside. Black circles represent oral kinetids, black ovals are oral dikinetids. c - cytostome, ib - inner pharyngeal basket, Nd - nematodesma, ob - outer pharyngeal basket, OF - oral fibres, pm - perpendicular microtubules, t - toxicyst

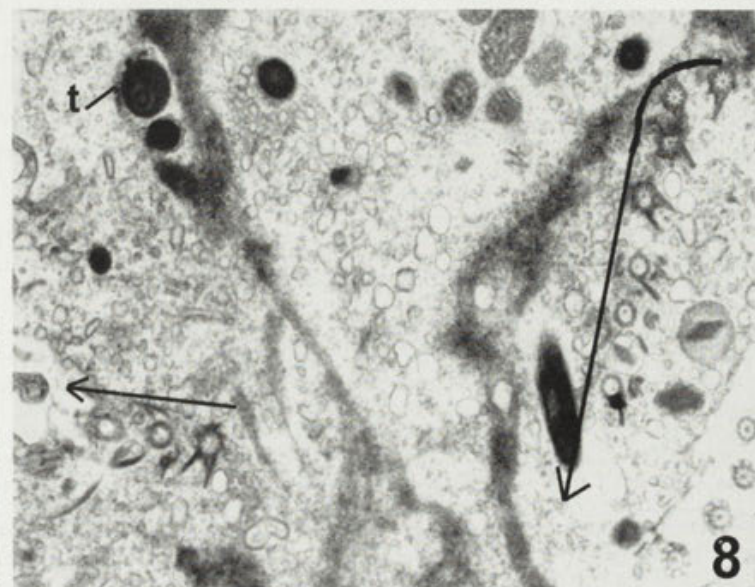
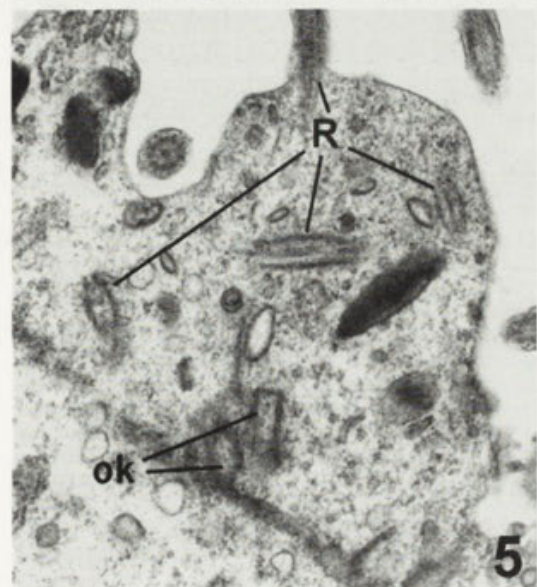
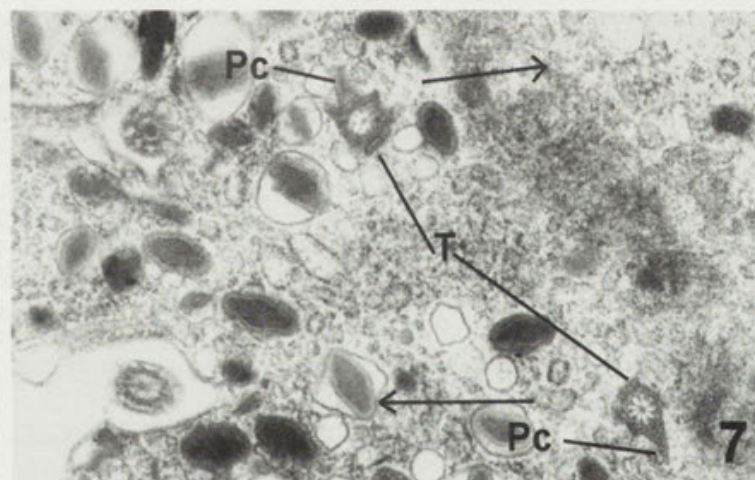
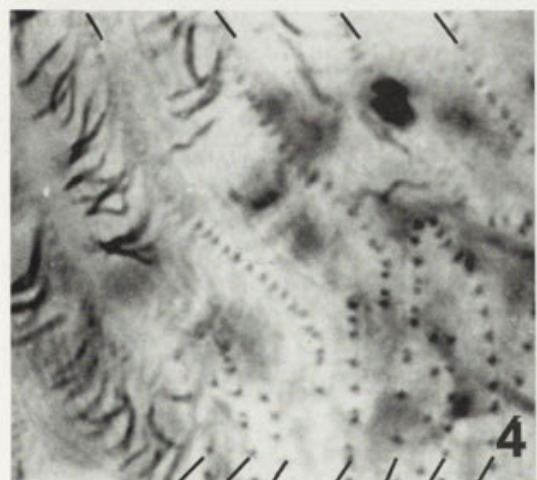
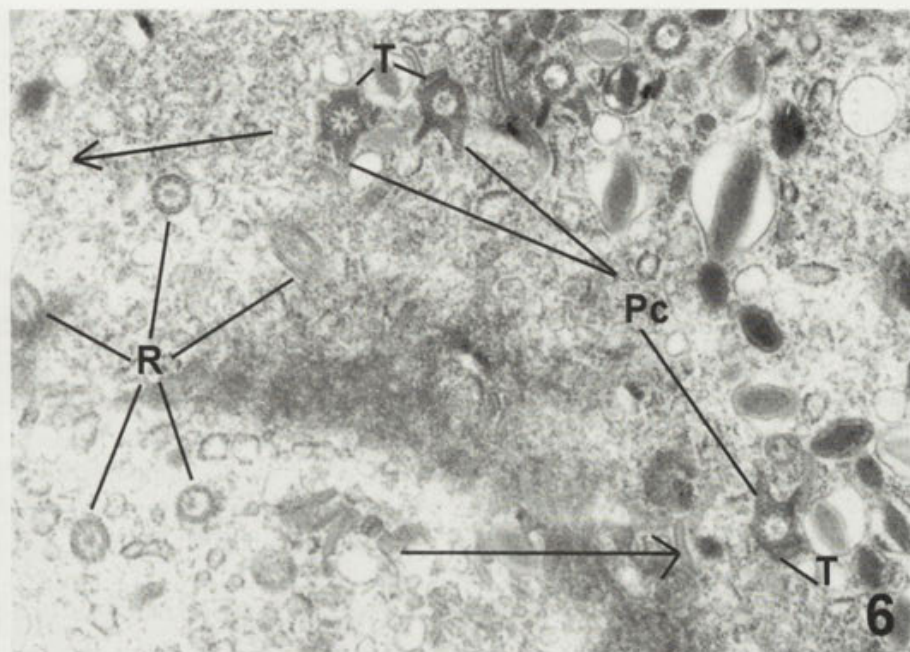
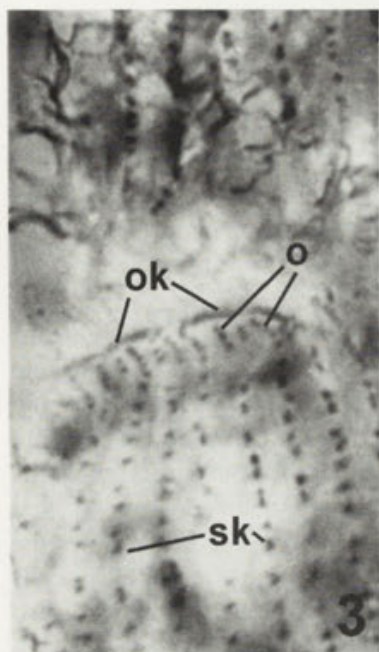
proboscis, distances in between oralized kinetids remain the same, regardless of their localization in wide or narrow part. It is unlike the distribution of other somatic kinetids in the region, which are located further apart when their kinetids come closer one to another.

Sensory cilia of *Dileptus* (Grain and Golińska 1969, later on in other ciliates termed the clavate cilia), are situated on the dorsal side of proboscis, at first glance in the prolongation of three somatic kinetids, as in many other haptorid ciliates. In reality, however, there rather exists an oblong region of sensory cilia, on its left side ending at the almost straight line (Fig. 15A). On the right side of the region sensory cilia are in prolongation of numerous right somatic kinetids when they reach the

dorsal side of proboscis. Most of somatic kinetids end before they enter the basal part of proboscis, similarly as do the somatic kinetids in posterior narrowing cell region.

The oral ciliature of *Dileptus* is represented by a single row of oral kinetids, which encircles the cytostomal field together with ventral band (Fig. 2). Each oral kinetid contains microtubular bundle of nematodesma (Nd) descending deeply into endoplasm, and a microtubular ribbon termed the oral fibre (OF) running under the surface of oral territory. Oral fibres are orientated with their short axes perpendicular to the cell surface, like no other microtubular ribbon in the cell. The OFs on the cytostomal field are all directed toward its centre, and some of them enter the cytostomal depression. On the

Figs. 3-8. Large *Dileptus margaritifer* cells belonging to activated and well-fed groups arrested in division in 20 mM KCl. 3 - protargol impregnated cell, after 5 h of activation to pregamic cell division. The beginning of resorption of oral kinetids. Note that the row of oral kinetids is disrupted. Oralized somatic kinetids are arranged into short rows, more numerous than their parental somatic kinetids. Cell anterior is in the upper part of the photograph (x 4500). 4 - protargol impregnated cell, after 24 h of activation. Pattern of somatic kinetids in midbody region, resorption of oral kinetids is already accomplished: Note that the number of kinetids in proter (upper part of the photograph) is much lower than in opisthe (lower part of the photograph). Kinetids shown with short black lines (x 6000). 5 - astomous cell, after 4.5 h of activation. Cilia and basal bodies withdrawn under the cell surface indicate that the resorption of oral primordium is under way. (x 22500). 6 - well-fed cell, after 24 h of the beginning of experiment. Equatorial region of the cell. Inverted kinety faces its neighbour with postciliary fibres. Arrows show orientation of kinetids. Note that interkinetal space is much wider than on Fig. 7 (x 26000). 7 - the same cell as on Fig. 6, inverted kinety faces its neighbour with transverse fibres. Arrows show the orientation of kinetids. Note that the interkinetal space is narrow, and no resorption of cilia can be found in the area (x 26000). 8 - the cell after 4 h of activation. Equatorial region of the cell arrested in pregamic division. Cell anterior is in the upper part of the photograph. Arrows show orientation of oralized kinetids. A toxicyst represent remnant of oral primordium (x 17500). o - oralized somatic kinetid, ok - oral kinetid, Pc - postciliary fibre, R - resorption of kinetids, sk - somatic kinetids, t - toxicyst, T - transverse fibre



ventral band, OFs run toward the midline of the band, then curve posteriorly (Fig. 2B). The left OFs are very long, and their curved distal parts form a stack of ribbons termed the central fibre (Figs. 2B, 11, 17). The right and cytostomal OFs are accompanied by perpendicular microtubules (p-microtubules), which represent a special category of microtubules anchored at subpellicular alveoli of oral field (Figs. 2, 17, 28). On the cytostomal field the p-microtubules not only accompany OFs, but also form a ring of bundles around the cytostome, termed the inner pharyngeal basket (Figs. 2, 11, 22, 28). The formation of the inner basket out of p-microtubules, was documented elsewhere (Golińska 1978). The outer margin of the cytostomal field is occupied by oral kinetids bearing the especially large Nds, which form a palisade of the outer basket. The inside of baskets is filled up with a specialized cytoplasm, called the phagoplasm, which contains numerous tubular vesicles intermingled with the loose ends of p-microtubules (Figs. 11, 28). The phagoplasm is deprived of the large endoplasmic organelles such as mitochondria, lipid granules, nuclei or food vacuoles.

Relationship between modifications of ciliary pattern and morphogenetic activity of cells

In *Dileptus* the rise in concentration of external potassium at first evokes ciliary reversal, lasting up to 20 seconds. Later on, in appropriate concentration of KCl, cells enter the adaptation period, and no ciliary reversal can be provoked by such stimuli as mechanical shock or mechanical injury. As shown by preliminary observations, the most useful concentration of KCl is 20 mM, since food uptake, regeneration and initiation of cell division was in this solution possible, while ciliary reversal was fully blocked. In 30 mM concentration the food intake was no longer possible, failed also the initiation of pregamic cell division. Moreover some percentage of cells in samples died during 24 h following the 30 mM KCl application. Concentrations of 5 or 10 mM KCl were not sufficient to block the ciliary reversal in all cells in a sample.

After 48 h of chronic KCl application ability to carry out the ciliary reversal was restored in many cells. During 24 h following KCl application also the active swimming of cells is restricted, and they simply lie down on the bottom of glass vessel and move around with their proboscis. Such cells can regenerate both oral and tail structures, can form complete oral primordia. Cells fission, however, is accomplished only occasionally, and oral primordia are usually resorbed.

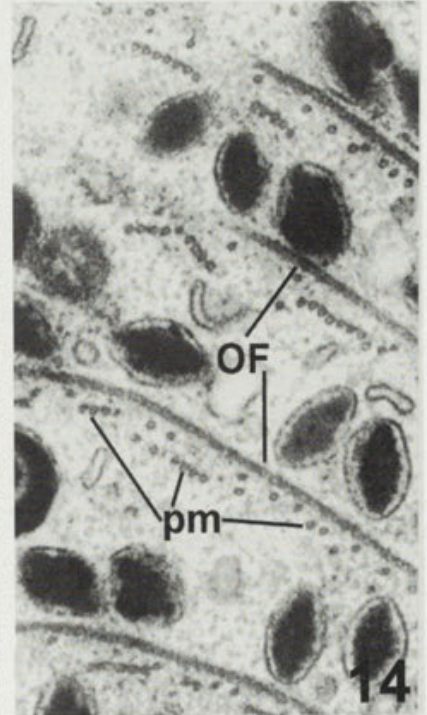
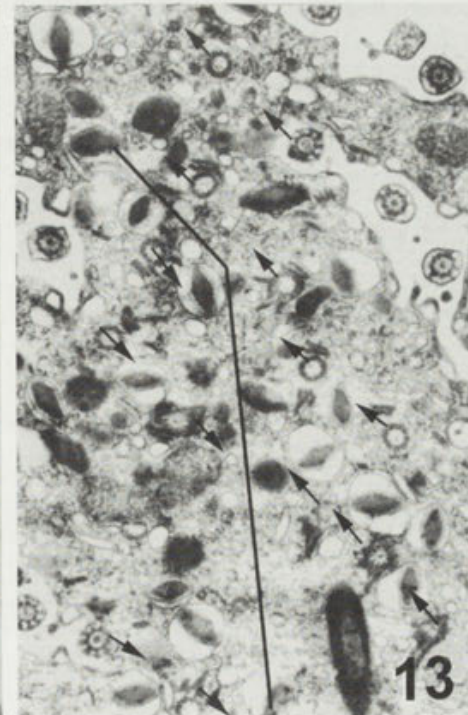
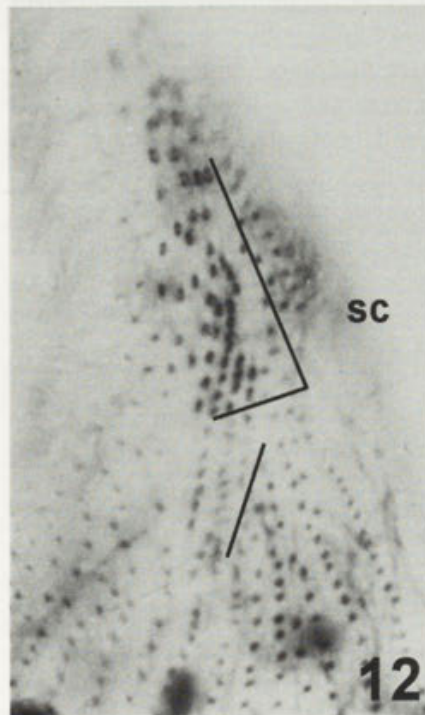
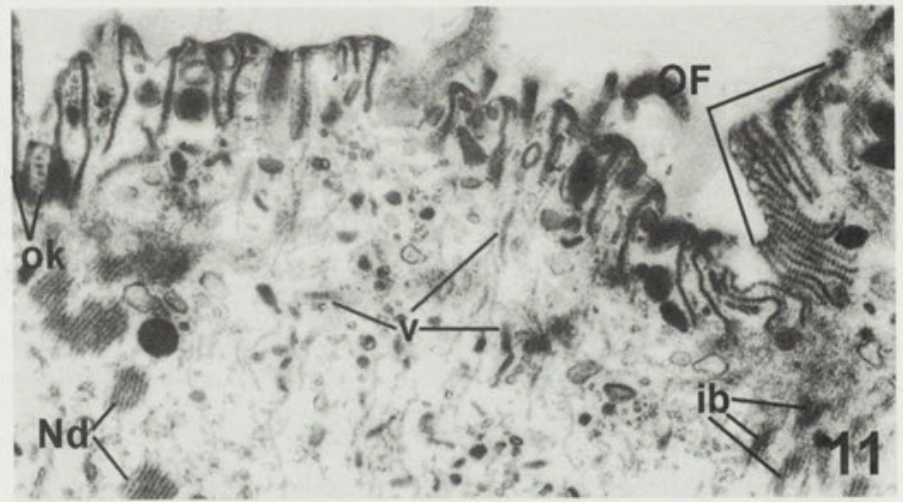
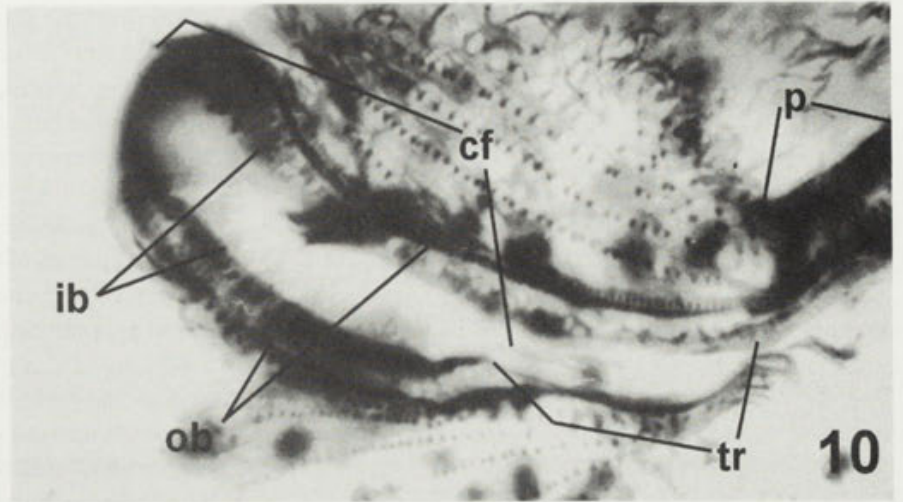
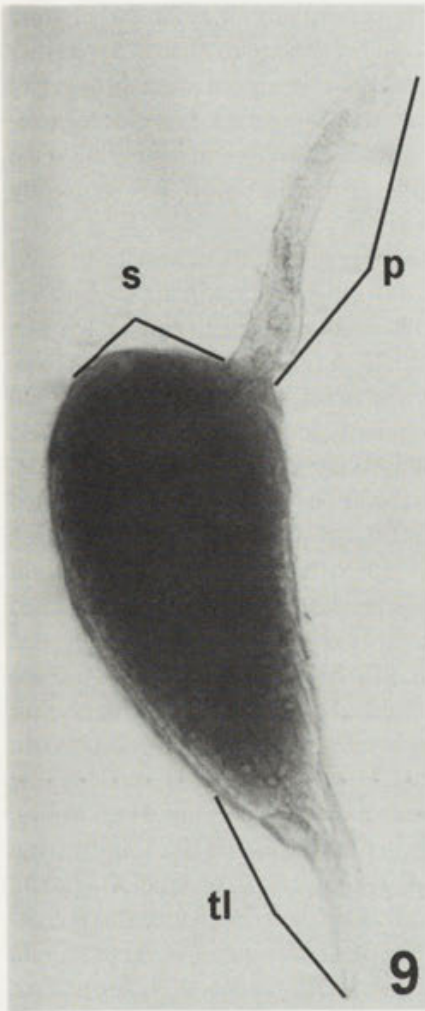
Modifications of the ciliary pattern evoked by 20 mM KCl in well-fed cells with intensely proliferating somatic kinetids are of two categories: firstly, supernumerary and inverted kinetids were found in the midbody region, representing a leftover of resorbed oral primordia. This modification was frequently encountered in activated cells: in 17% of cells ($n = 207$) fixed 24 h after the beginning of the experiment. In the group of growing cells such remnants of oral primordia were sometimes also found.

Another category of the modification in ciliary pattern was the rounding up of both posterior and anterior cell regions, accompanied with an increase in number of somatic kinetids on the rounded parts. Several types of this modification were named the humpbacked, astomous, and tailless cells.

The formation of supernumerary and inverted kinetids in the midbody region follows the inhibition of fission furrow development

In samples of the activated cells fixed 2.5 h after cell mixing, 46% of cells ($n = 33$) were found with oral primordia. On preparations made 5 h after the cell mixing, oral primordia in different stages of destruction were found in 16% of cells ($n = 170$). This indicates that between 2.5 and 5 h some of the dividing cells separate, and some of the early divisional primordia are resorbed without modifications to ciliary pattern. From 5 to 24 h after cell mixing, oral kinetids are completely resorbed, but disarrangement of pattern of somatic kinetids remains in

Figs. 9-14. Humpbacked *Dileptus margaritifer* cells found in samples of well-fed cells treated with 20 mM KCl. 9 - unstained cell fixed with saturated mercuric chloride after 24 h of KCl treatment. Note that the proboscis is very thin (x 2000). 10 - oral structure on protargol impregnated humpbacked cell after 24 h of experiment (orientation of the cell as in Fig. 9) suture is in the upper part of the photograph. Transformed part of ventral band, its cross section is shown on Fig. 11 (x 5000). 11 - cross section of transformed part of ventral band, 24 h after the beginning of experiment. Oral kinetids are dikinetids like on proboscis, but they bear large nematodesmata like at cytostomal field. Inner basket of microtubular bundles is arranged into single strand under a stack of oral fibres which on proboscis separates left and right portions of ventral band. Cytoplasm of this structure is deprived of toxicysts, contains few tubular vesicles characteristic of phagoplasm, and is penetrated by loose ends of p-microtubules (x 28000). 12 - the cell impregnated with protargol, 5 h after the beginning of experiment. The beginning of suture formation on dorsal side of proboscis. Heavy line shows place where about several somatic kinetids (x 6000). 13 - suture on humpbacked cell, 24 h after the beginning of experiment. Heavy line marks a border between two sets of kinetids which about the suture. Orientation of somatic kinetids is shown with arrows (x 21000). 14 - the cell fixed 2 h after the beginning of experiment. Right portion of ventral band, the beginning of its transformation into cytostomal field. Perpendicular microtubules assemble in unusually high number and form ribbons, later on arranged into bundles of inner basket (x 56500). cf - cytostomal field, ib - inner pharyngeal basket, Nd - nematodesma, ob - outer pharyngeal basket, OF - oral fibre, ok - oral kinetid, p - proboscis, pm - perpendicular microtubules, s - suture, tl - tail, tr - transformed part of ventral band, sc - group of sensory cilia, separated from their parental kinetids, v - tubular vesicles



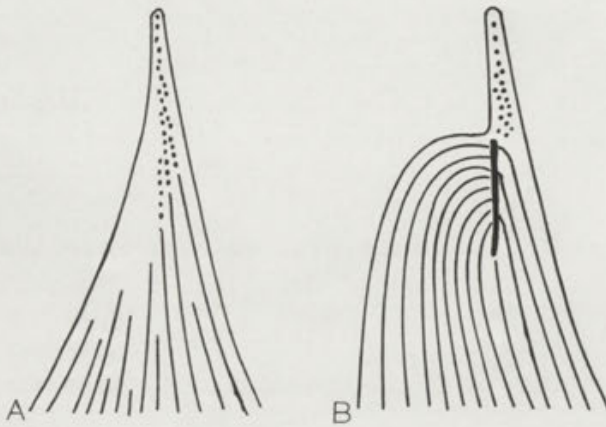


Fig. 15. Schematic representation of ciliary pattern on dorsal side in **A** normal, and **B** humpbacked cell. Dots represent pairs of sensory cilia, lines are somatic kinetids, black bar represents suture

midbody regions of 17% of large cells, probably the same cells which had oral primordia in 5th hour samples.

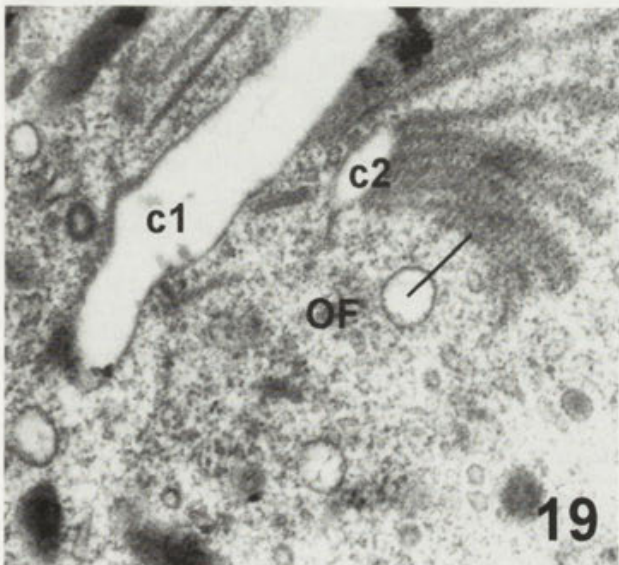
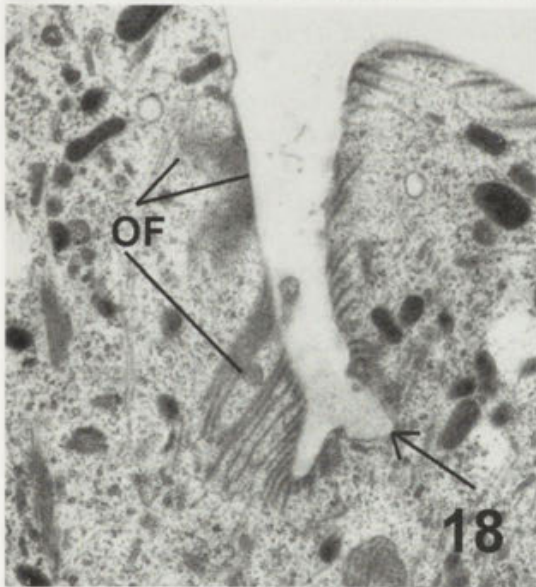
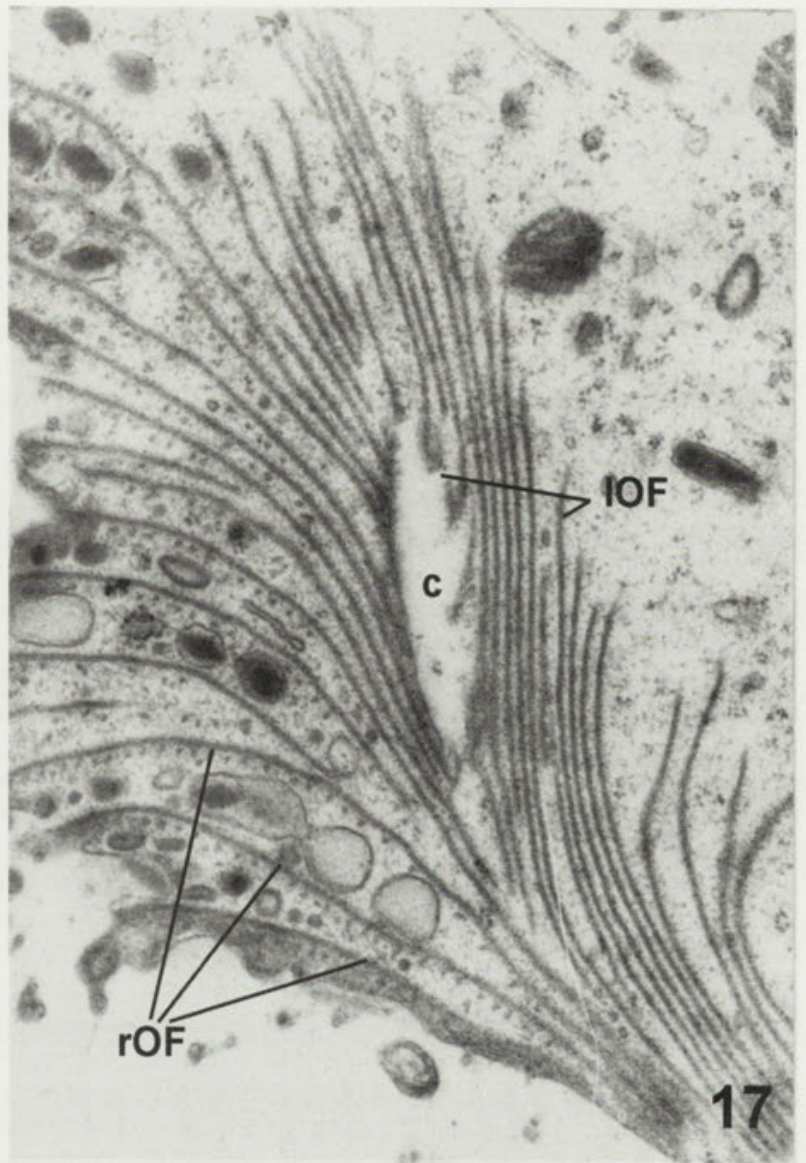
On preparations made 4 or 5 h after KCl application, both the well developed oral primordia were found (Fig. 3), and the images of their destruction (Fig. 5). Oral primordia formed by cells in the presence of elevated potassium are structurally not different from the normal ones. Remarkable difference lies in the presence or absence of resorption of somatic kinetids in front of fission line, on the territory destined to develop into the tail of anterior daughter. The appearance of oral primordia is always preceded by proliferation of somatic kinetids over the cylindrical part of the *Dileptus* body. This proliferation may be weak in small cells, and is always intense in large cells. The proliferation of somatic kinetids in normal medium lasts until the oral primordia develop into continuous structure around the cell body. Later on, in normal medium, the proliferation in front of fission line ceases and is replaced by resorption of somatic kinetids which precede and accompany the constriction of fission furrow. On protargol impregnated preparations the resorption can be observed as a shortening of some of the somatic kinetids in front of the fission line, and represents the beginning of tail formation for the anterior daughter. In elevated external potassium the proliferation of somatic kinetids around

oral primordia proceeds normally. It is the switch from proliferation to resorption processes that is apparently blocked in the presence of elevated potassium. In protargol impregnated preparations all somatic kinetids of the anterior daughter always reach down to oral primordia of the oral primordia, while the proliferation was frequently encountered there.

Oral kinetids of disintegrating oral primordia are invariably resorbed. The oralized somatic kinetids, which accompany oral kinetids in advanced primordia (Golińska 1995) are at last partially left on the cortex in midbody region, and apparently give rise to the supernumerary and inverted kinetids commonly found on preparations made 24 h of KCl treatment of activated cells (Figs. 4, 6, 7). There are several observations that confirm the origin of the supernumerary and inverted kinetids out of the oralized somatic kinetids. It is known that during cell division oral primordia on the dorsal and left cell sides are accompanied by oralized kinetids, formed from the bent and separated segments of somatic kinetids (Golińska 1995), and the number of the short oralized kinetids is always higher than the number of their parental somatic kinetids (Fig. 3). In cells treated with elevated potassium, the typical remnants of fission line are the numerous supernumerary kinetids, all extending posteriorly from the fission line (Fig. 4), some of them are inverted. The inversion of kinetofragments may result from distortions in their orientation that accompanies and follows the disappearance of oral primordia (Fig. 8). Later on, the kinetofragments elongate and are introduced into pattern of longitudinal kinetids, both in proper and in inverted configuration (Fig. 4).

Interesting features of ciliary pattern with inverted kinetids concerns spatial relations between the inverted kinetids and their normally orientated neighbours. When the inverted kinetid faces its neighbour with T fibres of its kinetids (Fig. 7), the interkinetal stripe is narrow and no resorption of kinetids occurs in the area. When, however, the interkinetal stripe contains double number of oppositely orientated Pc fibres (Fig. 6), the stripe is wide and a resorption of kinetids proceeds in vicinity, as visualized by the presence of numerous ciliary shafts withdrawn under the cell surface. It is not known whether the observed resorption may lead to an elimination of inverted

Figs. 16-20. Distortions of cytotomal depression under the influence of 20 mM KCl in *Dileptus margaritifer*. 16 - well-fed cell fixed 4 h after the beginning of experiment. Almost normally shaped cytotomal depression (x 34500). 17 - humpbacked well-fed cell, fixed 24 h after the beginning of experiment. Fissure-shaped depression on elongated cytotomal field. The depression is on one side flanked with left oral fibres, on the other by right oral fibres. Note the presence of p-microtubules along right oral fibres (x 40000). 18 - well-fed cell, 4 h after the beginning of experiment. Cross section of fissure-like depression. Oral fibres support walls of the depression, and small invaginations (arrow) may form inside the fissure (x 21000). 19 - well-fed cell, 24 h after the beginning of experiment. Cross section of fissure-like depression. Invaginations of fissure wall are also lined up with oral fibres (x 39500). 20 - the cell fixed 5 h after the beginning of activation. Cytostome-like structure on nearly destroyed cytotomal field in forming astomous cell. This probably is not the original cytotome, rather the place where numerous oral fibres happen to descend into cytoplasm (x 55500). c - cytotome, c1 - fissure-like depression, c2 - fissure wall, OF - oral fibres, l OF - left oral fibres, r OF - right oral fibres



kinety, since the modified ciliary pattern was observed no longer than 24 h after KCl application.

Formation of humpbacked cells

Another modification of ciliary pattern frequently found in KCl treated cells was formation of a humpback: the large convexity on the dorsal side of the cell, at the level of cytostomal field (Fig. 9). This deformation is not a specific one for 20 mM potassium, since it can be found whenever culture conditions are unfavourable, although in this case the percentage of disfigured cells is rather low. In elevated external concentration of potassium ions, the humpbacked cells were found both among the well-fed cells (24%, $n = 125$), and among the activated cells (60%, $n = 204$). In samples containing regenerating or starving cells, no humpbacks were formed.

The oral apparatus of a humpbacked cell is disfigured. Instead of a circular cytostomal field at the base of proboscis (Fig. 1), there is the transversely elongated oral field situated at the base of humpback (Fig. 10). The oral field terminates at a very narrow proboscis (Fig. 9). Usually the elongated oral field is twisted toward the right side and its anterior margin is in prolongation to right margin of ventral band on proboscis (Fig. 10) while the posterior margin merges with the left margin of ventral band. Sometimes, however, the oral field is twisted in the opposite way, the anterior border of oral field merging with the left margin of ventral band.

The elongated oral field of humpbacked cell is not equivalent to the circular cytostomal field, so far as its fine structure is considered. The part of elongated field closest to proboscis resembles the ventral band, because there are dikinetids at both its margins, and the central fibre usually separates left from right portion of the structure (Figs. 11, 17). This part of elongated field resembles also a cytostomal field, since the Nds at its oral dikinetids are much larger than those found on proboscis (Fig. 11, in normal proboscis bear several microtubules per Nd: Golińska 1991). Also the toxicysts are absent in right half of this structure (Figs. 11, 17). Moreover, p-microtubules during early stages of the humpback formation multiply in

this region, at first producing ribbons (Fig. 14), which later on are rearranged into bundles (Fig. 11). Usually, such bundles form the ring of inner pharyngeal basket (Fig. 2), but in this part of the elongated field no circular basket is present, rather a single strand of bundles extends just under the central fibre (Fig. 11).

The oral parts located further away from proboscis, structurally represent a true cytostomal field, although rather ovoid than circular in shape (Fig. 10). There are monokinetids at its margin, and the inner pharyngeal basket repeats outline of the outer basket (Fig. 10). The elongated oral fields contain numerous p-microtubules in their phagoplasm, but they almost totally lack the tubular vesicles (Figs. 11, 17-19). The cytostome, which on circular cytostomal field is a single permanent depression (Fig. 16) on the elongated field is represented by series of fissures in the places where converge OFs coming from opposite directions (Figs. 17-19). Inside of the fissures may form additional depressions (Figs. 18, 19). It is not clear whether such "cytostome" might function, since the humpbacked cells were never observed to swallow the prey.

The structure of the ventral band on proboscis of humpbacked cell does not structurally differ from that in the normal cell. The proboscis of humpbacked cell resembles the distal portion of normal proboscis, since its ciliature consists of oral, oralized and sensory kinetids, but no ordinary somatic kinetids can be found there (Figs. 9, 10). Structure of the narrow proboscis and structure of the elongated oral field allows to suppose that during the humpback formation the basal part of normal proboscis enlarges into the humpback, while its ventral band undergoes transformation into a part of the oral field. Further confirmation of such origin of the humpback is provided by the observations on patterning of somatic kineties in the humpback area.

Pattern of somatic kinetids on the dorsal side of normally shaped proboscis resembles the pattern on cell posterior, since in both tapered regions the somatic kineties approaching each other contain kinetids scattered further apart. Kineties end at different levels of the tapered region

Figs. 21-27. *Dileptus margaritifer* astomous cells and their formation in samples of cells activated in the presence of 20 mM KCl. 21 - unstained cell, fixed with mercuric chloride after 24 h of activation. Normally proportioned cell (x 2500). 22 - protargol impregnated cell after 5 h of activation. Beginning of destruction of cytostomal field. 5 h. Protargol impregnation. Inner pharyngeal basket is complete, although elongated toward the anterior pole. Outer basket is disrupted into several parts (arrows). Oralized kinetids are separated from their kineties and do not parallel row of oral kinetids (x 5500). 23 - protargol impregnated cell after 5 h of activation. Advanced stage of destruction of oral parts. Inner pharyngeal basket is not discernible and parts of outer basket are dislocated (x 5500). 24 - protargol impregnated cell after 5 h of activation. Remnant of cytostomal field with few oral kinetids. This is the last trace of oral apparatus, since proboscis is already resorbed (x 5500). 25 - protargol impregnated cell after 24 h of activation. Anterior part of astomous cell. The only remnant of cytostomal field is an area deprived of cilia (x 5000). 26 - unstained cell fixed with mercuric chloride after 24 h of activation. This cell is astomous and tailless (x 2000). 27 - protargol impregnated cell after 5 h of activation. Remnant of proboscis left on astomous cell. Structures of cytostomal field are completely resorbed. Note that somatic kineties curve toward the suture (x 7000). cf - cytostomal field, ib - inner pharyngeal basket, o - oralized somatic kinetid, ob - outer pharyngeal basket, p - proboscis, s - approximate location of suture, tl - tail

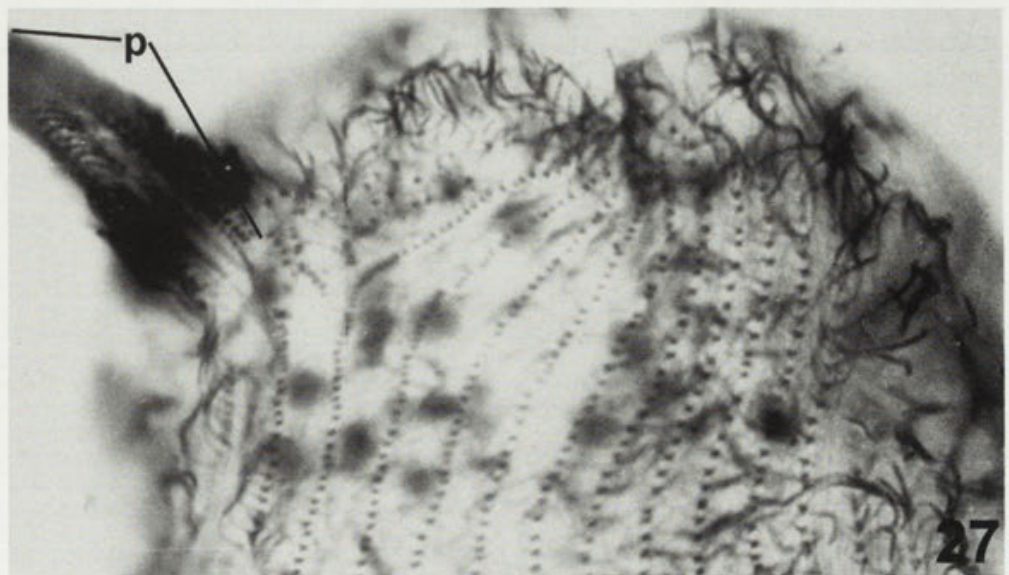
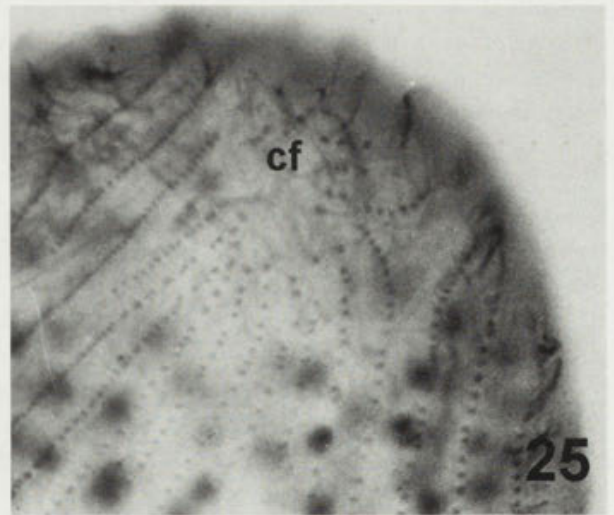
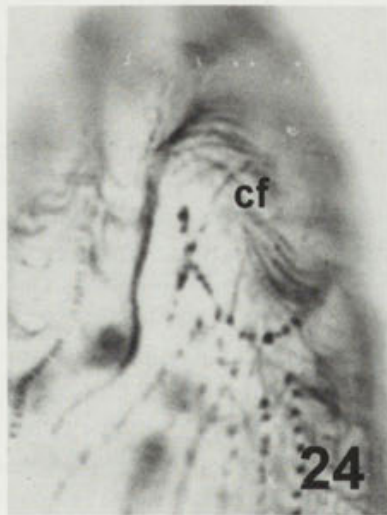
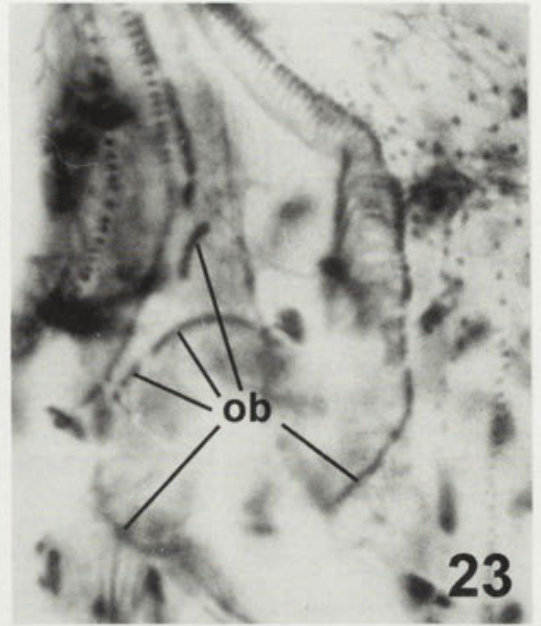
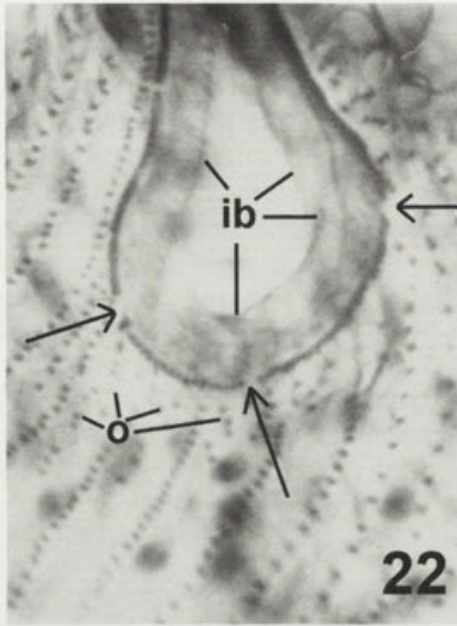
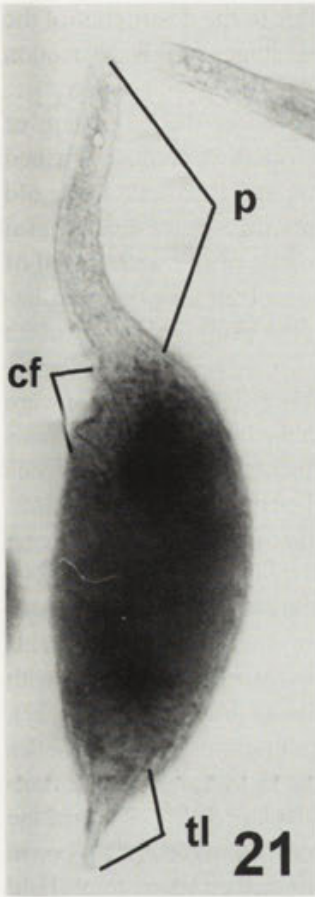


(Fig. 15A), and most of them do not reach the basal part of proboscis. During formation of a humpback, at first cells still have the normal oral structure and already swollen basal part of proboscis (Fig. 12). On the swollen region pattern of somatic kineties is changed, since the once shorter kineties elongate and enter the swollen region. The intense proliferation of somatic kinetids was found on swollen region in preparations made 5 h after KCl application. Well developed humpback is the place where end all the somatic kineties (Fig. 15B), except the kineties which abut the cytostomal field. Somatic kineties coming from right and left sides of the cell meet at a kind of suture, running on the top of humpback from proboscis toward the dorsal side (Figs. 9, 13, 15B). No sensory cilia are present along the suture, they all are crowded on the proboscis.

In humpbacks fixed 24 h after KCl application the proliferation of somatic kinetids is weak or absent. Presumably, all the somatic kineties are already prolonged up to the suture area. It is proposed that the unusual elongation of somatic kineties leads both to the humpback formation and to distortions of the oral structure.

Appearance of astomous cells

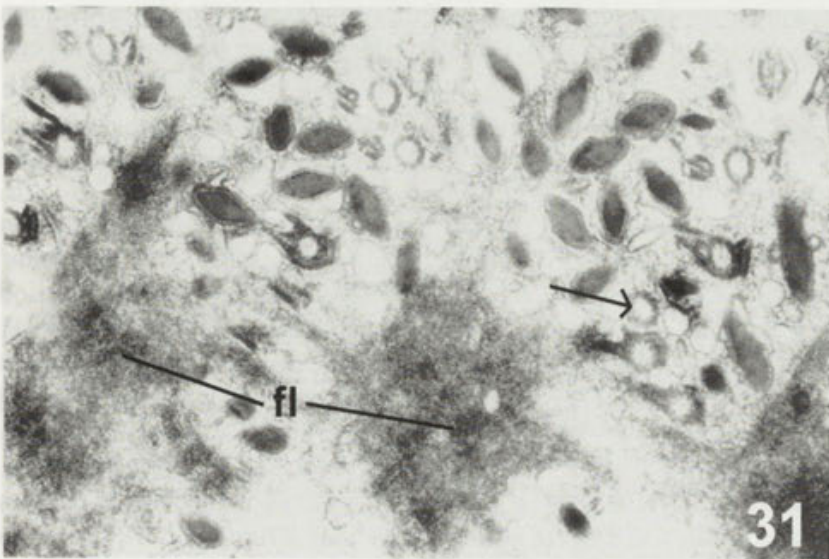
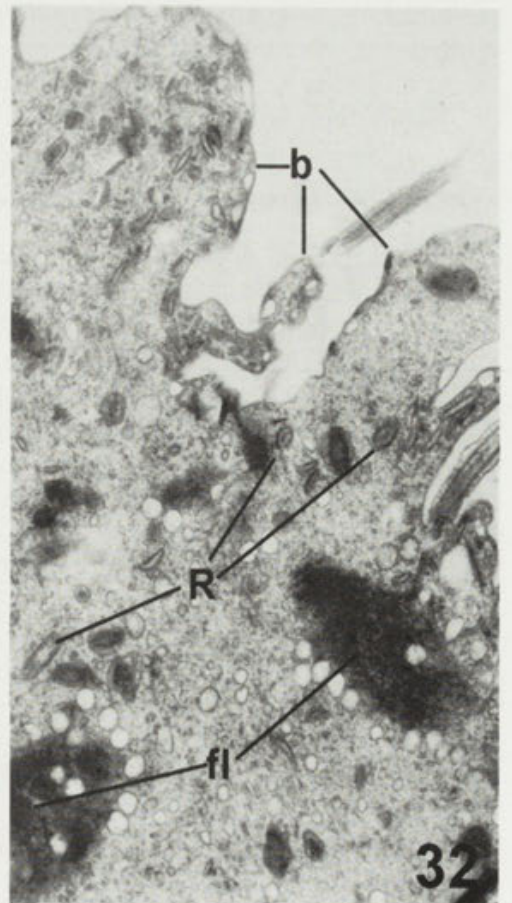
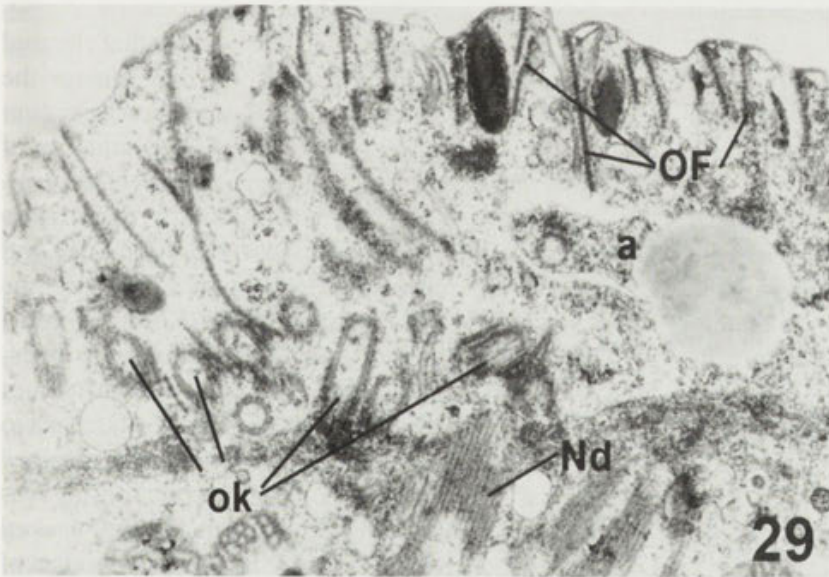
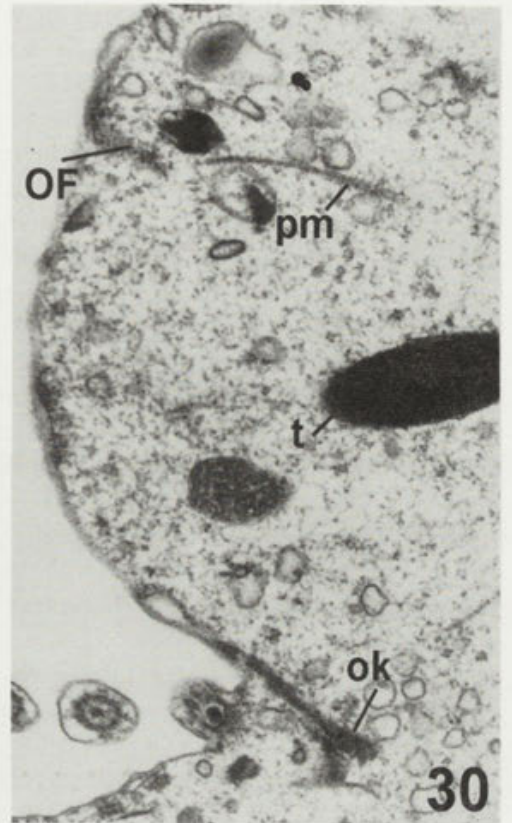
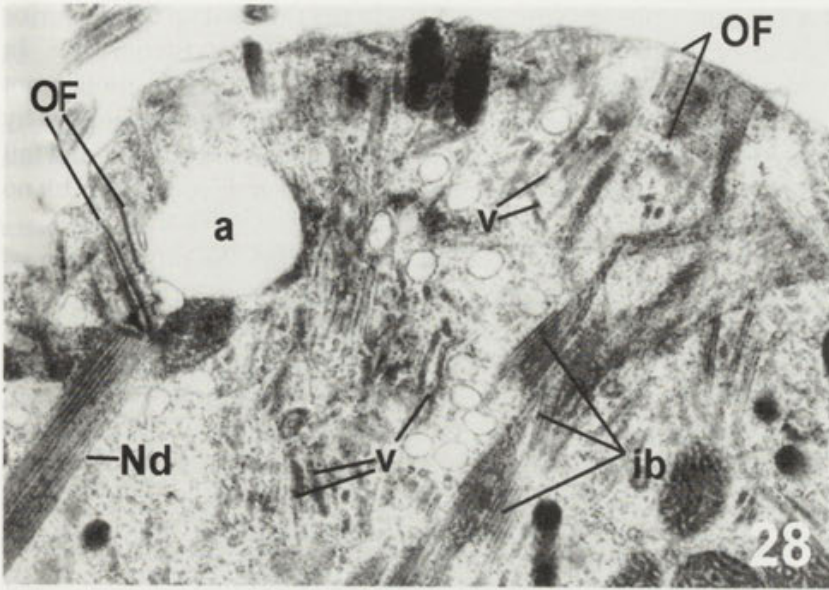
The second observed effect of 20 mM KCl upon the mature oral structure is its complete resorption. The anterior pole of an astomous cell is rounded up (Fig. 25), and resembles the humpback of humpbacked cell, since it is the place where all somatic kineties meet at a suture (Figs. 25, 31). The number of kineties in an astomous cell does not differ from the number of kineties on cells of normal appearance found on the same preparation slide. The astomous cells were produced only in samples of the activated cells. Astomous cells were never seen in samples of the well-fed cells and in cultures under unfavourable conditions (when humpbacks were forming). Astomous were always the large cells in a sample, many of them with traces of the fission line in the equatorial region. This indicates that the lack of oral apparatus is not due to abortive division (i.e. by separation of the astomous

posterior daughter), but it is due to the destruction of the mature oral apparatus. Several stages of this destruction were observed.

On preparations made 2 h after the beginning of activation, the only changes found were those ascribed to the oncoming conjugation, and localized in the old oral structure. These changes take place in the basal part of ventral band, and consist of the withdrawal of toxicysts and the appearance of an empty space between right and left halves of the ventral band (Golińska and Afon'kin 1993).

On preparations made after 5 h of activation were found both changes leading to the formation of astomous cells, and the astomous cells themselves. Two sequences are possible during the destruction of oral apparatus. Sometimes it is the proboscis that disappears first, leaving for some time the remnants of cytostomal field (Fig. 24). In other specimens, the remnants of proboscis last longer on cells already deprived of their cytostomal fields (Fig. 27). Destruction of the cytostomal field starts with disruptions in the circumoral row of oral kinetids (Fig. 22), and separation of the bent endings of somatic kineties from the margin of cytostomal field. Later on, the fragments of oral row are often displaced (Fig. 23), and the inner pharyngeal basket disappears completely. As seen in electron microscope, the destruction of cytostomal field starts with the appearance of autophagic vacuoles inside of phagoplasm (Figs. 28, 29). The content of autophagic vacuoles are often lipid droplets, easily washed out during the preparatory procedures (Fig. 28). Alongside to the formation of autophagic vacuoles, tubular vesicles and p-microtubules disappear from the phagoplasm (Fig. 31), until the remnants of a basket are filled up with scattered fibro-granular material, penetrated by a few p-microtubules. The disappearance of phagoplasm is accompanied by destruction of the oral kinetids of cytostomal field (Fig. 29). Basal bodies of the kinetids become tilted and displaced, their OFs pointing in different directions. Under the surface of cytostomal field, in places where converge OFs coming from different directions, form small addi-

Figs. 28-32. *Dileptus margaritifer* fine structure of astomous cells formed in the presence of 20 mM KCl. 28 - the cell fixed after 3 h of activation. Pharyngeal basket of almost normal appearance. Oral kinetid bearing its nematodesma and oral fibre is in its proper place and orientation. Tubular vesicles are still numerous between p-microtubules. Microtubular bundles of inner basket are, however, separated from cell surface, and autophagic vacuoles, appear in phagoplasma (x 21000). 29 - the cell fixed after 4 h of activation. Advanced stage of basket destruction. Oral kinetids are tilted and displaced, thus may point with oral fibres in different directions. Autophagic vacuoles are still present in the phagoplasm, p-microtubules and tubular vesicles become scarce. Nd - nematodesma (x 29000). 30 - the cell fixed after 4 h of activation. Almost destroyed basket: oral kinetids are scarce, and few oral fibres can be found under the surface of oral convexity. Tubular vesicles are absent, p-microtubules can be sometimes found. Toxicysts often invade the territory (x 27500). 31 - the cell fixed after 24 h of activation. Somatic kineties close to suture, which is situated in the upper part of the photograph. Filamentous layer that normally separates ecto- and endoplasm in *Dileptus* of this region is arranged into longitudinal strands. An arrow indicates new basal body, thus the proliferation of somatic kinetids proceed in the area (x 20000). 32 - the cell fixed after 24 h of activation. Remnant of oral structure on astomous cell, corresponding to nonciliated area on Fig. 25. The surface of the area is folded, presenting bulges of different size. Somatic kinetids are still resorbed in the area. Filamentous material is arranged into compact masses (x 14000). a - autophagic vacuole, b - nonciliated bulge, fl - filamentous layer, ib - inner pharyngeal basket, Nd - nematodesma, pm - perpendicular microtubule, OF - oral fibre, ok - oral kinetids, R - resorption of kinetids, t - toxicyst, v - tubular vesicles



tional "cytostomes" (Fig. 20), which are rather the temporary structures. The final stage in destruction of a cytostomal field is a series of blebs (Fig. 32), covered with the cell membrane which is underlined by alveoli but deprived of microtubular arrays. In vicinity of blebs, numerous cilia can be found under the cell surface of astomous cells, indicating that some somatic kineties are also resorbed after the oral structure is destroyed. The area of blebs remains in continuity to the suture of somatic kineties (Fig. 25).

In the anterior part of astomous cell the filamentous layer (which separates ecto- and endoplasm in *Dileptus*), becomes especially thickened along the somatic kineties (Fig. 30), and clusters into large compact masses in vicinity of blebs (Fig. 32). Similar large clusters of filamentous material were observed during destruction of oral structure in the encysting cells (Kink 1973), and were interpreted as the remnants of proboscis. The formation of clusters indicate that the filaments are not immediately resorbed, but rather are kept in storage. There is no evidence, however, whether this material could be reused by the cell.

The somatic kineties close to the suture are often of wavy appearance, since many of their kineties are situated out of the line (Fig. 10). Both the proliferation and the resorption of somatic kinetids is often seen on the region, even after 24 h of KCl application, suggesting instability of ciliary pattern close to the anterior pole in an astomous cell.

Modifications of ciliary pattern on the cell posterior

In normal cell of *Dileptus* the cell posterior is tapered ending with a slender tail (Figs. 1, 21). Somatic kineties on the narrowing part end at different distances from the tip of the tail, and their kinetids become scattered until it is hard to distinguish which kinety continues and which does not.

Under the influence of 20 mM KCl, the cell posterior becomes rounded up in many astomous (Fig. 25) and humpback cells. This abnormality is not specific for the potassium influence, because it is sometimes found in the humpbacked cells formed in standard culture medium under unfavourable conditions, and was observed in advanced stages of conjugation (Golińska and Afon'kin 1993). In elevated external potassium both humpbacked and astomous cells may have either the tapered or the rounded up posterior. Cells with normal anterior parts invariably have the normally tapered tail.

The rounded up posterior is similar to the humpback region, because it represents an orientation centre for

the somatic kinetids. On the rounded up cell posterior all the somatic kineties reach the posterior pole. In contrast to the humpback region, the pole itself is not suture-like but circular in shape, and it is often marked by a small convexity which resembles the tip of normal tail (Fig. 26). Numerous Pc fibres enter this convexity, but no kinetids can be found there.

On the rounded up posteriors the proliferation of somatic kinetids was frequently seen, in contrast to the tapered region of normal tail where no proliferation was ever encountered. Resorption of somatic kinetids was often observed in the tapered region of normal tail, while on the rounded up posteriors it was rather exceptional.

DISCUSSION

The observations presented above show that elevated concentration of external potassium may change the distribution of proliferation and resorption processes over the cell body in *Dileptus margaritifer*. The induction of proliferation of somatic kinetids spreads over cell extremities, where it is usually inhibited resulting in rounding up of polar regions. Similarly, a partial resorption of the oral structure in cells activated to conjugation spreads over the whole structure, resulting in formation of astomous cells.

Three main discussion topics emerge from this investigation. Firstly, the way in which potassium influences ciliates other than *Dileptus* and metazoan cells, needs to be recalled here and compared with the results obtained in this study. Secondly, an interesting relationship was found in this study between the maintenance of tapered form of cell extremities, and inhibition of proliferation of somatic kinetids, in these regions. Thirdly, a question arises whether a suture found on a rounded up cell anterior, has its counterpart in normal cells of *Dileptus*.

Consequences of chronic exposure to elevated external potassium concentration for ciliate and metazoan cells

Application of elevated concentration of potassium ions, first evokes hyperpolarization of cell membrane (ciliary reversal), later on followed by adaptation period when cell membrane is unable to generate action potential. Cell membrane during adaptation is depolarized both in ciliates (Schusterman et al. 1978, Dryl and Hildebrand 1979, Machemer 1989) and in metazoan cells (Chalazonitis and Fischbach 1980, Anqlister et al. 1982, Unsicker et al. 1983). This depolarization was ascribed either to changes in Ca^{2+} channels (Dryl and Hildebrand 1979), or to

increase in permeability to K^+ ions that tends to short-circuit the Ca^{2+} action current (Schusterman et al. 1978). Cells of *Dileptus* when in elevated potassium are also depolarized, because no ciliary reversal follows such stimuli like mechanical shock or mechanical injury to the cell.

In metazoan cells the influence of chronic rise in external potassium is best known for neurons. Generally, elevated external potassium improves both survival and differentiation of neurons (Lasher and Zagon 1972, Bennett and White 1979). Neurons grown in elevated potassium were depolarized and could not be excited with depolarizing current pulses (Chalazonitis and Fischbach 1980). Moreover, the shape of depolarized neurons was changed, since the area of growth cones was markedly increased (Anglister et al. 1982). In chromaffin cells, chronic depolarization induces the formation of neurite-like processes (Unsicker et al. 1983). The latter report indicates that in depolarized cells some inhibition that normally prevents neurite formation, becomes released.

For comparison with *Dileptus*, this release from inhibition is especially interesting, because the formation of the humpbacked, astomous and tailless cells can be explained as release from inhibition. In the case of *Dileptus* the inhibition concerns spreading of proliferation of somatic kinetids over the tapered cell extremities, or spreading of resorption of some oral structures over the whole oral apparatus (in astomous cells). Elevated concentration of potassium ions abolishes also the inhibition of kinetid proliferation in front of fission line, and inhibits resorption of oralized somatic kinetids during resorption of oral primordia.

What kind of relationship might exist between the depolarization of cell membrane and destruction of inhibition-activation pattern on cell cortex, remains unclear. An exciting possibility is nonuniform deployment of electric potentials along the cell membrane. In *Paramecium* it was found that the receptor potentials due to activated Ca and K mechanoreceptor channels, distribute over the cell surface in the manner of overlapping antero-posterior gradients (Ogura and Machemer 1980). In neurons, it was found that the intramembrane potential gradient is more positive in membranes of neurites than in membranes of somata (Bedlack et al. 1994). Membrane potential in highly integrated layer of cells in intestinal villi, was found to be the highest in cells at the top of a villus, and the lowest near the crypt region (Tsuchiya and Okada 1982). It cannot be excluded that in *Dileptus* membrane potential for proboscis and tail is different from that on cell body, allowing the segregation of activated and inhibited cell regions. Remains unclear, however, why a map of mor-

phogenetic activities is never abolished in small activated cells (forming oral primordia), but only in large ones. This does not allow to expect some simple relationship between the depolarization of cell membrane and maintenance (or formation) of cortical map of morphogenetic activities.

Inhibition of proliferation of somatic kinetids as prerequisite for the formation and maintenance of tapered cell extremities

Timing and distribution of proliferation and resorption of somatic kinetids are similar on the tapered regions of proboscis and of tail. The process of tail tapering is, however, easier to follow than the tapering of proboscis, because of lack of oral structures in the region of tail. Thus only the tapering of tail will be further discussed.

The tapering of cell posterior can be easily inhibited when it takes place during division of large cells, but it is hard to prevent during division of small cells and during regeneration. Regeneration of the tapered tail was so far inhibited only by puromycin (Golińska 1974), while other factors studied like Actinomycin D (Golińska and Bohatier 1975), or high concentration of potassium ions, may prevent tail formation during division but do not prevent the regeneration of tail. This difference in the sensitivity of tail tapering during regeneration and division, could be explained as a difference in feasibility of special preconditions for the tapering to occur in cortices of regenerating and of dividing cells of *Dileptus*.

During regeneration, the first reaction to transection in *Dileptus* is the resorption of somatic kinetids in wound vicinity, both at anterior and at posterior poles (Golińska and Grain 1969, Golińska and Kink 1977). Narrowing and elongation of the regenerating tail proceeds in the absence of proliferation of somatic kinetids, while their resorption is often encountered (Golińska 1991). Thus the tail tapering during regeneration starts and proceeds on a cortex where the proliferation of somatic kinetids is inhibited.

In cells dividing in ordinary culture medium, during the early stages of development proliferation of somatic kinetids proceeds in front of the fission line. During advanced stages of development of oral primordia, the proliferation in front of fission line becomes inhibited and replaced by the resorption of somatic kinetids. This switch from proliferation to resorption occurs before the fission line constriction, i.e. before the tapering of the posterior part of anterior daughter. When cells divide in the presence of elevated potassium, no resorption occurs in front of the fully developed oral primordia, while the proliferation of somatic kinetids is frequently seen. These observations strongly indicate that the inhibition of proliferation of

somatic kinetids (and/or induction of their resorption), is necessary for the tail tapering for anterior daughter to occur. The presented analysis of tail tapering in the dividing and regenerating cells shows that the exceptional sensitivity of cytokinesis in *Dileptus* to unfavourable factors may be due to the difficulty in setting in the inhibition of kinetid proliferation in the cortex where intense proliferation is under way. This is further confirmed by the observation that a weak proliferation of somatic kinetids in small dividing cells may fail to prevent cytokinesis in the presence of elevated potassium.

The difficulty to switch from proliferation to resorption in cells dividing in elevated potassium concentration, is not restricted to the somatic kinetids in front of a fission line. Just behind oral kinetids form the somatic kinetids of special category, termed the oralized somatic kinetids (Golińska 1995). These kinetids originate from somatic kineties, separate from them and arrange into multiple kinetofragments. When development of oral primordia is blocked in the potassium-treated cells, all oral kinetids are resorbed leaving the oralized kinetids arranged into additional somatic kineties, some of them in the reverse orientation. This was not observed in cells treated with Actinomycin D (Golińska and Bohatier 1975), and seems to represent the specific effect of elevated potassium on dividing cells of *Dileptus*.

As found in this study, the presence of elevated potassium hampers not only the switch from proliferation to resorption of somatic kinetids, but also the maintenance of tapered cell extremities. This leads to the formation of humpbacked and tailless cells. It is significant that the both deformities were found only in large cells, often with traces of fission line in midbody area, always with somatic kinetids proliferating everywhere on the cell body. Thus the proliferation may spread over the once-tapered cell extremities when it is sufficiently intense. These observations suggest that in a normal cell some barrier separates the area where somatic kinetids proliferate (mostly the midbody region) from the area where kinetids do not proliferate and are frequently resorbed (tapered parts). The elevated concentration of external potassium could intensify a signal for proliferation, in large cells leading either to the destruction of already existing barrier, or to prevention of its formation.

Orientation centre for somatic kinetids of *Dileptus margaritifer* in normal and disfigured cells

The main change resulting from the formation of astomous and humpbacked cells lies in the relationship between the anterior cell pole (as appointed by cell geometry) and the position of the anterior orientation

centre for somatic kineties. In normal cell of *Dileptus* the orientation centre for somatic kinetids seems to reside in the distalmost part of proboscis, which is also the anterior cell pole. During formation of humpback, an increase in the number of somatic kinetids reveals, however, the presence of a suture on dorsal side of basal part of proboscis. This suture extends from the top of a humpback down to the base of proboscis, and is not designated by any structural landmarks other than the orientation of somatic kinetids. The emerging pattern strongly resembles pattern around the anterior suture in *Paramecium* (Iftode et al. 1989), where all the somatic kineties abut either the suture or the anterior pole of the cell. Proboscis of *Dileptus* in such pattern would represent a part of oral structure emerging from the ventral side of the cell.

The elongated form of an anterior suture in *Dileptus* can be explained through mode of its formation during the cell fission. Somatic kineties posterior to oral primordia show a lateral gradient in intensity of basal body proliferation (Golińska 1995). Few (3 or 4) kineties on right side of the cell contain intensely proliferating kinetids. On a humpback, these kineties reach the right side of the suture. Several kineties on the ventral side show not-so-intense proliferation of their kinetids, while the majority of kineties on the dorsal and left sides contain very weakly proliferating kinetids. All the dorsal and left kineties reach the left side of the suture, while in normally shaped cell only few of these kineties continue on the basal part of proboscis. Thus the left and dorsal sides of the forming proboscis are ciliated by a majority of kineties but by relatively few kinetids, which allows for the symmetric shaping of proboscis in spite of asymmetric distribution of kinetid proliferation. Anyway, this asymmetry is apparently responsible for the elongated form of anterior suture, when numerous kineties of dorsal and left sides come to reach one side of the suture.

This is further confirmed by ciliary pattern found on the cell posterior in tailless cells. There is no lateral gradient in proliferation of somatic kinetids during rounding up of the cell posterior, and no suture forms at the posterior cell pole in tailless cells.

The comparison of the normal and humpbacked cells leads to a supposition that in the normal cell an orientation centre for somatic kinetids is situated not at the distal point of the proboscis, but that the invisible suture extends between the narrow distal part of proboscis and its wide basal part, along the endings of somatic kineties of the right side. In more general terms, the orientation centre for somatic kinetids of *Dileptus* is not identical with the anterior cell pole.

Acknowledgements. Author is very grateful to Dr Jerzy Sikora for special care on editorial matters concerning the manuscript (that is the last one written by the Author), and to Mrs Katarzyna Muszyńska for expert technical assistance. Financial support for this investigation was supported by a grant No 6P20406004 from the State Committee for Scientific Research to the Nencki Institute of Experimental Biology, Polish Academy of Sciences.

REFERENCES

- Anglister L., Farber I. C., Shahar A. and Grinvald A. (1982) Localization of voltage-sensitive channels along developing neurites: their possible role in regulating neurite elongation. *Dev. Biol.* **94**: 351-365
- Bedlack R. S., Wei M.-d., Fox S. H., Gross E. and Loew L. M. (1994) Distinct electric potentials in soma and neurite membranes. *Neuron* **13**: 1187-1193
- Bennett M. R., White W. (1979) The survival and development of cholinergic neurons in potassium-enriched media. *Brain Res.* **173**: 549-553
- Chalazonitis A., Fischbach G. D. (1980) Elevated potassium induces morphological differentiation of dorsal root ganglionic neurons in dissociated cell culture. *Dev. Biol.* **78**: 173-183
- Dragesco J. (1962) L'orientation actuelle de la systématique des Ciliés et la technique d'imprégnation au protéinate d'argent. *Bull. Microsc. Appl.* **11**: 49-58
- Dryl S., Hildebrand E. (1979) Modifying effects of chemical factors on behavior and excitability of ciliate Protozoa. *Acta Protozool.* **18**: 17-21
- Foissner W., Foissner I. (1988) The fine structure of *Fuscheria terricola* Berger et al., 1983 and a proposed new classification of the subclass Haptorida Corliss, 1974 (Ciliophora, Litostomatea). *Arch. Protistenk.* **135**: 213-235
- Golińska K. (1974) Effect of puromycin on regeneration processes in *Dileptus anatinus* Golińska, 1971. *Acta Protozool.* **12**: 289-306
- Golińska K. (1991) Cortical organellar complexes, their structure, formation and bearing upon cell shape in a ciliate, *Dileptus*. *Protoplasma* **162**: 160-174
- Golińska K. (1995) Formation and orientation of skeletal elements during development of oral territory in a ciliate, *Dileptus*. *Acta Protozool.* **34**: 101-113
- Golińska K., Afon'kin S. Yu. (1993) Preparatory changes and the development of the conjugation junction in a ciliate, *Dileptus*. *Protoplasma* **173**: 144-157
- Golińska K., Bohatier J. (1975) Action of Actinomycin D upon regenerative and divisional stomatogenesis in *Dileptus*. *Acta Protozool.* **14**: 1-15
- Golińska K., Grain J. (1969) Observations sur les modifications ultrastructurales lors de la régénération chez *Dileptus cygnus* Clap. et Lach., 1859, Cilié Holotriche Gymnostome. *Protistologica* **5**: 447-464
- Golińska K., Jerka-Dziadosz M. (1973) The relationship between cell size and capacity for division in *Dileptus anser* and *Urostyla cristata*. *Acta Protozool.* **12**: 1-21
- Golińska K., Kink J. (1977) Proportional regulation of body form and cortical organelle pattern in the ciliate *Dileptus*. *J. Cell Sci.* **24**: 11-29
- Grain J., Golińska K. (1969) Structure et ultrastructure de *Dileptus cygnus* Claparède et Lachmann, 1859, Cilié Holotriche Gymnostome. *Protistologica* **5**: 269-291
- Iftode F., Cohen J., Ruiz F., Torres Rueda A., Chen-Shan L., Adoutte A., Beisson J. (1989) Development of surface pattern during division in *Paramecium*. I. Mapping of duplication and reorganization of cortical cytoskeletal structures in the wild type. *Development* **105**: 191-211
- Kink J. (1973) The organization of fibrillar structures in the trophic and encysted *Dileptus vissscheri* (Ciliata, Rhabdophorina). *Acta Protozool.* **12**: 173-194
- Lasher R. S., Zagon C. S. (1972) The effect of potassium on neuronal differentiation in cultures of dissociated rat cerebellum. *Brain Res.* **41**: 482-488
- Leipe D. D., Oppelt A., Hausmann K., Foissner W. (1992) Stomatogenesis in the ditransversal ciliate *Homalozoon vermiculare* (Ciliophora, Rhabdophora). *Europ. J. Protistol.* **28**: 198-213
- Lynn D. H. (1988) Cytoterminology of cortical components of ciliates: somatic and oral kinetids. *BioSystems* **21**: 299-307
- Machemer H. (1989) Cellular behaviour modulated by ions: electrophysiological implications. *J. Protozool.* **36**: 465-437
- Miyake A. (1968) Induction of conjugation by chemical agents in *Paramecium*. *J. Exp. Zool.* **167**: 359-380
- Ogura R., Machemer H. (1980) Distribution of mechanoreceptor channels in the *Paramecium* surface membrane. *J. Comp. Physiol. A* **135**: 233-242
- Peyer J. E. de, Machemer H. (1977) Membrane excitability in *Stylonychia*: properties of the two-peak regenerative Ca-response. *J. Comp. Physiol.* **121**: 15-32
- Schusterman C. L., Thiede E. W., Kung C. (1978) K⁺-resistant mutants and "adaptation" in *Paramecium*. *Proc. Natl. Acad. Sci. USA* **75**: 5645 - 5649.
- Tsuchiya W., Okada Y. (1982) Membrane potential changes associated with differentiation of enterocytes in the rat intestinal villi in culture. *Dev. Biol.* **94**: 284-290
- Unsicker K., Hofmann H. D., Höhne I., Müller T. H., Schmidt R. (1983) Phenotypic plasticity of cultured bovine chromaffin cells. II. Fiber outgrowth induced by elevated potassium: morphology and ionic requirements. *Dev. Brain Res.* **9**: 369-379
- Wirnsberger E., Foissner W., Adam H. (1984) Morphologie und Infracilicatur von *Perispira pyriformis* nov. spec., *Cranotheridium foliosus* (Foissner, 1933) nov. comb. und *Dileptus anser* (O. F. Müller, 1786) (Protozoa, Ciliophora). *Arch. Protistenk.* **128**: 305-317

Received on 14th June, 1995; accepted on 15th May, 1996

The Predation of *Litonotus* on *Euplotes*: a Two Step Cell-cell Recognition Process

Nicola RICCI, Andrea MORELLI and Franco VERNI

Dipartimento di Scienze dell'Ambiente e del Territorio, Università di Pisa, Pisa, Italy

Summary. The study of the distribution kinetics of *Litonotus* (the predator) in a T-maze, with *Euplotes* as the prey, led to a series of findings useful to help us understand better its predation: (a) *Litonotus* did not perceive (in a wide sense) *Euplotes* from a distance by chance; (b) the chemical gradient of a thermolabile molecule enables the predator to trace the prey; (c) the attractions exercised by several species of *Euplotes* on *Litonotus* have different strengths: *E. vannus* > *E. crassus* > *E. minuta* > *E. raikovi* > *E. charon*; (d) *E. charon* attracts *Litonotus*, although weakly, but it does not elicit any toxicyst discharge by the predator; (e) *E. magnicirratu*s and *E. rariseta* (as well as *Aspidisca* sp., *Diophrys* sp. and *Euplotidium itoi*) are neither traced nor killed by *Litonotus*. These results show that a predator-prey recognition actually occurs from a distance (I step), before they come into contact with each other (II step).

Key words: cell-recognition, *Euplotes*, *Litonotus*, predation, T-maze

INTRODUCTION

Although in the natural environment the populations of ciliates tend to occur in patchy clusters (Taylor 1979, Taylor and Berger 1980, Landis 1981), they typically spend their lives as isolated, solitary entities: the only social event they cannot avoid, without risking extinction, is conjugation, the process bringing about sexuality (Nanney 1977). The phenomenon of chemo-orientation is known to play a key-role during the preconjugal cell interactions of *Blepharisma*

(Honda and Miyake 1975) and, more recently, it has been demonstrated also in *Euplotes woodruffi* (Kosaka 1991). On the other hand, several examples of cell-cell interactions regulating different adaptive strategies are well known among the ciliates: the case of the intraspecific cell-to-cell contacts, which induced the differentiation of giants for *Oxytricha bifaria* (Ricci and Banchetti 1993) together with that of the well known and widely spread phenomenon of predation (interspecific cell-cell interactions) [*Didinium* vs. *Paramecium* (Balbiani 1873); *Dileptus* vs. *Colpidium* (Visscher 1923); *Enchelys* vs. *Tetrahymena* and *Chaenea* vs. *Uronema* (Dragesco 1962); *Homalozoon* vs. *Paramecium* (Diller 1964)] offers an incredibly wide range of examples of more or less species specific and more or less direct cell

Address for correspondence: Nicola Ricci, Dipartimento di Scienze dell'Ambiente e del Territorio, Università di Pisa, via A. Volta 6, 56126 Pisa, Italy; Fax: 050-49694

interactions leading the organisms to the specific morphological [*Euplotes octocarinatus* vs *Lembadion* (Kuhlmann and Heckmann 1985)] or behavioural responses [*Litonotus* vs *Euplotes crassus* (Ricci and Verni 1988)].

Predation, indeed, is a phenomenon of relevance among ciliated protozoa, due to the fact that the protozoa themselves were the organisms which, in the primeval oceans, conquered the niche of the secondary consumers i.e. the carnivorous (Gould et al. 1977). This niche, beyond being very convenient from an energetic point of view, plays a relevant role in the course of evolution because (a) it creates new empty spaces for new populations to settle and (b) it is at the basis of the competition between predator and prey, to strike and to escape, respectively. Therefore, these unique cell-organisms, the protozoa (Fenchel 1987), could not but explore the way of cell-cell interactions as the new adaptive strategy guiding the first predators towards their prey target.

The model offered by *Litonotus lamella* preying on *Euplotes crassus* has already been analyzed thoroughly in terms of the successive steps guiding the predator to ingest the prey and the prey itself to escape (when possible) from the predator (Ricci and Verni 1994). This phenomenon was described as a succession of steps (direct contact-prey recognition-discharge of toxicysts-search-ingestion) differently affected by different agents (starvation, calcium ions, trypsin, cycloheximide, Con-A, prey homogenate). The synoptic scheme given by these authors, however, left an initial doubt as to the nature of the initial step: does *L. lamella* actively track *E. crassus* or, on the contrary, does it find the prey just by chance? The possible solution of the problem could be of great interest not only for the *Litonotus* and *Euplotes* model, but also and mainly as regards the general point of view of the understanding of the basic strategies which enabled the ancestors of *Litonotus* to specialize in this mode. After solving this problem, indeed, it will become possible to have answers also to many other questions such as the following: (a) if the first encounter is "guided", which kind of phenomenon guides *Litonotus* in its hunt? (b) is it a chemical gradient? (c) if this is the case then in turn, what kind of molecule is recognized by *Litonotus*? (d) is it a species-specific signal or just something like a secondary metabolite? (e) is such a species-specific phenomenon an all-or-none phenomenon or, rather, is it a graded one?

With all these questions in mind, a series of experiments was conducted to obtain as many answers as possible.

MATERIALS AND METHODS

New strains of *L. lamella* and *E. crassus* were collected *ex novo* in nature, namely along the sea shores of the Tyrrhennian sea close to Leghorn, cultured in our laboratory according to the standard protocols (Ricci and Verni 1988) and then studied experimentally. Many other species were also collected on the sandy shores of the Tyrrhennian and Ligurian seas, between Leghorn and the Camargue (France) and grown in our laboratory for the 16 months of our experiments: *E. charon*, *E. magnicirratu*s, *E. minuta*, *E. raikovi*, *E. rariseta*, *E. vannus*, *Aspidisca* sp., *Diophrys* sp., *Euplotidium itoi*. For the experimental sessions, the organisms were collected from the cultures through a nylon net with a 8.0 μ m mesh. To study the kinetics of the spatial distribution of *Litonotus* a bidimensional T-maze, obtained in a perspex slide by a milling cutter, was used (Fig. 1): the length of the principal arm was 6 cm and the shorter arm of 1 cm; their width was 4 mm; the depth of the T-maze was 7 mm and the populations were observed in sea water never deeper than 4 mm. Our device was designed according to Van Houten et al. (1975), only slightly changed to satisfy our need for small volumes, high efficiency (bidimensional), long time observation (large interface with air for the oxygen supply) and easy and readable observation under the microscope. Throughout our experiments, a total volume of 0.5 ml was used and 50 *Litonotus* were added in the N (neutral)-arm: their spreading and their distribution between the E (experimental)-arm and C (control)-arm was measured every 5 min for the first 60 min since the introduction of the predators. In the E-arm a modified Pasteur pipette was put in such a way that its tip was 2 mm under the surface of the water: the pipette itself was kept still by means of plasticine. In the standard experiments this E-pipette contained a concentrated population of *Euplotes*, and its tip was closed by means of a thick cotton stopper to avoid any leaking of prey through the T-maze. A gross measurement of the different flows of fluid from the different pipettes (obtained by coloured ink) was also made and their values never differed significantly due to our using (a) the same volume, (b) the same diameter of the tip and (c) the same difference between the level of the fluids themselves. The experimental *Euplotes* were concentrated (10^4 cells/ml) by mild centrifugation (5 minutes at 300 x g) then washed and incubated in sterilized sea water for 2 days. When the cell free fluid (cff) of *Euplotes* was tested it was obtained by

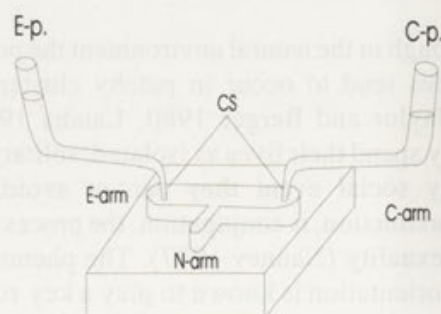


Fig. 1. The bidimensional T-maze: E - Experimental: it refers to the arm of the T-maze, to the pipette, to the different populations of ciliates tested. C - Control: it refers to the arm of the T-maze, to the marine water used as control. N - Neutral: it refers to the arm where the 50 *Litonotus* were added. CS - cotton stopper

filtering concentrated *Euplotes* through a BioRad membrane with a 0.42 μm pore to remove both bacteria and *Dunaliella salina* (used as food for *Euplotes*): it was then put into the E-pipette and the effects on *Litonotus* measured as already described. The C-pipette contained only standard artificial sea water. For each experiment the E and the C-arms were inverted to avoid unwanted possible mistakes: no difference due to the characteristics of our bidimensional T-maze between the two successive E-populations and the two C-populations was ever observed. The cells were counted directly under the stereo microscope (20x). Each type of experiment was performed 3 times. The data obtained are given in terms of mean values and standard deviations (Table I A,B,C,D and Table II A,B) and plotted in the Figs. 2 and 3 to show the kinetics of the phenomenon. In the figures the standard deviations have not been shown to avoid useless overlapping of information. The effects of the experiments were measured as the number of *Litonotus* observed at the successive times (time 0 corresponded to the introduction of the predators in the N-arm) in E-arm (E-*Litonotus*), in the C-arm (C-*Litonotus*) and in the N-arm (N-*Litonotus*). Their trends in the time were then studied statistically by means of the non parametric Wilcoxon test (Wilcoxon 1945, Snedecor and Cochran 1976). The data were plotted singly, as shown in Fig. 2. To compare the relative attraction strength of the different species, a series of experiments was also run using, in the same T-maze, two different species (one for each Pasteur pipette) contemporaneously: the dynamics of the spatial distribution of the 50 *Litonotus* were measured in the same way as in the basic experiments.

Litonotus was also treated by 1% Con-A (Sigma C 2010) for 60 min and then washed twice by transferring the experimental organisms into new artificial sea water. To control the specificity of Con-A, several experiments were run with 40 mM α -methyl-D-mannoside (Ricci and Verni 1994).

RESULTS

The first goal was to study whether *Litonotus* reacts to the presence of *Euplotes crassus* or not, and if it does, how it reacts. The results shown in Fig. 2A give the kinetics of the accumulation of *Litonotus* in the E-arm, namely in the arm of the T-maze with the pipette containing the prey. Three main conclusions can be drawn according to these results: (a) the predators indeed crowd where the prey is perceived; (b) the effect, in our apparatus, becomes evident after 25-30 min, on average; (c) the effect increases steadily, at least for the 60 min we monitored.

This kind of result indicated that *Litonotus* can track *Euplotes* also when it is not in physical contact. As a control, a new apparatus was prepared, where the E-pipette was filled by cff collected from cultures of *Euplotes*, and the results, plotted in Fig. 2B, showed that: (a) the effect of the cff is evident soon after introducing the E-pipette into the E-arm ($\Delta t=5$ min) and (b) the effect

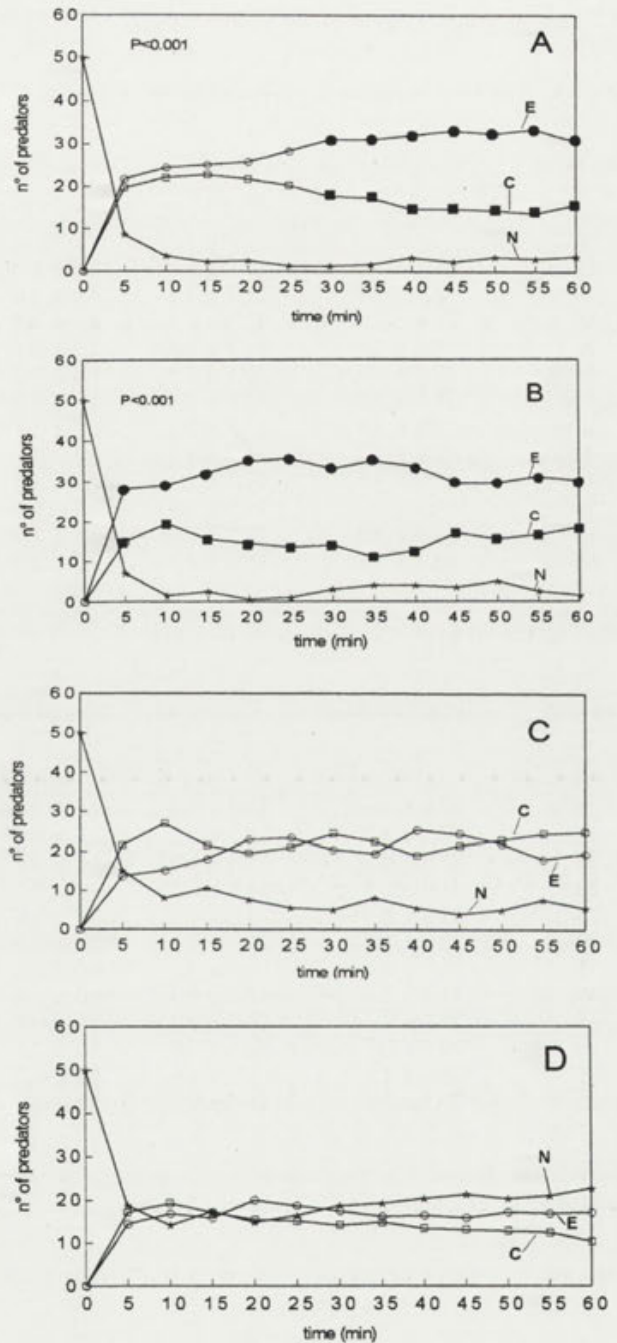


Fig. 2. The trends of spatial distribution of *Litonotus* in the E-arm (E), in the C-arm (C) and in the N-arm (N); the circle and the squares are black when a significant difference ($p < 0.05$) between them occurs; in the abscissa the time and in the ordinate the number of *Litonotus* in the different arms of the T-maze are given. (A) The basic experiment: the E-pipette contains *Euplotes*; (B) the E-pipette contains the cff of *Euplotes*: the effect is reached within 5 min; (C) the E-pipette contains the cff treated at 85 °C for 5 min; (D) the same experiment as the (A) but the predator had been pretreated by Con-A, as explained in the Material and Methods sections. When also α -methyl - D - mannoside was used as the specific competitor of Con-A the spatial distribution of *Litonotus* in the three arms of the T-maze followed the trend of the basic experiment (A): in both the (C) and (D) experiments no significant difference between the E and C arms ever occurred ($P > 0.1$)

Table I. Temporal distribution of the predators in the 3 arms of the T-maze

Table I A. The basic experiment: *E. crassus* in the E-pipette

Time (min)	Experimental arm	Control arm	Neutral arm
0	0	0	50
5	21.7 ± 1.5	19.7 ± 5.0	8.6 ± 6.0
10	24.3 ± 2.1	21.7 ± 3.5	4.0 ± 1.0
15	25.0 ± 2.0	22.7 ± 1.5	2.3 ± 0.6
20	25.7 ± 2.1	21.7 ± 2.5	2.6 ± 0.6
25	28.3 ± 3.8	20.3 ± 3.5	1.4 ± 0.2
30	31.0 ± 1.0	17.7 ± 0.6	1.3 ± 0.6
35	31.0 ± 4.4	17.3 ± 5.1	1.7 ± 1.1
40	32.0 ± 4.4	14.7 ± 3.3	3.3 ± 1.1
45	33.0 ± 3.6	14.7 ± 2.3	2.3 ± 1.5
50	32.3 ± 4.0	14.3 ± 3.8	3.4 ± 0.6
55	34.7 ± 5.7	12.7 ± 6.0	2.6 ± 2.0
60	30.7 ± 3.8	15.7 ± 4.0	3.6 ± 2.1

Table I B. The cff from *E. crassus* in the E-pipette

Time (min)	Experimental arm	Control arm	Neutral arm
0	0	0	50
5	28.0 ± 0.0	15.0 ± 1.4	7.0 ± 1.4
10	29.0 ± 1.4	19.5 ± 0.7	1.5 ± 0.7
15	32.0 ± 4.2	15.5 ± 4.9	2.5 ± 0.7
20	35.0 ± 2.8	14.5 ± 2.1	0.5 ± 0.7
25	35.5 ± 6.4	13.5 ± 7.8	1.0 ± 0.4
30	33.0 ± 4.2	14.0 ± 7.1	3.0 ± 2.0
35	35.0 ± 0.0	11.0 ± 4.2	4.0 ± 2.2
40	33.5 ± 2.8	12.5 ± 0.7	4.0 ± 2.8
45	29.5 ± 7.1	17.0 ± 5.7	3.5 ± 0.7
50	29.5 ± 0.7	15.5 ± 7.8	5.0 ± 2.1
55	31.0 ± 1.4	16.5 ± 4.9	2.5 ± 1.5
60	30.0 ± 7.1	18.5 ± 9.2	1.5 ± 0.5

Table I C. The cff from *E. crassus* was put in the E-pipette after being heated at 85°C for 5 min

Time (min)	Experimental arm	Control arm	Neutral arm
0	0	0	50
5	13.5 ± 2.1	21.5 ± 2.1	15 ± 4.2
10	15 ± 0.0	27 ± 4.2	8 ± 4.2
15	18 ± 5.7	21.5 ± 2.1	10.5 ± 3.5
20	23 ± 1.4	19.5 ± 0.7	7.5 ± 2.1
25	23.5 ± 3.5	21 ± 1.4	5.5 ± 4.9
30	20.5 ± 2.1	24.5 ± 4.9	5 ± 2.0
35	19.5 ± 0.7	22.5 ± 3.5	8 ± 3.2
40	25.5 ± 3.5	19 ± 1.4	5.5 ± 2.1
45	24.5 ± 4.9	21.5 ± 4.9	4 ± 0.0
50	22 ± 1.4	23 ± 2.8	5 ± 1.4
55	18 ± 0.0	24.5 ± 0.7	7.5 ± 0.7
60	19.5 ± 2.1	25 ± 2.8	5.5 ± 1.9

Table I D. The basic experiment with Con-A pre treated *Litonotus*

Time (min)	Experimental arm	Control arm	Neutral arm
0	0	0	50
5	14.3 ± 6.0	17.0 ± 0.0	18.7 ± 6.6
10	16.7 ± 2.9	19.3 ± 3.2	14.0 ± 3.5
15	15.7 ± 5.0	17.0 ± 2.6	17.3 ± 7.5
20	20.0 ± 5.0	15.3 ± 3.0	14.7 ± 6.5
25	18.7 ± 10.7	15.0 ± 6.2	16.3 ± 9.9
30	17.3 ± 6.0	14.0 ± 5.6	18.7 ± 6.1
35	16.0 ± 4.6	14.7 ± 5.0	19.3 ± 3.5
40	16.3 ± 4.0	13.3 ± 4.2	20.4 ± 2.5
45	15.7 ± 2.3	13.0 ± 6.6	21.3 ± 4.9
50	17.0 ± 3.6	12.7 ± 4.0	20.3 ± 4.2
55	16.7 ± 3.0	12.3 ± 4.0	21.0 ± 4.6
60	17.0 ± 2.6	10.3 ± 4.0	22.7 ± 3.0

Table II. The effects of attracting/non-attracting prey

Table II A. The basic experiment conducted with *E. vannus* in the E-pipette

Time (min)	Experimental arm	Control arm	Neutral arm
0	0	0	50
5	19.3 ± 4.8	13.0 ± 6.8	17.7 ± 11.4
10	21.5 ± 5.8	12.8 ± 2.6	15.7 ± 6.9
15	27.0 ± 8.5	12.0 ± 6.4	11.0 ± 6.0
20	27.3 ± 8.8	12.7 ± 6.2	10.0 ± 5.0
25	26.5 ± 7.4	14.3 ± 7.9	9.2 ± 4.4
30	25.5 ± 8.7	16.8 ± 10.8	7.7 ± 5.1
35	23.8 ± 8.6	17.5 ± 9.2	8.7 ± 4.4
40	25.5 ± 8.7	16.8 ± 9.1	7.7 ± 3.3
45	26.5 ± 7.0	15.0 ± 7.3	8.5 ± 1.7
50	25.3 ± 6.1	16.7 ± 10.7	8.0 ± 4.7
55	24.8 ± 10.8	15.2 ± 10.0	10.0 ± 1.8
60	27.0 ± 7.6	15.3 ± 10.8	7.7 ± 3.6

Table II B. The basic experiment conducted with *E. magnicirratu* in the E-pipette

Time (min)	Experimental arm	Control arm	Neutral arm
0	0	0	50
5	18.3 ± 5.7	22.0 ± 4.5	9.7 ± 5.6
10	19.3 ± 5.3	23.3 ± 4.6	7.4 ± 4.4
15	20.5 ± 8.3	24.5 ± 8.2	5 ± 2.0
20	21.3 ± 9.4	25.0 ± 7.2	3.7 ± 3.1
25	20.7 ± 10.3	25.7 ± 10.1	3.6 ± 3.0
30	22.8 ± 10.6	22.3 ± 10.7	4.9 ± 2.6
35	22.8 ± 10.9	21.5 ± 8.2	5.7 ± 3.6
40	21.3 ± 10.3	23.8 ± 11.2	4.9 ± 2.6
45	22.2 ± 12.1	22.5 ± 12.3	5.3 ± 2.4
50	23.8 ± 11.2	21.8 ± 10.4	4.4 ± 2.6
55	24 ± 10.7	21.2 ± 10.6	4.8 ± 2.2
60	24 ± 8.8	19.7 ± 8.2	6.3 ± 2.6

is fairly constant with time (up to 60 min, at least). To investigate the nature of the soluble principle released by the *Euplotes* into the cff, this fluid was kept at 85 °C for 5 min and then tested again. Fig. 2C clearly shows that this "temperature-treated" cff does not affect the behaviour of *Litonotus*: the predators in the E-arm are more or less of the same number as those in the C-arm, while a certain number (5-10) remains in the N-arm. The fourth experiment was carried out with *Litonotus* pretreated by Con -A: the results are shown in Fig. 2D. These results show that *Litonotus*, once pretreated by Con-A, does not react any more to the soluble factor released by the *Euplotes* as demonstrated by the numbers of *Litonotus*, which are more or less equivalent in the three different arms. What must be noticed is the relatively large number of *Litonotus* in the N-arm in comparison with the small number of *Litonotus* in the E- and C-arms. As a control for the effect of Con-A, other *Litonotus* were pretreated with Con-A + α -Methyl-D-mannoside and the results showed that (a) the effect of Con-A is indeed a specific one and (b) the Con-A itself does not react in the medium with the factor(s) released by *Euplotes*: these data have not been shown in any specific figure, because they completely overlap the kinetics of the basic experiment given in Fig. 2A.

The species specificity of the prey, already reported by Ricci and Verni (1988) as occurring at the moment of the direct contact between the predator and the prey, was also studied by the T-maze apparatus, to ascertain whether a

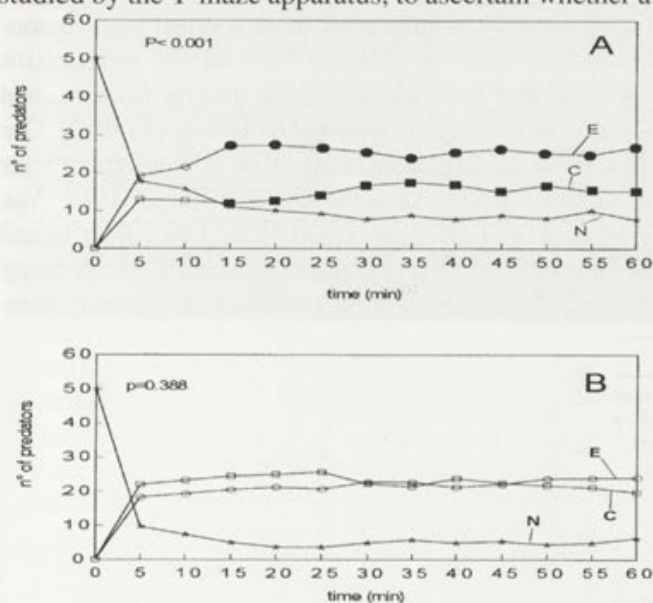


Fig. 3. The species-specificity of the attraction of the potential prey on the predator. (A) The attracting species, *E. vannus* has been considered as the typical example; (B) the non-attracting species, *E. magnicirratum* has been considered as the typical example

similar species specificity does exist also at the level of the recognition of the prey from a distance. Many species of *Euplotes* as well as of the genera *Euplotidium*, *Diophrys*, and *Aspidisca* were tested with the same kind of experiment and the results are given in Fig. 3. It is evident that *E. vannus*, *E. minuta*, *E. raikovi* and *E. charon* (Fig. 3A) behave like *E. crassus*, from the point of view of their capability of attracting the predators, while *E. magnicirratum*, *E. rariseta*, *Euplotidium itoi*, *Diophrys* sp. and *Aspidisca* sp. (Fig. 3B) do not attract *Litonotus*. Peculiar is the case of *E. charon* (more clearly shown in Table III). This species indeed does attract *Litonotus*, which, however, does not discharge its toxicysts against it, even when strongly bumped. The attraction of predators by different species becomes evident (i.e. the difference between the number of *Litonotus* in the E-arm and in the C-arm is significant) at different times. (Table III, 3-rd column, Δt). According to these results *E. vannus* has the strongest effect ($\Delta t \approx 15$), followed by *E. crassus* ($\Delta t \approx 27$), by *E. minuta* ($\Delta t \approx 35$), by *E. raikovi* and *E. charon* ($\Delta t \approx 40$).

The last experiment involved the use of two species at a time (one at either extreme of the T-maze), to enable the 50 *Litonotus* to "choose" between them. To differentiate clearly the relative attractiveness of the different species we observed (A) the first statistically significant difference between the number of *Litonotus* in the E vs. the C arm (FDN - First Difference Number) and we measured the time lag between the beginning of the experiment and the onset of this difference (FDT - First Difference Time), (B) the longest numerical difference between the predator in the E vs. the C arm (MDN: Maximum Difference Number) and the time lag of its occurrence (MDT - Maximum Difference Time). The results obtained are shown in Table IV. They can be summarized by the following points: (a) *E. vannus* is the most effective species, as far as its attraction of *Litonotus* is concerned; (b) *E. crassus* is the most similar to *E. vannus*, followed by *E. minuta*, as shown by the number of predators in the arms of the T-maze and by the time needed for the first difference to become significant; (c) *E. raikovi* and *E. charon* represent a sort of third level of attraction for *Litonotus*, while *E. magnicirratum* and *E. rariseta* are silent from this point of view, as shown by a comparison between the numbers of *Litonotus* in the E-vs those in the C-arm and the number of *Litonotus* in the N-arm. The fact that both the $FD\Delta t$ and $MD\Delta t$ are quite similar to those of the other species seems to be due to some intrinsic structural characteristic of the T-maze itself, determining the establishment of the chemical gradient guiding the predators to their targets.

Table III. The different attraction powers

	Attraction	TD	Δt (min)
<i>E. vannus</i>	+	+	15
<i>E. crassus</i>	+	+	27
<i>E. minuta</i>	+	+	35
<i>E. raikovi</i>	+	+	40
<i>E. charon</i>	+	∞	40
<i>E. magnicirratu</i>	∞	∞	♦
<i>E. rariseta</i>	∞	∞	♦
<i>Aspidisca</i> sp.	∞	∞	♦
<i>Euplotidium itoi</i>	∞	∞	♦
<i>Diophrys</i> sp.	∞	∞	♦

The effects of different species (column on the left) on *Litonotus*, are shown in terms of attraction (+ = yes; ∞ = no), of toxicyst discharge (direct observation) (TD) (+ = yes; ∞ = no) and of Δt of the first significant difference between the E-arm and the C-arm (∞ = no difference)

Table IV. The direct choice tests

Comparison between	FDN	FDT(min)	MDN	T(min)
<i>E. vannus</i> (E-arm) and other species (C-arm)				
<i>E. crassus</i>	25/12 (13)	35	20/5 (25)	60
<i>E. minuta</i>	28/14 (8)	20	37/4 (9)	35
<i>E. raikovi</i>	25/14 (11)	15	34/12 (4)	30
<i>E. charon</i>	29/9 (13)	15	37/3 (10)	30
<i>E. magnicirratu</i>	34/12 (4)	15	41/7 (2)	30
<i>E. rariseta</i>	29/8 (13)	15	38/8 (4)	30

E. vannus is placed in the E-arm while different species (left column) are successively placed in the C-arm to test their relative strengths in attracting *Litonotus*. FDN (First Difference Number): the number of *Litonotus* in the E-arm vs. that in the C-arm (in parentheses: the number of *Litonotus* in the N-arm) at the moment of the first significant difference; FDT (First Difference Time): the time lag necessary for the first significant difference to occur; MDN (Maximum Difference Number): the number of predators in the E-arm vs. the same number in the C-arm (in parentheses the number of *Litonotus* in the N-arm) at the moment of the greatest difference; MDT (Maximum Difference Time): the time lag between the onset of the experiment and the occurrence of the greatest difference

A	B	C	D	E
<i>Litonotus</i> recognizes from a distance the soluble factor of <i>Euplotes vannus</i> , <i>E. crassus</i> , <i>E. minuta</i> , <i>E. raikovi</i> , <i>E. charon</i> [the first level of recognition of prey individuals].	<i>Litonotus</i> changes its behaviour and finishes close to the prey.	<i>Litonotus</i> discharges its toxicysts, upon direct cell to cell contact, against: <i>E. vannus</i> ; <i>E. crassus</i> ; <i>E. minuta</i> ; <i>E. raikovi</i> ; (not <i>E. charon</i>). [the second level of recognition of prey individuals].	<i>Litonotus</i> creeps backwards and starts searching for the stricken prey: <i>E. vannus</i> , <i>E. crassus</i> , <i>E. minuta</i> , <i>E. raikovi</i> .	<i>Litonotus</i> engulfs stricken specimens of: <i>E. vannus</i> , <i>E. crassus</i> , <i>E. minuta</i> , <i>E. raikovi</i> .

Fig. 4. A scheme showing the principal steps following each other in the predation of *Litonotus* on *Euplotes*: the A and B steps represent the main results of this round of experiments, while the C, D, and E steps are just the rearrangement of the more detailed data reported by Ricci and Verni (1994)

DISCUSSION

The predator *Litonotus lamella* can recognize from a distance its prey, (I recognition step) to intercept them and, upon direct cell-cell recognition (II recognition step), to discharge its toxicysts before to kill. This is the main result obtained by our experiments, but a careful discussion is necessary to deepen our understanding of such a complex phenomenon. First of all it represents the solution of the question proposed by Ricci and Verni (1994) who, describing the series of steps guiding *L. lamella* to feed on *E. crassus*, left undefined the very first stage of the interacting relationships between *L. lamella* and *E. crassus*. This is namely the way by which the former contacts the latter. The data obtained rule out any random exploration by *L. lamella* while searching for its preys: the species indeed proved it was capable of approaching the prey efficiently. Such a capability, in turn, shows a predatory strategy which is quite sophisticated and somehow different from that of other predator ciliates, such as *Enchelys mutans* and *Chaenea vorax* (Dragesco 1962) or *Dileptus anser* (Miller 1968), which can only intercept their prey by chance and which, very likely due to such a handicap, do not show any alimentary specialization, being capable of feeding on flagellates, amoebae, ciliates and even planarians. This non-oriented predatory behaviour, suggesting interesting possibilities of mathematical modelling (Voit 1984), is very likely to be more primitive, it being less specialised than the oriented predation. The latter case, on the contrary, implies a far more sophisticated chemorientation from the point of view of the mechanisms involved: that this could be the case also for *Litonotus* had already been indirectly reported by Dragesco (1962). Our data, however, have been obtained by *ad hoc* experiments using the T-maze technique (cf. also Berger 1980, Van Houten et al. 1981, Leick and Helle 1983, Francis and Hennessey 1995) and this makes them indicative of many different characteristics of the *Litonotus* - *Euplotes* system.

In the apparatus described in Fig. 1, *Litonotus* proved it was able to track *Euplotes* from a distance of at least 3 cm. According to the nature of the habitat of *Euplotes*, namely the tridimensional net of tunnels existing in the sandy substrate preferred by this organism (Ricci 1989), we can put forward the hypothesis that the detection distance between *Litonotus* and its prey in nature can be even greater than 3 cm: the water volume containing the chemical(s) from *Euplotes* indeed is more dispersed amid the sandy granules than in the unique volume of our T-maze. Furthermore, our experiments showed that the effects of *Euplotes* in conditioning chemically the water in the T-maze become evident after 20 min and last for more than 60 min: within this time lag a gradient forms which is capable of guiding *Litonotus* to its prey. The same results showed also that *Euplotes* releases into the medium some chemical(s) which induce in the predator a creeping behaviour leading it to the prey. Although the adaptive meaning for *Litonotus* is self-evident, the nature of its changed behaviour (is it a taxis or a kinesis?) is still unknown and being currently analysed according to the standard ethological techniques (Ricci 1992). Con-A, a well known agent perturbing the cortical glycoproteins (Ricci and Verni 1994), generally reduces the motility of the predator (as shown by the number of *Litonotus* in the N-arm, Fig. 2D) and their capability of tracking *Euplotes*. This might indicate that a kinesis, rather than a taxis could represent the adaptive answer of *Litonotus* once stimulated by the *Euplotes* themselves.

The data here reported tend to indicate that the molecule released by *Euplotes* could be a large one (or even a complex of molecules) as indicated by its thermolability and this distinguishes the *Litonotus* - *Euplotes* system from that of *Didinium*, which is attracted by a thermostable molecule (Van Houten et al. 1981). The finding that *E. crassus* releases some substance(s) into the environment must be considered as a rather unexpected one. The species, indeed, seems to use a different adaptive strategy, for instance, as far as the cell bound gamones, mediating its sexuality, are concerned (Heckmann and Siegel 1964; Nobili et al. 1978, 1987). On the other hand, the soluble substance released by *Euplotes* seems to be an aspecific one, (at least from the point of view of the prey's biology) and, thus (differently from the mating substances) really specific only to guide the predator to its prey. Quite a new story, in the wider context of the predation behaviour among the ciliates, is shown by the demonstration that *L. lamella* is capable of finding and killing several species (*E. vannus*, *E. crassus*, *E. minuta*,

E. raikovi), while it can only find (and not kill) *E. charon* and it ignores completely *E. magnicirratu*s and *E. rariseta* together with *Euplotidium itoi*, *Aspidisca* sp. and *Diophrys* sp. The fact that the time lags between the beginning of the experiments and the onset of the gradient affecting the behaviour of *Litonotus* are progressively longer for *E. vannus*, *E. crassus*, *E. minuta*, *E. raikovi* and *E. charon*, together with the fact that the direct choicetests (Table IV) show that the relative attracting forces could be ordered according to a decreasing strength (*E. vannus* > *E. crassus* > *E. minuta* > *E. raikovi* > *E. charon*) tends to indicate that even among the potential preys a difference occurs, at least as far as their capability of eliciting the searching behaviour by *Litonotus* is concerned. The research being carried out to isolate attractant(s) released by *Euplotes*, is expected to throw new light also on the problem of the difference in the attracting forces of the various species: does it depend upon different amounts of the attractant(s) released? Does it depend upon different affinities that different attractant(s) have with the receptors of *Litonotus*? With regard to the latter question a ligand-receptor reaction (Esteve 1981, Ricci and Verni 1994) occurs on the basis of the specific effects of Con-A on the predation of *Litonotus* on *Euplotes*. These effects actually show that the soluble substance released by *Euplotes* does not cross react with Con-A in the medium, but, rather, that it binds at the cortical level of the predator. Beyond being interesting in itself, the peculiar fact that *E. charon* can be tracked by *Litonotus* without evoking any discharge of its toxicysts (what sort of mechanism might account for such an observation?) demonstrates that the recognition of the prey actually occurs at the two different levels and with the two different mechanisms reported in Fig. 4. The figure is drawn also according to the whole complex of data here reported: (A) *Litonotus lamella* perceives the presence of *Euplotes* from a distance before changing its behaviour in such a way that (B) it can intercept the prey (C) *Litonotus* contacts directly *Euplotes*, the second recognition occurs, triggering the discharge of the predator's toxicysts. The overall picture of the predation of *Litonotus* on *Euplotes* is now far clearer than before and the next two steps, presently investigated in our laboratory, are expected to define it at least from a general point of view: (a) does *Litonotus* undergo any morpho-physiological change while creeping upgradient as Marciano-Cabral et al. (1987) found in *Naegleria*? (b) does *Euplotes* sense the presence of *Litonotus* and, if this is the case, does it undergo any adaptive change as *E. octocarinatus*

does against *Lembadion* (Kuhlmann and Heckmann 1985) ?

The outcome of these experiments demonstrate that the study of predatory systems, like that of *Litonotus* - *Euplotes*, actually represents a multifaceted precious approach to the biology of these unique organisms, the first eukaryotes to conquer the trophic niche of the secondary consumers, the predators.

Acknowledgments. The enthusiastic and precious help of many students must here be acknowledged.

REFERENCES

- Balbani E.G. (1873) Observations sur le *Didinium nasutum*. *Arch. Zool. Exp.* **2**: 363-394
- Berger J. (1980) Feeding behaviour of *Didinium nasutum* on *Paramecium bursaria* with normal or apochlorotic zoochlorellae. *J. Gen. Microbiol.* **118**: 397-404
- Diller W.F. (1964) Observation on the morphology and life history of *Homalozoon vermiculare*. *Arch. Protistenk.* **107**: 351-362
- Dragesco J. (1962) Capture et ingestion des proies chez les infusoires Ciliés. *Bull. Biol. Fr. Belg.* **96**: 123-127
- Esteve J.C. (1981) Perturbation du comportement alimentaire par atteinte du revêtement cellulaire chez le cilié *Dileptus*. *Protistologica* **17**: 479-488
- Fenchel T. (1987) Ecology of Protozoa Springer Verlag, Berlin
- Francis J.T., Hennessey T.M. (1995) Chemorepellents in *Paramecium* and *Tetrahymena*. *J. Euk. Microbiol.* **42**: 78-83
- Gould S. J., Raup D.M., Sepkoski J. J., Jr., Schopf T.J.M., Simberloff D.S. (1977) The shape of evolution. A comparison of real and random clades. *Paleobiology* **3**: 173-181
- Heckmann K., Siegel R.W. (1964) Evidence for the induction of mating type substances by cell to cell contacts. *Exp. Cell Res.* **36**: 688-691
- Honda H., Miyake A. (1975) Taxis to a conjugant-inducing substance in the ciliate *Blepharisma*. *Nature* **257**: 678-679
- Kosaka T. (1991) Mature cells attracting cells of the complementary mating type in *Euplotes woodruffi* syngen 3 (Ciliophora, Hypotrichida). *Zool. Sci.* **8**: 681-692
- Kuhlmann H.-W., Heckmann K. (1985) Interspecific morphogens regulating prey-predator relationship in protozoa. *Science* **227**: 1347-1349
- Landis W.G. (1981) The ecology, role of the killer trait, and interactions of five species of the *Paramecium aurelia* complex inhabiting the littoral zone. *Can. J. Zool.* **59**: 1734-1743
- Leick V., Helle J. (1983) A quantitative assay for ciliate chemotaxis. *Analytical Biochem.* **135**: 466-469
- Marciano-Cabral F., Cline M. (1987) Chemotaxis by *Naegleria fowleri* for bacteria. *J. Protozool.* **34**: 127-131
- Miller S. (1968) The predatory behavior of *Dileptus anser*. *J. Protozool.* **15**: 313-319
- Nanney D.L. (1977) Cell-cell interactions in ciliates: evolutionary and genetic constraints. In: Microbial interactions (Ed. J.L. Reissig). Chapman & Hall, London, 353-397
- Nobili R., Luporini P., Dini F. (1978) Breeding systems, species relationships and evolutionary trends in some marine species of *Euplotidae* (Hypotrichida, Ciliata). In: Marine organisms (Eds. B. Battaglia and J. Beardmore). Plenum Publishing Corporation, 591-616
- Nobili R., Luporini P., Esposito F. (1987) Compatibility systems in ciliates. In: Invertebrate models: cell receptors and cell communication (Ed. A.H. Greenberg). Karger-Basel, 6-28
- Ricci N. (1989) Locomotion as a criterion to read the adaptive biology of protozoa and their evolution towards metazoa. *Boll. Zool.* **56**: 245-263
- Ricci N. (1992) Qualitative study and quantitative analysis of behavior of ciliated protozoa: principles, techniques, tricks. In: Protocols in protozoology (Eds. J.J. Lee and A.T. Soldo). Allen Press, Lawrence (USA), 14.1-14.6
- Ricci N., Banchetti R. (1993) The peculiar case of the giants of *Oxytricha bifaria* (Ciliata, Hypotrichida): a paradigmatic example of cell differentiation and adaptive strategy. *Zool. Sci.* **10**: 393-410.
- Ricci N., Verni F. (1988) Motor and predatory behavior of *Litonotus lamella* (Protozoa, Ciliata). *Can. J. Zool.* **66**: 1973-1981
- Ricci N., Verni F. (1994) Experimental perturbations of the *Litonotus-Euplotes* predator-prey system. *Zool. Sci.* **11**: 309-406
- Snedecor G. W., Cochran W. G. (1976) Statistical methods. The Iowa state University Press, 1-593
- Taylor W.D. (1979) Sampling data on the bactivorous ciliates of a small pond compared to neutral models of community structure. *Ecology* **60**: 876-883
- Taylor W.D., Berger J. (1980) Microspatial heterogeneity in the distribution of ciliates in a small pond. *Microb. Ecol.* **6**: 27-34
- Van Houten J., Hansna H., Kung C. (1975) Two quantitative assays for chemotaxis in *Paramecium*. *J. Comp. Physiol.* **127**: 167-174
- Van Houten J., Hauser D.C.R., Levandowsky M. (1981) Chemosensory behavior in protozoa. In: Biochemistry and physiology of protozoa (Eds. M. Levandowsky and H.S. Hutner). Academy Press, New York, 67-124
- Visscher J.P. (1923) Feeding reactions in the ciliate *Dileptus gigas* with special reference to the function of the trichocysts. *Biol. Bull.* **45**: 113-143
- Voit E.O. (1984) Encounters in predator-prey systems: a simple discrete model. *Biosystems* **17**: 57-63
- Wilcoxon F. (1945) Individual comparison by ranking methods. *Biometrics Bull.* **1**: 80-83

Received on 16th October, 1995; accepted on 22nd March, 1996

The Sludge Biotic Index for the Evaluation of the Activated-sludge Plant Performance: the Allocation of the Ciliate *Acineria uncinata* to its Correct Functional Group

Paolo MADONI

Dipartimento di Scienze Ambientali, Università di Parma, Parma, Italy

Summary. In this paper the position of the ciliate *Acineria uncinata* Tucolesco 1962 into the functional groups of the protistan community of the activated-sludge process was investigated. Ciliate communities colonizing four different activated-sludge plants receiving domestic and industrial waste were monitored. The dynamics of the observed ciliate species was studied through the microscopical analysis of the samples collected in the aeration tank. The sludge biotic index (SBI) method was applied to the observed microfauna and the results obtained were compared to the chemical and operational parameters. Statistical analysis of these data, revealed a negative linear relation between *A. uncinata* and crawling ciliates, possibly due to competition. Lastly, the hypothesis was put forward that *A. uncinata* is a crawling form rather a free-swimming form in the activated sludge.

Key words: *Acineria uncinata*, activated sludge, ciliated protozoa community, functional groups, sludge biotic index

INTRODUCTION

It is well known that the performance of the activated-sludge sewage-treatment process is strictly associated to both density and structure of the protistan community (ciliates, flagellates, amoebae) colonizing the activated sludge in the plant aeration tank (Curds and Cockburn 1970, Curds 1975, Madoni and Ghetti 1981, Antonietti et al. 1982, Madoni 1982). In sewage-treatment processes the components of the microbial community and their ecological valency can be utilized as indicators of different operational conditions of the plants.

In particular, the sludge biotic index (SBI), an objective

index based on protistan community, has been devised to monitor activated-sludge plant performance (Madoni 1994). This method is based on two principles. First, the dominance of protistan keygroups changes in relation to environmental and operational conditions of the plant. Secondly, cell density and number of taxa diminish as the efficiency of the plant drops.

Since the majority of ciliates present in biological sewage-treatment plants feed upon populations of dispersed bacteria, protistan keygroups consist chiefly of bacterivorous ciliates which can be subdivided into three functional groups on the basis of their behaviour: free-swimmers, crawlers, and attached. All bacterivorous ciliates rely upon ciliary currents to force suspended bacteria into the oral region. So, while free-swimming and attached ciliates are in competition for bacteria dispersed in the liquid phase, crawling forms, that are in proximity to

Address for correspondence: Paolo Madoni, Dipartimento di Scienze Ambientali, Università di Parma, Viale delle Scienze, I-43100 Parma, Italy; FAX: +39 - 521 - 905402

surface growths, feed upon particles that lightly adhere to the sludge and that are dislodged easily by the feeding currents (hypotrichous ciliates) or by scraping (cyrtophorian ciliates). Due to the different food habits preventing competition, crawling and attached ciliate functional groups co-dominate the protistan community in activated-sludge plants. On the contrary, swimming bacterivorous ciliates are more abundant in the early phases of developing plant, when sludge flocs are still scarce and, consequently, sessile ciliates are absent. Nevertheless, when the plant reaches the optimum efficiency, soon they are competitively displaced by attached ciliates which are more efficient than free-swimming ciliates in enforcing suspended bacteria and flagellates into the oral region. Moreover, free-swimming forms are washed out of the system, whereas attached and crawling forms are re-inoculated with the return sludge. This explains why an efficient activated-sludge plant presents a protistan community composed chiefly by crawling and attached ciliates, with almost no swimming ciliates and flagellates.

Nevertheless, among ciliated protozoa commonly found in activated sludges, there are some species, such as *Acineria uncinata*, *Trachelophyllum pusillum*, and *Drepanomonas revoluta*, which position into a well defined functional group appear problematic in the application of the SBI method. These three ciliate species are considered free-swimming forms but their grazing activity seems to depend more on the floc phase than the liquid one. The arrangement of these species into the appropriate functional group would make the sludge biotic index a more reliable measure to evaluate plant operating conditions.

In order to resolve this problem four different activated-sludge plants were analyzed. In each plant the protistan community was characterized by *Acineria uncinata* Tucolesco 1962 as important component in term of abundance and frequency. The protistan communities and the main operational conditions of the plants were monitored to obtain information useful in determining the SBI functional group to which *A. uncinata* belongs.

MATERIALS AND METHODS

Sampling

The study was carried out in four activated-sludge plants located in the Po River plain (Northern Italy). The plants were monitored weekly. The activated-sludge plant receiving domestic and industrial sewage from the town of Bergamo (BG) was monitored over a two-

year period from May 1993 to May 1995. One of the two plants receiving domestic waste from the town of Reggio Emilia (M1) was monitored from March 1989 to April 1990, while the second plant (M2) was monitored from April to September 1989. The plant at Roncocesi (RO), treating domestic and industrial sewage from a wide area in the province of Reggio Emilia, was monitored from November 1990 to July 1991.

On each sampling event, samples of settled sewage, mixed liquor, and final effluent were collected and conveyed to the laboratory for chemical and biological analysis. Samples of mixed liquor for microscopical observations were kept alive during both carriage and analysis period, by aerating them sufficiently to keep all solids in suspension.

Physico-chemical and operational parameters

In each sampling event, biological oxygen demand (BOD₅), chemical oxygen demand (COD), suspended solids (MLSS), volatile solids (MLVSS) and oxygen uptake rate (OUR) were determined following the *Standard Methods* (APHA 1985). Flow data necessary for the calculation of retention time, sludge age and loading rate, were also registered. The operational conditions of the plants are shown in Table 1. Values of BOD₅ in the effluent were low, indicating a good purification efficiency with values of organic matter removed ranging from 78.3 % to 90.4 %. During the sampling period, dissolved oxygen in the aeration tank was always present at concentrations sufficient to maintain the activated sludge in aerobic conditions. Mean values of D.O. ranged from 2.9 mg/l at plant M2 to 7.3 mg/l at plant BG. During the two-year study the mixed liquor suspended solids (MLSS) in the aeration tank of the plant BG ranged from 3.0 to 4.5 g/l and volatile solids were on average 70% of suspended solids (Goffredi et al. 1996). The other plants showed mean values of MLSS ranging from 2.1 g/l (plant M2) to 5.1 mg/l (plant RO).

Identification and enumeration of microorganisms

Microscopic analysis was performed as soon as possible, and in any case within 2-3 h since sample collection, using both bright field and phase contrast illumination. Ciliated protozoa were identified according to Madoni (1988) and Foissner et al. (1991-1995) and by using special staining techniques such as ammoniacal silver carbonate (Fernandez-Galiano 1976). Other protists than ciliates were not identified but some characteristic forms were assigned to generic level following Streble and Krauter (1981) and Lee et al. (1985).

In each sample, estimates of protozoan population densities were based on enumerations from sub-samples extracted with an automatic micropipette. The most appropriate drop size and number of replicate counts were selected each time, according to the sub-sampling technique described by Madoni (1984). Mostly, 25 µl sub-samples of activated-sludge mixed liquor were taken and two replicates of this volume were counted.

Evaluations of the biological performance of the activated-sludge plant - performed on the basis of the protistan community present - were made using the sludge biotic index (SBI) devised by Madoni (1994).

Statistical analysis of data was performed using the PC application program Stat View II (Feldman et al. 1987), and transforming percent values in $\arcsin \sqrt{P/100}$

RESULTS AND DISCUSSION

During the whole period of study, 32 taxa of ciliated protozoa and 2 taxa of testate amoebae were identified. Not all ciliates were identified to species level, and the testate amoebae not at all. Other protists, such as naked amoebae and flagellates, were also observed. Table 2 shows the list of ciliates and other groups observed in the activated-sludge plants and their relative frequencies and abundances. In the aeration tank of the four plants, density values of ciliated protozoan communities were higher than 1×10^6 individuals per liter of activated-sludge mixed liquor. At plant BG, mean abundance values were 15.4×10^6 ind./l with the greatest density reached in January '94 with 33.3×10^6 ind./l, and the smaller values of density observed in October '93 with 6.5×10^6 ind./l. At plants M1 and M2 mean abundance values were 22.1×10^6 ind./l and 13.6×10^6 ind./l respectively, while at plant RO the ciliate density ranged from 5.1 to 50.7×10^6 ind./l, with a mean value of 17.6×10^6 ind./l.

The dynamics of the three functional groups (free-swimming, crawling, and attached) of the ciliate community are reported in Fig. 1. In most cases, the species making up the ciliate community were present during most of the study period with the exception of free-swimming ciliates of which only *Acineria uncinata* was present during the whole period. The ciliate communities were almost always dominated by attached and crawling forms of which the most representative species were *Vorticella convallaria* and *Aspidisca cicada*, respectively. In some occasions (August '93 and July '94 at plant BG; March, July, and August '89 at plant M2; March '90 at plant RO) the ciliate community was

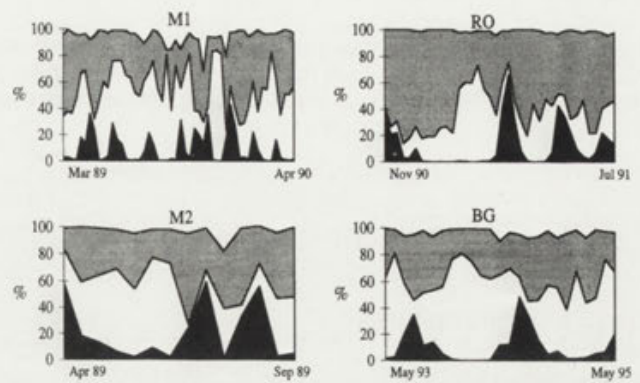


Fig. 1. Temporal changes in the proportion of the three functional groups (free-swimming, crawling, and attached) of the ciliate community in the four studied activated sludge plants, measured in terms of numerical abundance. (Black area- free-swimming ciliates; white area- crawling ciliates; gray area- attached ciliates). Some protists, such as carnivorous ciliates and testate amoebae are not represented here.

dominated by free-swimming forms, represented principally by *Acineria uncinata*.

The values of the sludge biotic index (SBI) are represented in Fig. 2. The judgements obtained from this type of analysis corresponded in most cases to plants belonging to a first quality class (SBI=10) with very well colonized and stable sludge, excellent biological activity, and very good performance (Madoni 1994). Whenever free-swimming forms, represented by *Acineria uncinata*, predominated, the SBI values resulted lower than 6, corresponding to a third class of quality. These values did not agree with the prevalent physico-chemical and operational parameters which indicated a good purifying efficiency.

In the application of the sludge biotic index (SBI), the species *A. uncinata* was assigned to the group of free-swimming ciliates. It is to be underlined that this species

Table 1. Summary of the mean, minimum and maximum values of some physico-chemical and operational parameters in four activated-sludge plants

Parameter	BG	M1	M2	RO
Mixed-liquor temperature (°C)	16.8 (8.8-24.1)	16.6 (8.5-24.6)	19.1 (14.8-25.1)	16.1 (7.0-23.8)
D.O. (mg/l)	7.3 (6.5-7.9)	3.5 (0.9-7.8)	2.9 (0.6-7.7)	5.2 (3.5-8.1)
BOD ₅ influent (mg/l)	116 (70-186)	180 (45-420)	153 (68-350)	187 (54-285)
BOD ₅ effluent (mg/l)	16 (8-46)	41 (8-67)	33 (14-60)	18 (4-46)
Purification efficiency (%)	80.2 (70.1-89.6)	81.4 (69.5-90.1)	78.3 (68.8-93.0)	90.4 (50.0-98.3)
MLSS (g/l)	4.1 (3.0-4.5)	2.4 (1.5-3.0)	2.1 (1.1-3.5)	5.1 (3.5-6.8)
Sludge loading (kgBOD ₅ /kgMLSS d)	0.52 (0.23-0.84)	0.20 (0.16-0.25)	0.21 (0.16-0.28)	0.03 (0.01-0.07)

Table 2. List of ciliates and other protists observed in four activated-sludge plants and their relative frequencies (F) and mean abundances (A) (F- percentage of samples containing the species; A- the average ratio calculated considering the number of individuals belonging to a species divided by the total number of individuals sampled, and expressed as percentage)

Plant	BG		M1		M2		RO	
	F	A	F	A	F	A	F	A
BACTERIVOROUS CILIATES								
Free-swimming forms:								
<i>Acineta uncinata*</i>	96	9.4	90	9.1	100	21.1	91	4.2
<i>Cinetochilum margaritaceum</i>	3	<1	3	<1	-	-	-	-
<i>Colpidium colpoda</i>	23	<1	-	-	-	-	4	<1
<i>Drepanomonas revoluta*</i>	13	<1	100	2.0	43	<1	56	<1
<i>Glaucoma scintillans</i>	<1	<1	-	-	-	-	-	-
<i>Paramecium caudatum</i>	4	<1	-	-	-	-	-	-
<i>Tetrahymena pyriformis</i>	5	<1	-	-	-	-	-	-
<i>Trachelophyllum pusillum*</i>	-	-	-	-	-	-	4	<1
<i>Uronema nigricans</i>	7	<1	25	<1	7	<1	-	-
Crawling forms:								
<i>Aspidisca cicada</i>	100	41.3	100	47.2	100	37.1	100	40.4
<i>Aspidisca lynceus</i>	9	<1	7	<1	-	-	-	-
<i>Chilodonella uncinata</i>	95	4.9	42	<1	71	1.0	52	<1
<i>Euplotes</i> sp.	71	2.3	83	1.3	78	1.9	30	<1
<i>Strylonychia</i> sp.	6	<1	-	-	-	-	-	-
<i>Trithigmostoma cucullulus</i>	85	1.5	3	<1	7	<1	-	-
<i>Trochilia minuta</i>	3	<1	27	1.5	78	1.4	65	<1
Attached forms:								
<i>Carchesium</i> sp.	-	-	5	<1	14	<1	56	5.7
<i>Epistylis</i> spp.	94	6.3	73	3.8	100	11.9	100	13.4
<i>Opercularia</i> spp.	90	5.1	93	7.6	93	5.2	100	15.5
<i>Stentor</i> sp.	<1	<1	-	-	-	-	-	-
<i>Vorticella aquadulcis</i>	83	2.7	93	3.7	93	2.3	100	13.0
<i>Vorticella convallaria</i>	99	11.7	95	13.2	100	12.6	91	5.2
<i>Vorticella microstoma</i>	75	1.0	93	4.4	100	3.3	9	<1
<i>Vorticella</i> sp.	99	6.6	-	-	-	-	-	-
<i>Zoothamnium</i> sp.	96	2.5	29	3.2	21	<1	26	<1
CARNIVOROUS AND OMNIVOROUS CILIATES								
<i>Acineta</i> sp.	64	<1	25	<1	14	<1	35	<1
<i>Amphileptus</i> sp.	2	<1	-	-	7	<1	-	-
<i>Coleps hirtus</i>	<1	<1	-	-	-	-	-	-
<i>Litonotus</i> spp.	67	<1	59	<1	93	<1	39	<1
<i>Podophrya</i> sp.	72	<1	46	<1	64	<1	17	<1
<i>Prorodon</i> sp.	<1	<1	-	-	-	-	-	-
<i>Tokophrya</i> spp.	11	<1	41	<1	50	<1	26	<1
Naked amoebae								
Testate amoebae:								
<i>Arcella</i> sp.	3	<1	19	<1	43	<1	96	<1
<i>Euglypha</i> sp.	4	<1	17	<1	14	<1	39	<1
Large flagellates:								
<i>Euglena</i> sp.	2	<1	42	<1	50	<1	13	<1
<i>Peranema</i> sp.	47	<1	-	-	-	-	-	-

* Incertae sedis: these species are considered free-swimming forms but their grazing activity seems to be linked to the floc (Madoni 1994)

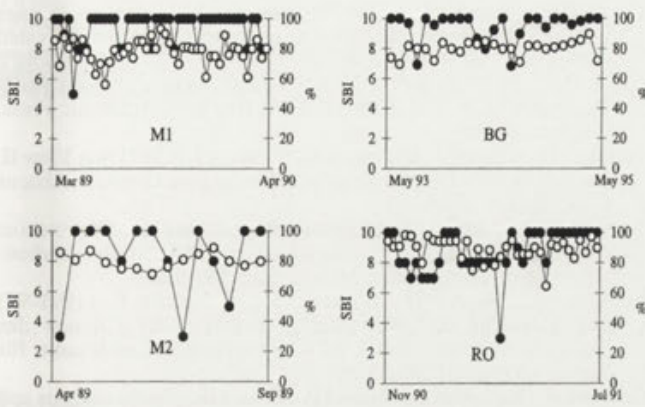


Fig. 2. Values of sludge biotic index SBI (•), obtained with the protistan community for the four activated-sludge plants, compared with the concomitant percentage of BOD₅ removal (o). (The SBI values were obtained including *Acineria uncinata* in the free-swimming ciliate functional group)

was the only component of the free-swimmer group in the major part of samples collected. Consequently, the estimate of the SBI values reported in Fig. 2 resulted in some occasions heavily influenced by having considered *A. uncinata* as a free-swimming form. In these cases estimated SBI values were not in agreement with purification efficiency revealed by chemical and operational parameters (Fig. 2, Table 1). Moreover, comparing the values of sludge loading (Table 1) with the trend of free-swimming ciliates (Fig. 1) emerges that *A. uncinata* showed the highest abundance values on occasions of low sludge loading (< 0.2 kg BOD₅/kg MLSS d). This is in contrast with Curds and Cockburn (1970) who found free-swimming forms to dominate ciliate community at high sludge loadings (0.6-0.9 kg BOD₅/kg MLSSd).

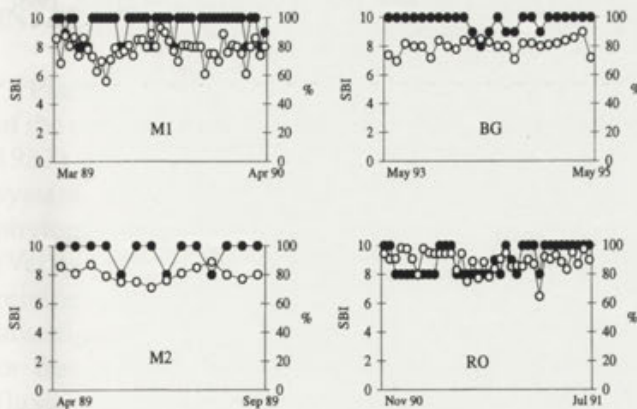


Fig. 3. Values of sludge biotic index SBI (•), obtained transferring *Acineria uncinata* in the crawling ciliate functional group, and compared with the concomitant percentage of BOD₅ removal (o)

The above observations suggest that *A. uncinata* should not be regarded as a free-swimming form, and the results obtained in this paper strengthened the critical position assigned by Madoni (1994) to this species, classified as “incertae sedis” when the SBI method is used. If *A. uncinata* would be transferred to the crawling ciliates the SBI values would always be higher than 7, i.e. to a first class of quality, in agreement with purification efficiency revealed by chemical and operational parameters (Fig. 3).

By testing the existence of possible relationships between *A. uncinata* and the other functional groups (crawling and attached ciliates) was an expedient to see whether data collected in the present work could be useful to the widening of this important question. For this purpose, statistical analysis of regression was performed on the data. Results obtained (Fig. 4) revealed a negative linear relation between *A. uncinata* and crawling ciliates, whilst no correlation was observed between this species and attached ciliates. In addition we performed a non-parametric correlation analysis (Kendall τ); results obtained confirm the previous outcomes of parametric regression test (RO: $\tau = -0.431$, $p = 0.0001$; BG: $\tau = -0.601$, $p = 0.0001$; M1: $\tau = -0.424$, $p = 0.0001$; M2: $\tau = -0.495$, $p = 0.01$). It appears thus that in the activated sludge *A. uncinata* puts itself in a relationship of competition with crawling ciliates, occupying the same ecological niche. It is well-known, in fact, that in activated sludge sessile and crawling forms normally coexist without competition because of their different ecological niches. By contrast, sessile and free-swimming ciliates compete for bacteria and small flagellates dispersed in the mixed

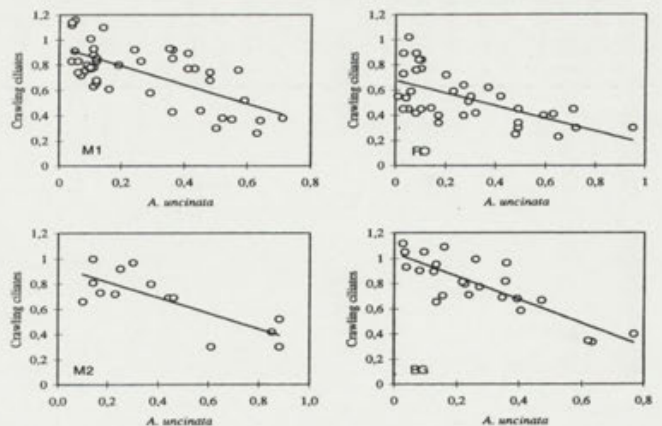


Fig. 4. Relationship between crawling ciliates and *Acineria uncinata* in the four activated-sludge plants during the studied period (BG: $y = -0.893x + 1.039$; $r^2 = 0.675$; M1: $y = -0.745x + 0.939$; $r^2 = 0.456$; M2: $y = -0.617x + 0.938$; $r^2 = 0.609$; RO: $y = -0.473x + 0.663$; $r^2 = 0.415$). Data are represented as arcsin $\sqrt{p/100}$ of abundance percentage values

liquor (Madoni 1994). Moreover, every species within each functional group competes with each other depending on the ecological niche occupied. According to Augustin et al. (1987) *A. uncinata* eats only small prey (flagellates) because of its restricted cytostome. The data presented here, however, suggest that *A. uncinata* in the activated sludge might be considered more similar to that of effluent clarifiers such as filter feeding ciliates than that of carnivorous ciliates, even though *A. uncinata* carry out its activity on the floc rather in the mixed liquor. Nevertheless, further direct microscopical examination of *A. uncinata* isolated from an activated-sludge plant might give a clue as to whether it adopts a "free-swimming" or a "crawling" mode of behaviour.

In conclusion, this study revealed that in the activated-sludge process a close correlation exists between *A. uncinata* and crawling ciliates, indicating it is unlikely that this species is a free-swimming form. Nevertheless, more supporting experimental evidence is needed, in order to confirm this and to clarify the position of *A. uncinata* in the SBI functional groups as a crawling form rather a free-swimming form.

Acknowledgments. This research was supported by grants from the Italian Ministry of University and Scientific & Technological Research (MURST).

REFERENCES

- Antonietti R., Broglio P., Madoni P. (1982) The evaluation of biological parameters as indicators of purification efficiency in activated sludge plants. *Ingegneria Ambientale* **11**: 472-477
- APHA (1985) Standard Methods for the Examination of Water and Wastewater. American Public Health Association, Washington
- Augustin H., Foissner W., Adam H. (1987) Revision of the genera *Acineria*, *Trimyema* and *Trochiliopsis* (Protozoa, Ciliophora). *Bull. Br. Mus. nat. Hist. (Zool.)* **52**: 197-224
- Curds C.R., Cockburn A. (1970) Protozoa in biological sewage treatment processes. II. Protozoa as indicators in the activated sludge process. *Wat. Res.* **4**: 225-236
- Curds C.R. (1975) Protozoa. In: Ecological Aspects of Used Water Treatment, (Eds. C.R. Curds & H.A. Hawkes). Academic Press, London, 203-268
- Feldman D., Gagnon J., Hofmann R., Simpson J. (1987) Stat View II. The Solution for Data Analysis and Presentation Graphics. Abacus Concepts Inc., Berkeley.
- Fernandez-Galiano D. (1976) Silver impregnation of ciliated protozoa: procedure yielding good results with the pyridinated silver carbonate method. *Trans. Amer. Micros. Soc.* **99**: 52-60
- Foissner W., Berger H., Blatterer H., Kohmann F. (1991-95) Taxonomische und ökologische Revision der Ciliaten des Saprobiensystems. Band 1-IV. Bayerisches Landesamt für Wasserwirtschaft, München
- Goffredi A., Benedetti L., Madoni P. (1996) Microfauna analysis and sludge biotic index evaluation of Bergamo's waste treatment plant. *Acqua-Aria* **4**: 421-425
- Lee J.J., Hunter S.H., Bovee E.C. (1985) An Illustrated Guide to the Protozoa. Society of Protozoologists, Lawrence, Kansas
- Madoni P. (1982) Growth and succession of ciliate populations during the establishment of a mature activated sludge. *Acta Hydrobiol.* **24**: 223-232
- Madoni P. (1984) Estimation of the size of freshwater ciliate populations by a subsampling technique. *Hydrobiologia* **111**: 201-206
- Madoni P. (1988) I Protozoi Ciliati nel Controllo di Efficienza dei Fanghi Attivi. C.I.S.B.A., Reggio Emilia
- Madoni P. (1994) A sludge biotic index (SBI) for the evaluation of the biological performance of activated sludge plants based on the microfauna analysis. *Wat. Res.* **28**: 67-75
- Madoni P., Ghetti P.F. (1981) The structure of ciliated protozoa communities in biological sewage-treatment plants. *Hydrobiologia* **83**: 207-215
- Streble H., Krauter D. (1981) Das Leben im Wassertropfen. W. Keller & Co., Stuttgart
- Tucolesco J. (1962) Etudes protozoologiques sur les eaux Roumaines. I. Espèces nouvelles d'infusoires de la mer Noire et des bassins salés paramarins. *Arch. Protistenk.* **106**: 1-36

Received on 24th December, 1995; accepted on 29th March, 1996

Interactions between Planktonic Protozoans and Metazoans after the Spring Bloom of Phytoplankton in a Eutrophic Lake, the Belauer See, in the Bornhöveder Seenkette, North Germany

Heike ZIMMERMANN

Max-Planck-Institut für Limnologie, Plön, Germany

Summary. To obtain information about the planktonic protozoans that form a link in the flux of matter from bacterio- to metazooplankton in the eutrophic Belauer See, one of the lakes in the Bornhöveder Seenkette of North Germany, abundance, biomass, production, and grazing loss rates of the planktonic bacteria, algae, ciliates, flagellates, rotifers, and crustaceans were estimated. Different trophic levels were isolated using the size fractionation technique, and each was exposed for 24 and 48 h to ambient conditions. Changes in their population densities were recorded. Toward the end of winter, herbivorous protozoan plankton developed together with small algae. Protozoans that feed on algae were predominant during our experiments in spring. They were preyed upon in turn by rotifers and crustaceans. The protozoan community structure was influenced by the presence of cyclopoid copepods, which were also the main predators on rotifers. Cyclopoids were the main top-down controlling organisms in the pelagic food web during the spring.

Key words: energy flux, eutrophic lake, metazoa, pelagic food web, protozoa.

INTRODUCTION

Planktonic protozoans constitute an important part of the microbial food web (Pomeroy 1974, Azam et al. 1983) and play two principal roles in the aquatic system. They are the intermediate organisms that link phytoplankton and bacteria with higher trophic levels (Verity 1991), and they are important sources of remineralized nutrients (Caron 1991). Quantitative investigations of all components of the protozooplankton in freshwater systems with calculations of energy fluxes (Weisse et al. 1990, Gaedke and Straile 1994) are rare. Protozoa were investigated in Lake Oglethorpe

(Sanders et al. 1989), the Lake of Constance (Weisse et al. 1990, Geller et al. 1991), the Müggelsee (Arndt and Nixdorf 1991), and water bodies near Schwerin (Mathes and Arndt 1995).

In recent years, studies on the activity and biomass of bacteria and protozoans showed that the bacterioplankton is controlled mainly by protozooplankton (Güde 1989, Weisse 1990), while metazooplankton has an impact on the protozoa (Güde 1988, Stoecker and Capuzzo 1990, Arndt 1993, Jürgens 1994). There is little information about interactions among the species in the protozooplankton (Weisse 1990, Arndt and Nixdorf 1991) and about their impact on phytoplankton in early spring. The authors who formulated the PEG-model (Sommer et al. 1986, Sommer 1994) thought that small phytoplankton was consumed mainly by small metazooplankton. The im-

Address for correspondence: Heike Zimmermann, Institut für Hydrobiologie und Fischereiwissenschaft, Universität Hamburg, Zeiseweg 9, D-22765 Hamburg, Germany; E-mail: hz@rrz.uni-hamburg.de

pect of protozooplankton on phytoplankton was not even considered by the authors of the PEG-model.

The experiments performed at the Belauer See are the first to encompass all components of the microbial food web in an eutrophic lake during spring. They are designed to assess the importance of protozooplankton, which includes the first herbivorous species to develop a large biomass during the spring phytoplankton bloom. Their interactions with various functional groups were studied while the phytoplankton was developing.

MATERIALS AND METHODS

Study site

Belauer See, a lake in the Bornhöveder Seenkette in North Germany, is a holomictic, dimictic, eutrophic lake with an area of 1.13 km² and a maximal depth of 29.6 m (Müller 1981).

Sampling

Water samples were collected at seven different depths: 1, 3, 5, 10, 15, 20 and 25 m, from the deepest part of the lake at biweekly intervals from January to June.

Picoplankton and flagellate abundance

Samples for determination of picoplankton and flagellate abundance were fixed in 1.5% formalin and stained with the fluorochrome, 4',6-diamidino-2-phenylindole (DAPI), according to Porter and Feig (1980). The picoplankton was counted on black membrane filters.

Chlorophyll *a* biomass

The lake water was filtered through a 47 mm Whatman GF/F glassfiber filter and frozen at -20°C. The pigments were extracted with ethanol according to the methods of Nusch (1980). A 2.0 l sample was filtered.

Primary production

Primary production within the particulate fraction was calculated as incorporated ¹⁴C according to Tilzer and Beese (1988).

Ciliate abundance

Samples of 0.2 l used to investigate the ciliates were fixed immediately after sampling by adding 0.06% HgCl₂. Ciliates were counted under the Utermöhl inverted microscope (Utermöhl 1958). Samples of 0.01 l were allowed to settle for 24 h; then, the entire surface of the settling chamber was examined at 200 x magnification. Ciliates were determined in most cases to the level of genus and sorted according to their size groups.

Crustacean abundance

The abundance of crustaceans was recorded in samples fixed with 4% formalin.

Size fractionation technique

To study the growth rates, grazing impact, and energy fluxes from the picoplankton to the metazoans in spring, the size fractionation technique (Arndt 1990, Landry 1994) was employed in April 1991. The water column below 3 m was sampled by making four hauls with a 3.6 l Haney chamber (Haney 1971).

To separate the species at the higher trophic levels in the plankton, the water was filtered through 150, 44 and 15 µm sieves. Filtered and unfiltered water (UF) as well as water enriched with zooplankton (3 x >150 µm and unfiltered water, ZP) was placed in 1 l glass bottles. All procedures were performed on triplicate samples. The bottles were exposed on a rotating wheel under ambient conditions.

Abundance and biomass of the autotrophic picoplankton (APP), bacteria, algae and protozoa were determined at the beginning of the experiment and after incubation periods of 24 and 48 h. The protozoa were separated into several groups: nanoflagellates (NF), flagellates smaller than 20 µm, large heterotrophic flagellates (LF), flagellates larger than 20 µm, nanociliates smaller than 20 µm (NC), and ciliates larger than 20 µm (LC). Rotifers and crustaceans were counted at the start and at the end of the experiments.

The phytoplankton, ciliate, and rotifer species were identified in samples fixed in Lugol's solution as described above. The abundance of bacteria, APP, NF, rotifers, and crustaceans were determined as described above. The size of the bacteria, APP, and NF was measured using an image analysis system developed and described by Schröder and Krambeck (1991). The sizes of the algae, ciliates, and rotifers were measured under the microscope, and the volume was calculated using appropriate formulas (Ruttner-Kolisko 1977). Crustacean abundance was converted to biomass according to known relationships between body length and dry weight (Downing and Rigler 1984).

The number of cells and their biovolumes were used to calculate the amount of carbon using the following conversion factors: for bacteria 15 fg C cell⁻¹ (Simon and Tilzer 1987); NF 220 fg C µm⁻³ (Børsheim and Bratbak 1987); ciliates 110 fg C m⁻³ (Turley et al. 1986); rotifers 50% of dry weight, and crustaceans 43% of dry weight (Weisse et al. 1990). For a rough calculation of total phytoplankton C, we converted chlorophyll *a* values to C, assuming a C: chlorophyll *a* ratio of 25:1, which is typical for phytoplankton during spring blooms in lakes (Bell and Kuparinen 1984).

Protozoan production was estimated from the mean cell concentrations and the calculated size specific growth rates (Zimmermann 1994). The production of metazooplankton was derived from the calculated community ingestion rates, assuming a growth efficiency of 25% (Bosselmann and Riemann 1986). To determine the food supply of the protozoa, their ingestion rates were calculated, assuming that 200% of the body weight per day must be ingested by individuals in the size class from 5 to 50 x 10³ µm³, when their production efficiency is 50%. An ingestion rate greater than 300% of the body weight is assumed for smaller individuals, and 150% for larger ones (Laybourn-Parry 1984).

RESULTS

In early spring algae were dominated in the eutrophic Belauer See by Bacillariophyceae, followed in abundance by crysophyceans. The centric diatoms, *Cyclotella radiosa* (Grunow) Lemmermann 1900, *Stephanodiscus minutulus* (Kützing) Cleve and Möller 1878 and *Stephanodiscus*

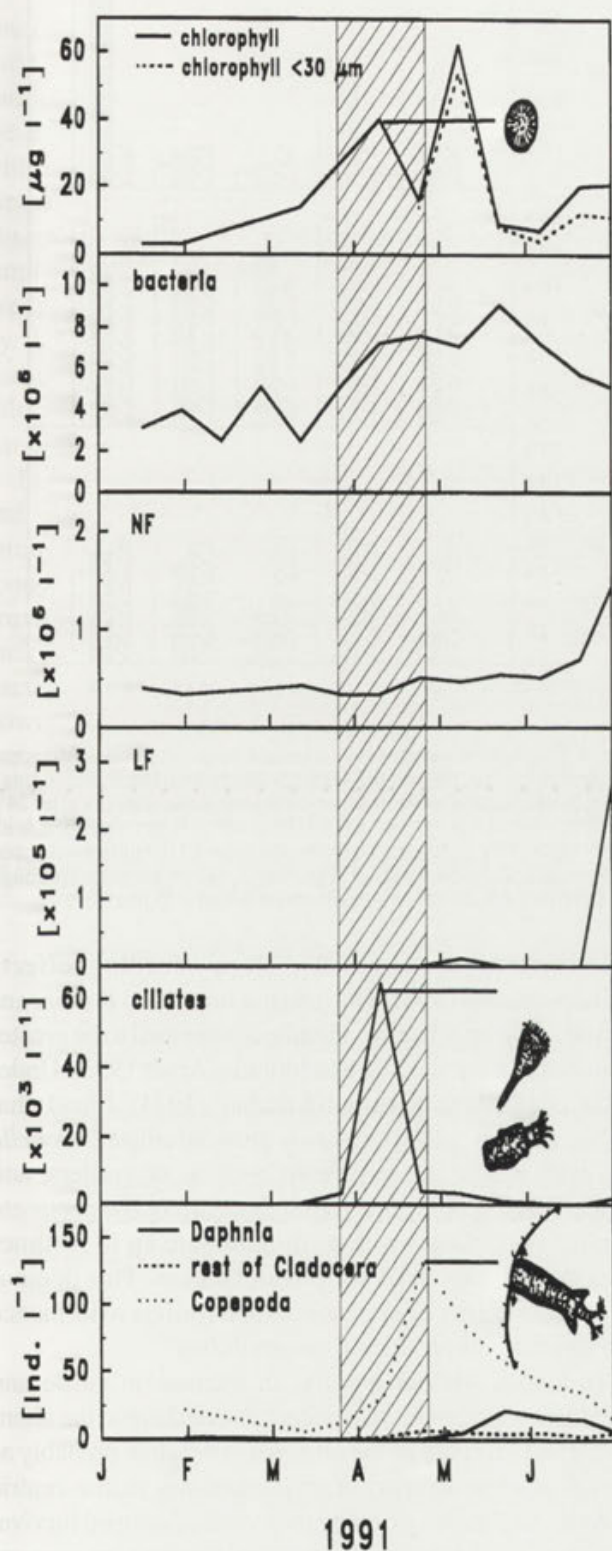


Fig. 1. Seasonal changes in total chlorophyll *a* ($\mu\text{g l}^{-1}$) and chlorophyll *a* in the $<30 \mu\text{m}$ fraction ($\mu\text{g l}^{-1}$), bacteria (cells $\times 10^5 \text{ l}^{-1}$), NF - nanoflagellates (cells $\times 10^6 \text{ l}^{-1}$), LF (flagellates $>20 \mu\text{m}$ (cells $\times 10^5 \text{ l}^{-1}$), ciliates (cells $\times 10^3 \text{ l}^{-1}$), and crustaceans (individuals l^{-1}) in 1991. Data are available at the ÖSF-database, University of Kiel, Project Centre Ecosystem research, D-24118 Kiel

parvus Stoermer and Håkansson 1984, were most numerous until the middle of April. Planktonic bacteria (Fig. 1) showed much less variability in abundance. APP was not significantly represented during spring. Ciliates were scarce in winter (Fig. 1) but became more abundant during the first phytoplankton bloom, which was produced by diatoms. NF and LF (Fig. 1) were not numerous in spring. The crustaceans (Fig. 1) were most numerous in spring, when copepods were predominant.

The experiments were performed in the middle of April, three days before the phytoplankton abundance maximum in spring of $650 \text{ mg chlorophyll } a \text{ m}^{-2}$ (Fig. 1) was recorded. In April 1991, several weeks of calm, sunny weather produced a rapid increase in the surface water temperature and an incipient thermal stratification. When the surface temperature reached about 5.5°C , the chlorophyll *a* concentration started to rise rapidly (Fig. 1). During the first phytoplankton peak, the centric diatoms, *Cyclotella radiosa*, *Stephanodiscus minutulus* and *Stephanodiscus parvus*, were predominant. The algae at this time were small and could be consumed by the ciliates. Of the 12×10^9 bacterial cells l^{-1} , 5×10^9 bacteria l^{-1} were in the size class $>0.54 \mu\text{m}$. They began to become more abundant in the middle of April together with the phytoplankton. The maximal abundance of the ciliates was 65×10^3 individuals l^{-1} . The ciliate community consisted primarily of 13 ciliate species. *Vorticella rhabdostyloides* Kellicot 1885, (18×10^3 cells l^{-1}) and *Tintinnidium fluviatile* (Stein 1863) Kent 1881 (47×10^3 cells l^{-1}) were the most abundant of them. The NF increased to about 6.87×10^6 cells l^{-1} and the LF, mainly *Gymnodinium helveticum* var. *apiculatum* (Zacharias) Utermöhl 1925, to about 36×10^3 cells l^{-1} . The only crustaceans present were the copepods, *Cyclops kolensis* Lilljeborg 1901, *Cyclops vicinus* Uljanin 1875, and *Eudiaptomus graciloides* Lilljeborg 1888. They were mostly copepodids, and only a few adults were present. Populations of the cladocerans, *Daphnia longispina* O. F. Müller 1785, *Bosmina longirostris* O. F. Müller 1785, and *Chydorus sphaericus* O. F. Müller 1784, were also present, together with 13 rotifer species, the most abundant of which was the raptorial *Synchaeta pectinata* Ehrenberg 1832.

Dissolved P decreased sharply near the surface of the water while the bloom was developing. During the peak, TDP decreased. $\text{NO}_3\text{-N}$ and silica concentrations also decreased during the course of the bloom.

Figure 2 shows that five size fractions were used: ZP, UF, $<150 \mu\text{m}$, $<44 \mu\text{m}$ and $<15 \mu\text{m}$. In bottles to which metazoans, such as *Cyclops* sp., were added, there were significant reductions in the abundance of protozooplankton

(ANOVA: $p < 0.05$). After 48 h, 50% of the ciliates and 25% of the LF and NF communities had been eliminated.

All protozoan species increased in abundance. The LF showed a decrease of about 75% in bottles with organisms $< 150 \mu\text{m}$. There was a significant increase in the NF in bottles with organisms $< 44 \mu\text{m}$ and $< 15 \mu\text{m}$. The ciliates also increased in abundance in bottles $< 15 \mu\text{m}$.

DISCUSSION

The growing season started with the onset of thermal stratification in spring. Due to the stratification, turbulent mixing was reduced, and therefore, the average light intensity to which phytoplankton was exposed increased. Nutrients had accumulated in the water column during the winter and the onset of stratification ended the period of light limitation. Favourable light conditions and nutrient availability promote rapid algal growth and seasonal changes in phytoplankton abundance. The events followed typical patterns of a succession that have been described for eutrophic lakes (Sommer et al. 1986). The subsequent increase in phytoplankton biomass and the first peak in primary production occur during the spring phytoplankton bloom. The phytoplankton was dominated by centric diatoms during its peak in spring. The zooplankton consisted of mainly herbivorous organisms, which developed together with the phytoplankton (Fig. 1). These included *Tintinnidium* and *Gymnodinium*, two protozoans, that graze on centric diatoms (Zimmermann 1994). The turnover of herbivorous metazooplankton was low in early spring. Ciliates and LF include important phytoplankton grazers. These utilized plants for most of their food. A close relationship between algal biomass and bacterial abundance (Bell and Kuparinen 1984, Lancelot and Billen 1984) is apparent in Fig 2. Aquatic bacterial production is currently thought to be largely controlled by NF and LF, which are the most important consumers of bacteria (Sherr and Sherr 1984, Porter et al. 1985).

Cyclops kolensis, a raptorial feeder, was the most important top-down controlling organism in the planktonic community during spring. In bottles without copepods, the rotifers, *Asplanchna priodonta* Gosse 1850, and *Synchaeta pectinata*, increased in abundance, while ciliates and LF became scarce. Rotifers ingested two to five ciliates per hour under natural conditions (Zimmermann 1994), and like crustaceans (Berk et al. 1977), they are able to meet their energy requirements by feeding on protozoans. Experiments with labelled *Cyclidium* sp. demonstrated that ciliates were really consumed rather

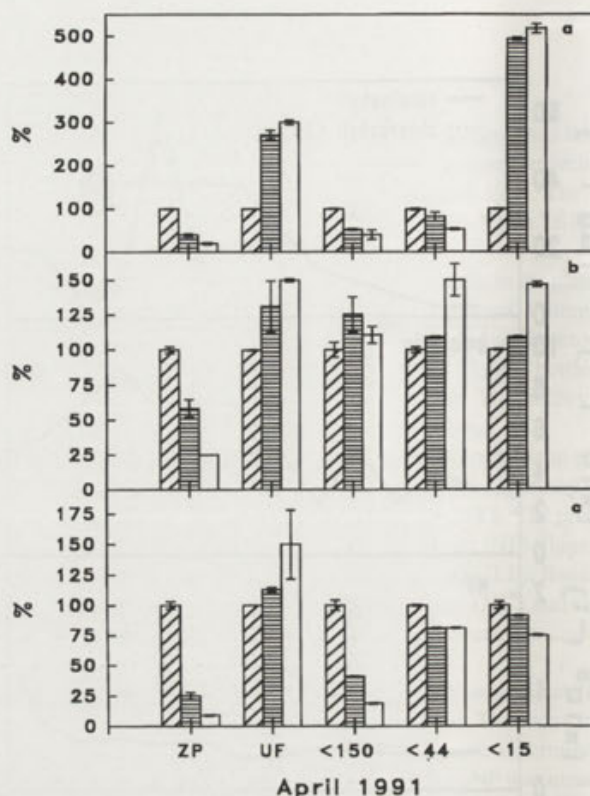


Fig. 2. Changes in percent and standard error of: ciliates (diagonal hatched columns), NF - nanoflagellates (horizontal hatched columns), and LF - flagellates $> 20 \mu\text{m}$ (open columns) at the start (a), after 24 h (b) and after 48 h (c), in April 1991. ZP - water enriched with zooplankton ($3 \times < 150 \mu\text{m}$ and unfiltered water), UF - unfiltered water, < 150 - water filtered through a $150 \mu\text{m}$ sieve, < 44 - water filtered through a $44 \mu\text{m}$ sieve and < 15 - water filtered through a $15 \mu\text{m}$ sieve

than merely destroyed by sloppy-feeding effects (Zimmermann 1994). The grazing impact on protozoans by rotifers with grasping mouthparts seemed to be greater than that of filter feeding brachionids (Arndt 1993). Under field conditions, Ejsmont-Karabin (1974) found that *Asplanchna* sp. fed on the slowly growing ciliate *Codonella* sp., with nearly the same efficiency as on rotifers, and Gilbert and Jack (1993) found that *Synchaeta pectinata* can feed on ciliates with a filtration rate up to 50 times greater than that used for phytoplankton. This demonstrated the ability of crustaceans and rotifers to influence the structure of protozoan communities.

In bottles without grazers, an increase in ciliate and flagellate abundance was evident. Nevertheless, the abundance and diversity of the protozoans was low probably as a result of a low diversity of prey organisms, such as centric diatoms and bacteria. Some protozoans developed survival strategies during the spring to escape the predator pressure by rotifer and cyclopoids. *Ceratium* and *Gymnodinium*, two dinoflagellates, produced large single cells, unwieldy for most grazers. *Vorticella rhabdostyloides*, a peritrich ciliate, was not evident during cursory examinations because it attaches to centric diatoms, and many ciliates, including

Tintinidium fluviatile, *Tintinidium cylindrata* Kofoid and Campbell 1929, and *Codonella cratera* Leidy 1877, had loricas that serve as refuges from raptorial feeders. Nevertheless, many copepods ingested tintinnids together with their loricas, which were sometimes visible in the faecal pellets of the copepods. However it was sometimes observed that only the tintinnids were eaten and their empty loricas were discarded (Zimmermann unpubl.). Predators kept their abundance below the carrying capacity. In spring, 50% of the ciliate standing stock was consumed through metazooplankton grazing. Similar results were described by Stoecker and Capuzzo (1990) and Sanders and Wickham (1993).

In contrast to that the most phytoplankton, nanoflagellate and ciliate can nearly compensate for grazing losses through their more rapid rates of reproduction when ample food is available (Jürgens, Arndt and Zimmermann unpubl.). It was observed that protozoans were below their carrying capacity while food, phytoplankton and bacteria, were not limited. They were controlled top down and were replaced by large, effective grazing metazooplankton, which produced the first metazooplankton peak.

Although the size fractionation technique is considered to be an effective method to manipulate the planktonic

community, evidence suggests that predators and prey are not unambiguously separated by filters (Fuhrman and McManus 1984, Goldman and Caron 1985) and that the fractionation step may cause cell damage and enrichment with dissolved organic substances (Fuhrman and Bell 1985). These fundamental problems might cause the growth rates of prey determined in "predator-free" controls to be either depressed by grazers or stimulated artificially by organic enrichment. The situation is further complicated by the fact that the larger size fraction includes producers, grazers, and nutrient regenerators with varied feedback relationships with the growth of the microbial populations (Sieburth and Davis 1982, Sherr et al. 1988, Stone 1990). However, the amount of error was small, and so we used the results to estimate the causal relationships within the plankton community in the C flow model (Fig. 3). There was no direct energy flow in the C flow model from the lowest trophic level, picoplankton and phytoplankton, to the highest level, *Cyclops* sp. Both ciliate groups, large ciliates and nanociliates, consumed mainly phytoplankton. Herbivorous metazooplankton was unimportant. It is obvious that a large fraction of primary production was channelled through the microbial loop during the spring bloom. Judging from the ciliate species present, it is concluded that relatively few bacteria are

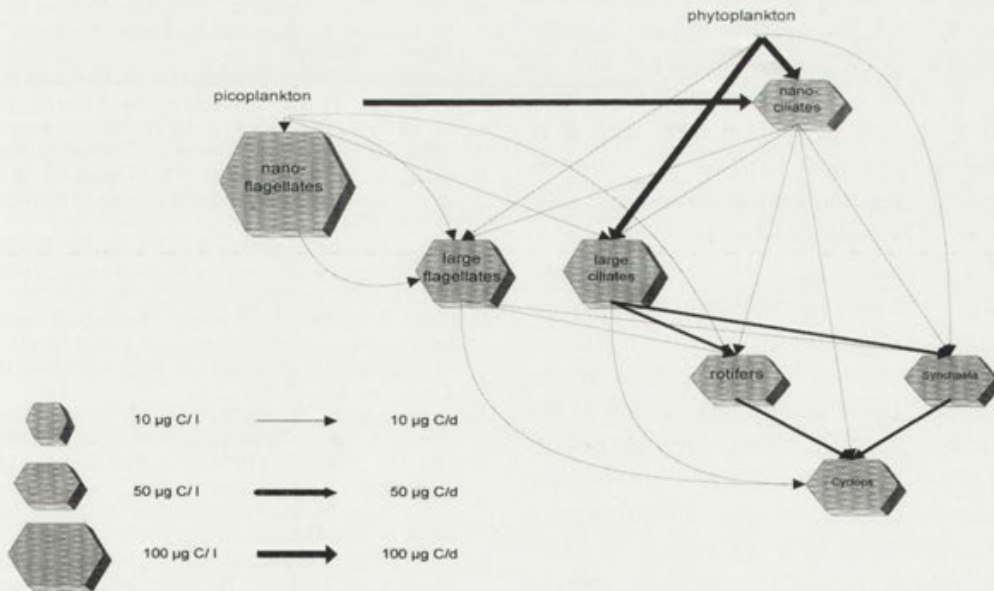


Fig. 3. Biomass (mg C l⁻¹) and matter flux (mg C d⁻¹) in the microbial food web of the Belauer See in April 1991

consumed by ciliates in spring (Müller 1989, Müller et al. 1990). Some small ciliates, such as *Urotricha* sp., preferred picoplankton, which consisted chiefly of bacteria, because the APP was not abundant at that time. The C demand of NF, 25%, was low relative to bacterial production. In contrast to the results of Weisse et al. 1990, the production by NF was low and there was little consumption of NF by ciliates in the Belauer See during those experiments. In the Belauer See, the situation was different, but the LF, especially the herbivorous *Gymnodinium helveticum*, also seemed to be an important component of the microbial food web. Compared to the combined protozoan consumption, the feeding impact of metazoans, especially copepods, was slight. The top-down controlling function of copepods during spring seemed to be similar to that of the cladocerans during the clear water phase. One result of the present study showed the necessity to determine protistan standing stocks and their grazing impact on the planktonic food webs during spring. It was obvious that a large fraction of the phytoplankton is channelled through the microbial food web during the spring bloom (Weisse et al. 1990), because herbivorous protozoans developed together with the phytoplankton and earlier than the herbivorous metazooplankton. Grazing by herbivorous metazooplankton is generally believed to play a major role. As biomass of larger herbivorous zooplankton such as small copepodids and rotifer, was low in April, the grazing impact on phytoplankton should have been mainly due to microzooplankton. Pelagic protozoa with their high intrinsic growth rates are better able to respond to the rapid increase in food supply than in the metazooplankton. Ciliates and LF were important phytoplankton grazers. They obtained most of their food as herbivores. Furthermore, they are likely to constitute a major part of the diet of cyclopoid copepodids at the beginning of the year. In this way a substantial amount of phytoplankton may reach larger zooplankton organisms, especially if growth efficiency of the ciliates turns out to be high in spring. Another important fact is that the microbial food web components, with their short doubling time, produce the spring peak in response to the increased substrate supply originating from phytoplankton secretion, cell lysis, and the crushing of the prey during feeding. In contrast to the findings of Azam et al. (1983) and Porter et al. (1988), in eutrophic waters, the microbial food web was assumed to be of major importance.

Acknowledgements. I am indebted H. Arndt, K. Jürgens, H. Kausch and W. Lampert who provided much information during discussions of the work. I also gratefully acknowledge the support of my colleagues S. Barkmann, W. Fleckner, K. Moaledj, and P. Witzel, who provided data on chlorophyll *a* and APP, zooplankton, bacterial plankton, and chemistry. Thanks are also due to C. W. Heckman, who corrected the English, and the two anonymous reviewers for constructive criticism of an earlier version of this manuscript. This work was supported by the Bundesministerium für Forschung und Technologie (BMFT) with a research grant to Heike Zimmermann as part of "Ökosystemforschung im Bereich der Bornhöveder Seenkette".

REFERENCES

- Arndt H. (1990) Das pelagische "microbial web" in einem eutrophen Flachsee: Jahreszeitliche Unterschiede in der Wechselwirkung zwischen Proto- und Metazooplankton. Deutsche Gesellschaft für Limnologie, Erweiterte Zusammenfassung der Jahrestagung in Essen, 112-116
- Arndt H. (1993) Rotifer as predators on components of the microbial web (bacteria, heterotrophic flagellates, ciliates) - a review. *Hydrobiol.* **76**: 387-396
- Arndt H., Nixdorf B. (1991) Spring clear water phase in aneutrophic lake: Control by herbivorous zooplankton enhanced by grazing on components of the microbial web. *Verh. Int. Ver. Limnol.* **24**: 879-883
- Azam F., Fenchel T., Field J. G., Gray J. S., Meyer-Reil L. S., Thingstad F. (1983) The ecological role of water-column microbes in the sea. *Mar. Ecol. Progr. Ser.* **10**: 257-263
- Bell R. T., Kuparinen A. J. (1984) Assessing phytoplankton and bacterioplankton production during early spring in lake Erken, Sweden. *Appl. Environ. Microbiol.* **48**: 1221-1230
- Berk S. G., Brownlee D. C., Heinle D. R., Kling H. S., Colwell R. R. (1977) Ciliates as a food source for marine planktonic copepods. *Microb. Ecol.* **4**: 27-40
- Børsheim K. Y., Bratbak G. (1987) Cell volume to carbon conversion factor for a bacterivorous *Monas* sp. enriched from seawater. *Mar. Ecol. Progr. Ser.* **36**: 171-175
- Bosselmann S., Riemann B. (1986) Zooplankton. In: Carbondynamics in eutrophic temperate lakes, (Eds. B. Riemann, M. Sondergaard). Elsevier, 199-236
- Caron D. A. (1991) Evolving role of Protozoa in aquatic nutrient cycles. In: Protozoa and their role in marine processes, (Eds. P. C. Reid, C. M. Turley, P. H. Burkil). Springer-Verlag, Berlin, Heidelberg. *NATO/ASI Series G, Ecological Science* **25**: 387-415
- Downing J. A., Rigler F. (1984) A manual on methods for the assessment of secondary productivity in fresh water, 2nd ed. IBP Handbook 17. Blackwell
- Ejsmont-Karabin P. (1974) Studies on the feeding of planktonic polyphage *Asplanchna priodonta* Gosse (Rotatoria). *Ekol. Pol.* **22**: 311-317
- Fuhrman J. A., Bell T. M. (1985) Biological considerations in the measurement of dissolved free amino acids in seawater and implications for chemical and microbiological studies. *Mar. Ecol. Progr. Ser.* **25**: 13-21
- Fuhrman J. A., McManus G. B. (1984) Do bacteria-sized eukaryotes consume significant bacterial production? *Science* **224**: 1257-1260
- Gaedke U., Straile D. (1994) Seasonal changes of the quantitative importance of protozoans in a large lake. An ecosystem approach using mass-balanced carbon flow diagrams. *Mar. Microb. Food Webs* **8**: 163-188
- Geller W., Berberovic R., Gaedke U., Müller H., Pauli H. R., Tilzer M. M., Weisse T. (1991) Relations among the components of autotrophic and heterotrophic plankton during the seasonal cycle 1987 in Lake Constance. *Verh. Int. Ver. Limnol.* **24**: 831-836
- Gilbert J. J., Jack D. (1993) Rotifer as predators on small ciliates. *Hydrobiologia* **255/256**: 247-253
- Goldman J. C., Caron D. A. (1985) Experimental studies on an omnivorous microflagellate: implications for grazing and nutrient

- regeneration in the marine microbial food chain. *Deep-Sea Res.* **32**: 899-915
- Güde H. (1988) Direct and indirect influences of crustacean zooplankton on bacterioplankton of Lake Constance. *Hydrobiologia* **159**: 63-73
- Güde H. (1989) The role of grazing on bacteria in plankton succession. In: *Plankton Ecology: Succession in Plankton Communities*, (Ed. U. Sommer). Springer-Verlag, Berlin, Heidelberg, New York, 337-364
- Haney J. F. (1971) An in situ method for the measurement of zooplankton grazing rates. *Limnol. Oceanogr.* **16**: 970-977
- Jürgens K. (1994) Impact of *Daphnia* on planktonic microbial food webs. A review. *Mar. Microb. Food Webs* **8**: 295-324
- Lancelot C., Billen G. (1984) Activity of heterotrophic bacteria and its coupling to primary production during the spring phytoplankton bloom in the southern bight of the North Sea. *Limnol. Oceanogr.* **29**: 721-730
- Landry M. J. (1994) Methods and controls for measuring the grazing impact of planktonic protists. *Mar. Microb. Food Webs* **8**: 37-57
- Laybourn-Parry J. (1984) *A Functional Biology of Free-Living Protozoa*. Croom Helm, Australia
- Mathes J., Arndt H. (1995) The cycle of protozoans (ciliates, flagellates, sarcodines) in relation to phytoplankton and metazooplankton in Lake Neumühlen (Mecklenburg, Germany). *Arch. Hydrobiol.* **134**: 337-358
- Müller H. (1989) The relative importance of different ciliate taxa in the pelagic food web of Lake Constance. *Microb. Ecol.* **18**: 261-273
- Müller H., Geller W., Schöne A. (1990) Pelagic ciliates in Lake Constance: Comparison of epilimnion and hypolimnion. *Int. Ver. Theor. Angew. Limnol.* **24**: 846-849
- Müller H. E. (1981) Vergleichende Untersuchungen zur hydrochemischen Dynamik von Seen im schleswig-holsteinischen Jungmoränengebiet. *Kieler Geographische Schriften* **53**
- Nusch E. A. (1980) Comparison of different methods for chlorophyll and phaeopigment determination. *Ergebn. Limnol.* **14**: 14-36
- Pomeroy L. R. (1974) The ocean's food web, a changing paradigm. *Bioscience* **24**: 499-504
- Porter K. G., Feig Y. S. (1980) The use of DAPI for identifying and counting aquatic microflora. *Limnol. Oceanogr.* **25**: 943-948
- Porter K. G., Sherr E. B., Sherr B. F., Pace M., Sanders R. W. (1985) Protozoa in planktonic food webs. *J. Protozool.* **32**: 409-415
- Porter, K. G., Pearl H., Hodson R., Pace M., Priscu J., Riemann B., Scavia D., Stockner J. (1988) Microbial interactions in lake food webs. In: *Complex interactions in lake communities*, (Ed. S. R. Carpenter), Springer Verlag, New York, 209-227
- Ruttner-Kolisko A. (1977) Suggestions for biomass calculation of planktonic rotifer. *Arch. Hydrobiol. Suppl. Ergebn. Limnol.* **8**: 71-76
- Sanders R. W., Porter K. G., Bennett S. J., Debiase A. E. (1989) Seasonal patterns of bacterivory by flagellates, ciliates, rotifer, and cladocerans in a freshwater planktonic community. *Limnol. Oceanogr.* **34**: 673-687
- Sanders R. W., Wickham S. A. (1993) Planktonic protozoa and metazoa: predation, food quality and population control. *Mar. Microb. Food Webs* **7**: 197-223
- Schröder D., Krambeck H. J. (1991) Advantages in digital image analysis of bacterioplankton with epifluorescence microscopy. *Verh. Int. Ver. Limnol.* **24**: 2601-2604
- Sherr B. F., Sherr E. B. (1984) Role of heterotrophic protozoa in carbon and energy flow in aquatic ecosystems. In: *Current perspectives in microbial ecology*, (Eds. M. J. Klug, C. A. Reddy). Am. Soc. Microbiol. 312-423
- Sherr B. F., Sherr E. B., Hopkinson C. S. (1988) Trophic interactions within pelagic microbial communities: indications of feedback regulation of carbon flow. *Hydrobiol.* **159**: 19-26
- Sieburth J. McN., Davis P. G. (1982) The role of heterotrophic nanoplankton in the grazing and nutrition of planktonic bacteria in the Sargasso and Caribbean Seas. *Ann. Inst. océanogr. (Paris)(Suppl.)* **58**: 285-296
- Simon M., Tilzer M. M. (1987) Bacterial response to seasonal changes in primary production and phytoplankton biomass in Lake Constance. *J. Plankton Res.* **9**: 535-553
- Sommer U. (1994) *Planktologie*. Springer Verlag, Berlin, Heidelberg, New York
- Sommer U., Gliwicz Z. M., Lampert W., Duncan A. (1986) The PEG-model of seasonal succession of planktonic events in freshwaters. *Arch. Hydrobiol.* **106**: 433-471
- Stoecker D. K., Capuzzo J. M. (1990) Predation on Protozoa: its importance to zooplankton. *J. Plankton Res.* **12**: 891-908
- Stone L. (1990) Phytoplankton-bacteria-protozoa interactions: a qualitative model portraying indirect effects. *Mar. Ecol. Prog. Ser.* **64**: 137-145
- Tilzer M. M., Beese B. (1988) The seasonal productivity cycle of phytoplankton and controlling factor in lake Constance. *Schweiz. Z. Hydrol.* **50**: 1-39
- Turley C., Newell R. C., Robins D. B. (1986) Survival strategies of two small marine ciliates and their role in regulating bacterial community structure under experimental conditions. *Mar. Ecol. Progr. Ser.* **33**: 57-70
- Utermöhl H. (1958) Zur Vervollkommnung der quantitativen Phytoplankton-Methodik. *Internat. Verein. Limnol.* **9**: 1-39
- Verity P. G. (1991) Feeding in planktonic protozoans: Evidence for non-random acquisition of prey. *J. Protozool.* **83**: 69-76
- Weisse T. (1990) Trophic interactions among heterotrophic microplankton, nanoplankton, and bacteria in Lake Constance. *Hydrobiologia* **191**: 111-122
- Weisse T., Müller H., Pinto-Coelho M., Schweizer A., Springmann D., Baldinger G. (1990) Response of the microbial loop to the phytoplankton spring bloom in a large pre-alpine lake. *Limnol. Oceanogr.* **35**: 781-794
- Zimmermann H. (1994) *Untersuchungen zur Bedeutung der Ciliaten im mikrobiellen Nahrungsnetz des Belauer Sees*. Dissertation Universität Hamburg

Received on 15th March, 1995; accepted on 14th February, 1996

A *Sarcocystis* Species from Goshawk (*Accipiter gentilis*) with Great Tit (*Parus major*) as Intermediate Host

Milena SVOBODOVÁ

Department of Parasitology, Faculty of Science, Charles University, Prague, Czech Republic

Summary. One hundred and seventy five passerine birds from the Czech Republic were examined for the presence of sarcosporidia; only 5 (all great tits) were positive for muscle cysts. Three great tits experimentally fed sporocysts (12.2 x 8.4, 11-13 x 7.5-9 µm) from a goshawk developed cysts while 2 house sparrows (*Passer domesticus*) were not infected. The cysts from great tits muscles were morphologically similar to those found in natural infections. The thin-walled cysts contained banana-shaped cystozoites 6.9 x 1.8 (5.9-8.5 x 1.3-2.3) µm in size. The natural life cycle of this *Sarcocystis* species involves goshawks and great tits. The relation of this species to *S. accipitris* is discussed.

Key words: Apicomplexa, birds, coccidia, host specificity, life cycle, *Sarcocystis*, transmission.

INTRODUCTION

Although birds have been known to harbour *Sarcocystis* cysts in their muscles since 1865 (Kühn ex Erickson 1940), it was only in 1977 that Munday and colleagues described the first sarcosporidian life-cycle with a bird (*Gallus gallus*) as the intermediate host and a carnivore (*Canis familiaris*) as the final host. Sarcosporidia have since been found in dozens of bird species (Kalyakin and Zasukhin 1975) but their life-cycles have been elucidated only in a few cases, mostly with a carnivore as final host (Levine 1986). In his abstract, Ashford (1975) was the first to suggest the existence of a sarcosporidian life cycle involving birds as both final (*Accipiter nisus*) and intermediate (*Serinus canaria*) host. The only named species involving birds as both final (*A. gentilis*) and intermediate

(*S. canaria*) hosts in its life cycle is *Sarcocystis accipitris* (Černá and Kvašňovská 1986); the life cycle was investigated only in laboratory experiments.

During our investigation of sarcosporidiosis in passerine birds, the great tit was the only species found to be infected; the morphology of the cysts and cystozoites suggested this *Sarcocystis* species could have a bird of prey as final host (Munday et al. 1977). Among raptors living in the investigated area the genus *Accipiter* most often preys on birds (Hudec and Černý 1977), and the existence of a sarcosporidian life cycle with the goshawk as final and the great tit as natural intermediate host therefore seemed probable.

MATERIALS AND METHODS

Birds examined for the presence of muscular stages of sarcosporidia were unintentionally caught during trapping of mice or were collected for other investigations (house sparrows). They originated from Prague or from other localities in Czech Republic. The inoculum used in experimental infections originated from a single goshawk obtained from a

Address for correspondence: Milena Svobodová, Department of Parasitology, Faculty of Science, Charles University, Viničná 7, 128 44 Prague 2, Czech Republic; E-mail: Volf @beba.cesnet.cz

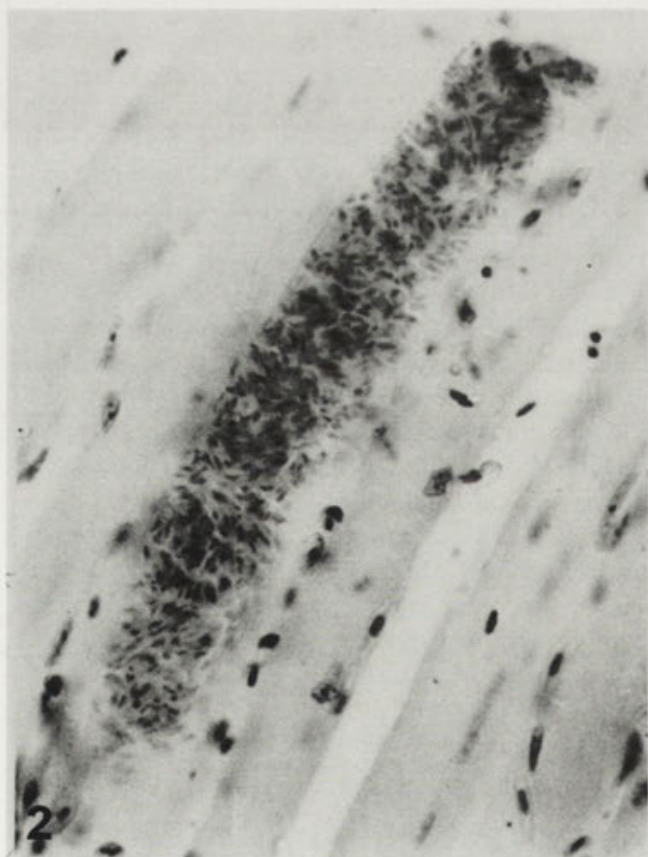
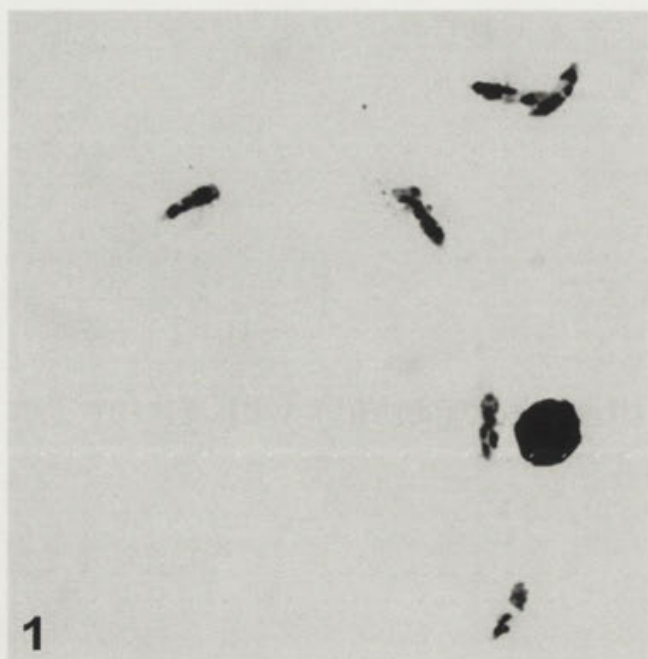


Fig. 1. Individual cystozoites from the muscle homogenate of a naturally infected great tit. Giemsa staining, x 1500

Fig. 2. Muscular cyst of *Sarcocystis* sp. in the great tit. Note the thin wall without any protrusions. Histological section, Harris hematoxylin, x 1000

taxidermist workshop DIPRA, Prague; the raptor was probably shot on an unknown locality in Czech Republic. Three great tits and 2 house sparrows were net-caught, each species caged separately and reared in an animal room. The birds were fed with a combined animal and plant feed (live insect larvae, seeds, vegetables, eggs) and subsequently infected *per os* with decanted gut contents of the goshawk containing an unknown number of sarcosporidian sporocysts. The probability that all the 3 tits were infected with sarcosporidia before the experiment is $(5/79)^3 = 0.00025$ (based on our data concerning the prevalence in great tits). Two tits were killed 2 months, 2 sparrows 4 months and 1 tit 5 months after infection. The muscles from half of the body of experimental as well as free-living birds were homogenized in saline using a grinding mortar, filtered through gauze and centrifuged for 15 min at approx. 1000 g. The sediment was smeared on slides, Giemsa-stained and examined for the presence of cystozoites under immersion objective. In the case of positive result, cystozoites (Fig. 1) were measured ($n=10$ in each specimen), their lengths compared using the multiple range test (ANOVA); muscles from the second half of the body were fixed in Bouin's fixative, embedded in paraplast, histologically processed and stained with Harris hematoxylin (Fig. 2).

RESULTS

One hundred and seventy five passerine birds were examined for the presence of muscular sarcosporidia. Among them, only 5 great tits were found to be infected, representing 2.9 % of all birds and 6.3 % of great tits examined (Table 1). These tits originated from different localities in the Czech Republic (2 from Prague, 50.05 N, 14.20 E; 3 others from the vicinity of Mělník, Central Bohemia, 50.21 N, 14.29 E; Choceň, East Bohemia, 50.00 N, 16.13 E; and Mikulov, South Moravia, 48.48 N, 16.38 E, resp.)

Table 1. Passerine birds examined for the presence of muscular sarcosporidiosis

Bird species	Examined	Infected
<i>Carduelis carduelis</i> Goldfinch	1	0
<i>Emberiza citrinella</i> Yellowhammer	3	0
<i>Erithacus rubecula</i> Robin	25	0
<i>Fringilla coelebs</i> Chaffinch	2	0
<i>Hippolais icterina</i> Icterine Warbler	1	0
<i>Parus caeruleus</i> Blue Tit	1	0
<i>Parus major</i> Great Tit	79	5
<i>Parus palustris</i> Marsh Tit	2	0
<i>Passer montanus</i> Tree Sparrow	2	0
<i>Passer domesticus</i> House Sparrow	47	0
<i>Phylloscopus trochilus</i> Willow Warbler	1	0
<i>Prunella modularis</i> Hedge Sparrow	3	0
<i>Serinus serinus</i> Serin	1	0
<i>Sitta europaea</i> Nuthatch	4	0
<i>Turdus merula</i> Blackbird	2	0
<i>Turdus philomelos</i> Song Thrush	1	0
Total	175	5

All 3 great tits fed experimentally with sporocysts, which measured $12.2 \times 8.4 \mu\text{m}$ (11-13 \times 7.5-9, $n=20$, SE 0.12 and 0.13, resp.), developed muscular cysts, while the 2 sparrows remained uninfected. The morphology of cystozoites and muscular cysts was similar in naturally and experimentally infected individuals; after Giemsa staining the cystozoites were banana-shaped with light blue cytoplasm and violet, slightly out of the center nucleus; their length and width was $6.9 \times 1.8 \mu\text{m}$ (5.9-8.5 \times 1.3-2.3, $n=80$, SE 0.07 and 0.02, resp.); fresh thin-walled muscular cysts measured $57 \mu\text{m}$ (45-84, $n=4$) in width. The cystozoites from experimental infection measured $7.0 \times 1.7 \mu\text{m}$ (5.9-8.5 \times 1.3-2.0, $n=30$, SE 0.13 and 0.04, resp.), those from natural infections $6.9 \times 1.8 \mu\text{m}$ (5.9-8.5 \times 1.3-2.3, $n=50$, SE 0.07 and 0.03, resp.) The similarity of cystozoites from natural and experimental infection was confirmed using the multiple range test (ANOVA).

DISCUSSION

The successful experimental inoculation of sarcosporidian sporocysts isolated from the goshawk to the great tit, and the similarity of sarcocysts and cystozoites derived from experimental and natural infections suggests this passerine bird acts as natural intermediate host of this *Sarcocystis* species.

Although goshawks usually prey upon larger birds, small passerines are also found in their diet (Goszczyński and Piłatowski 1986), especially in the nesting period (Hudec and Černý 1977); and the great tit was also reported from goshawk diet (Mañosa 1994).

The great tit was the only bird species in which sarcocysts were found, although a relatively high number of sparrows (47) were also examined; after being fed sporocysts the sparrows were not infected, and they are probably not involved in the life cycle of this parasite.

Oocysts/sporocysts isolated from the goshawk were reported to be infective for the canary (*Serinus canaria*) (Černá and Kvašňovská 1986). The canary, however, cannot act as intermediate host in central European area due to its range (the Canaries, the Azores and Madeira (Heinzel et al. 1983)); on the contrary, the ranges of goshawk and great tit overlap in the whole Europe (Heinzel et al. 1983). Therefore, it would be tempting to conclude that the *Sarcocystis* species in our work is *Sarcocystis accipitris* and that the great tit is the natural intermediate host of this species; the morphology of cystozoites and muscular cysts being similar to those reported by Černá and Kvašňovská (1986) further sup-

ports this hypothesis. However, sporocysts used for inoculation differ in their morphology and size, being relatively wide and measuring $15-17 \times 13-15 \mu\text{m}$ in the case of *S. accipitris* (Černá and Kvašňovská 1986), while those used in our experiment measured $11-13 \times 7.5-9$; they resemble sporocysts from sparrowhawk (*A. nisus*) which were not infective for the canary (Černá and Kvašňovská 1986) but it is unclear if in their experiment the sporocysts were still viable. Unfortunately, we had no sparrowhawk available for transmission study.

The fact that the great tit and the canary belong to different families (Paridae and Fringillidae, resp.) also does not help to answer the question if those findings are identical or not. From the species with well-known life cycles, *Sarcocystis falcatula*, a species with opossum (*Didelphis virginiana*) as final host, develops muscle cysts in members of 2 different bird orders (Box and Smith 1982); oocysts of *Sarcocystis dispersa* from barn owl (*Tyto alba*) are infective for all the members (7 genera tested) of the family Muridae except the laboratory rat (*Rattus norvegicus*) but not for family Cricetidae and Caviidae (Votýpka, unpub. obs.) The question is which of these two *Sarcocystis* species should we chose for comparison with "*Sarcocystis accipitris*"? Oocysts/sporocysts from the goshawk are also known to be infective for laboratory mice (Černá 1977, confirmed by Kolářová ex Černá 1986) but, to our knowledge, there is no *Sarcocystis* species with an intermediate host spectrum including both mammals and birds.

For the above reasons, the species identity of *Sarcocystis* species using great tit as intermediate and goshawk as final host remains unclear.

Acknowledgements. I thank Lucie Brejšková, MSc., Dr. Daniel Frynta and co-workers for providing the material for examination.

REFERENCES

- Ashford R. W. (1975) Preliminary observations on the life cycle of *Isospora buteonis*. *J. Protozool.* **22**: 48A
- Box E. D., Smith J. H. (1982) The intermediate host spectrum in a *Sarcocystis* of birds. *J. Parasitol.* **68**: 668-673
- Černá Ž. (1977) The importance of rodents as vectors of sarcocystosis. *Bratisl. lek. listy* **68**: 63-67 (in Czech)
- Černá Ž. (1986) Sarcosporidia, their importance and relation to other coccidia. Thesis, Dept. Parasitol., Charles Univ., Prague (in Czech)
- Černá Ž., Kvašňovská Z. (1986) Life cycle involving bird-bird relation in *Sarcocystis* coccidia with the description of *Sarcocystis accipitris* sp. n. *Folia Parasitol.* **33**: 305-309
- Erickson A. B. (1940) *Sarcocystis* in birds. *Auk* **57**: 514-519
- Goszczyński J., Piłatowski T. (1986) Diet of common buzzards (*Buteo buteo* L.) and goshawks (*Accipiter gentilis* L.) in the nesting period. *Ekol. Pol.* **34**: 655-667
- Heinzel H., Fitter R., Parslow J. (1983) Pareys Vogelbuch. Alle Vögel Europas, Nordafrikas und des Mittleren Ostens. Verlag Paul Parey, Hamburg und Berlin

- Hudec K., Černý W. (1977) The Fauna of ČSSR, Birds - Aves II. Academia, Prague (in Czech)
- Kalyakin V. N., Zasukhin D. N. (1975) Distribution of *Sarcocystis* (Protozoa: Sporozoa) in vertebrates. *Folia Parasitol.* **22**: 289-307
- Levine N. D. (1986) The taxonomy of *Sarcocystis* (Protozoa, Apicomplexa) species. *J. Parasitol.* **72**: 372-382
- Mañosa S. (1994) Goshawk diet in a Mediterranean area of northeastern Spain. *J. Raptor Res.* **28**: 84-92
- Munday B. L., Humphrey J. D., Kila V. (1977) Pathology produced by, prevalence of, and probable life-cycle of a species of *Sarcocystis* in the domestic fowl. *Avian Dis.* **21**: 697-703
- Munday B. L., Hartley, W. J., Harrigan, K. E., Presidente, P. J. A., Obendorf, D. L., (1979) *Sarcocystis* and related organisms in australian wildlife: II. Survey findings in birds, reptiles, amphibians and fish. *J. Wildl. Dis.* **15**: 57-73

Received on 11th December, 1995; accepted on 1st March, 1996

A Redescription of the Marine Ciliates *Uroleptus retractilis* (Claparède and Lachmann, 1858) comb. n. and *Epiclintes ambiguus* (Müller, 1786) Bütschli, 1889 (Ciliophora, Hypotrichida)

Weibo SONG¹ and Alan WARREN²

¹College of Fisheries, Ocean University of Qingdao, Qingdao, P. R. China; ²Department of Zoology, The Natural History Museum, Cromwell Road, London, U.K.

Summary. The morphology and infraciliature of two marine ciliates was observed on living cells and investigated using protargol silver impregnation. *Uroleptus retractilis* (Claparède and Lachmann, 1858) comb. n., formerly *Epiclintes radiosa* (= *Mitra retractilis*), a ciliate with a highly contractile "tail" whose systematic position has been unresolved for over a century, has a ciliature pattern that is typical of the genus *Uroleptus*. Based on the results presented in this paper, *E. radiosa* should be transferred to *Uroleptus* and thus a new combination has been erected. The infraciliature of the large contractile hypotrich *Epiclintes ambiguus* is also described confirming the descriptions of many previous authors. As an additional contribution, biometric data for both species are supplied.

Key words: *Epiclintes ambiguus*, hypotrichs, marine ciliates, morphology, new combination, *Uroleptus retractilis*.

INTRODUCTION

Ciliates assigned to the hypotrich genus *Epiclintes* have been isolated from all over the world for over a century (Claparède and Lachmann 1858, Calkins 1902, Kahl 1932, Bullington 1940, Carey and Tatchell 1983, Wicklow and Borror 1990 and references therein). Very few, however, have been described in detail, or following silver impregnation to reveal the infraciliature, so their taxonomic positions remain doubtful. In their revision of the genus, Carey and Tatchell (1983) recognized three species of *Epiclintes*: *E. caudatus* Bullington, 1940, *E. felis* (Müller, 1786) Carey and Tatchell, 1983 and *E. radiosa* Calkins, 1902. Wicklow and Borror (1990)

subsequently rejected *E. radiosa* as a member of the genus *Epiclintes* suggesting that it is probably an oxytrichid. They also preferred the name *E. ambiguus* to *E. felis* indicating that *felis* is probably a *nomen oblitum*. We support this view as the last previous record of the name *felis* in the literature was that of Bory St. Vincent (1824) over 160 years ago. *Epiclintes caudatus* still awaits rediscovery since it was first described by Bullington (1940).

The opportunity to re-examine two species of *Epiclintes*, *E. ambiguus* (= *E. felis sensu* Carey and Tatchell 1983) and *E. radiosa*, came with the discovery of large numbers of both in a marine shellfish pond at Taipingjia in Qingdao, China. The resulting observations, made of both living and protargol stained cells, are presented. The objective of this paper is to determine the correct taxonomic position of *E. radiosa* and to provide further information on the morphology of *E. ambiguus*.

Address for correspondence: Alan Warren, Department of Zoology, The Natural History Museum, Cromwell Road, London SW7 5BD, U.K. ; Fax: [+44](0)171-938.8754; E-mail (INTERNET): a.warren@nhm.ac.uk

MATERIALS AND METHODS

Both species were collected (March-April, 1995) in an eutrophic pond used for storing marine shellfish, in Taipingjiao, Qingdao (Tsingtao), China. The salinity was about 32‰, water temperature 12-15°C and pH ca 8.3.

Field specimens were used for the investigations. Protargol silver impregnation (Wilbert 1975) was applied to reveal the infraciliature. Counts and measurements on stained specimens were performed at a magnification of x 1250. Body shapes were drawn from slides without cover glasses. Details of living cells were studied using the oil immersion objective with bright field and Nomarski optics. Drawings were made with the help of a camera lucida.

To illustrate the changes occurring during physiological reorganizing processes (Fig. 10), old (parental) cirri are depicted by contour, whereas new cirri are shaded black. Terminology is mainly according to Borror (1972), Corliss (1979), Hemberger (1982) and Song et al. (1992).

The protargol stained specimens of both species are deposited in the Laboratory of Protozoology, College of Fisheries, Ocean University of Qingdao, China.

RESULTS AND DISCUSSION

Redescription of the morphology and infraciliature of *Uroleptus retractilis* comb. n. (Figs. 1-11, Table 1)

Oxytricha retractilis Claparède and Lachmann, 1858

Oxytricha longicaudata Strethill-Wright, 1862

Mitra radiosa Quennerstedt, 1867

Epiclintes retractilis (Claparède and Lachmann, 1858)

Kent, 1882

Epiclintes radiosa (Quennerstedt, 1867) Calkins, 1902

Mitra retractilis (Claparède and Lachmann, 1858)

Kahl, 1932

Micromitra retractilis (Claparède and Lachmann, 1858)

Kahl, 1933

Micromitra brevicauda (Claparède and Lachmann, 1858) Kahl, 1933

Psammomitra retractilis (Claparède and Lachmann, 1858) Borror, 1972

Psammomitra brevicauda (Kahl, 1933) Borror, 1972

This cosmopolitan species has been reported from all over the world for more than a century as an epibenthic ciliate from marine interstitial sediments (Ehrenberg 1830, Claparède and Lachmann 1858, Strethill-Wright 1862, Quennerstedt 1867, Bütschli 1889, Calkins 1902, Kahl 1932, Carey and Tatchell 1983). Yet its detailed morphology, infraciliature and even the nuclear apparatus have never been adequately described and until now it has been

considered as a member *incertae sedis* (Carey and Tatchell 1983, Wicklow and Borror 1990). Hence, a general detailed redescription will be added here based on our new investigations.

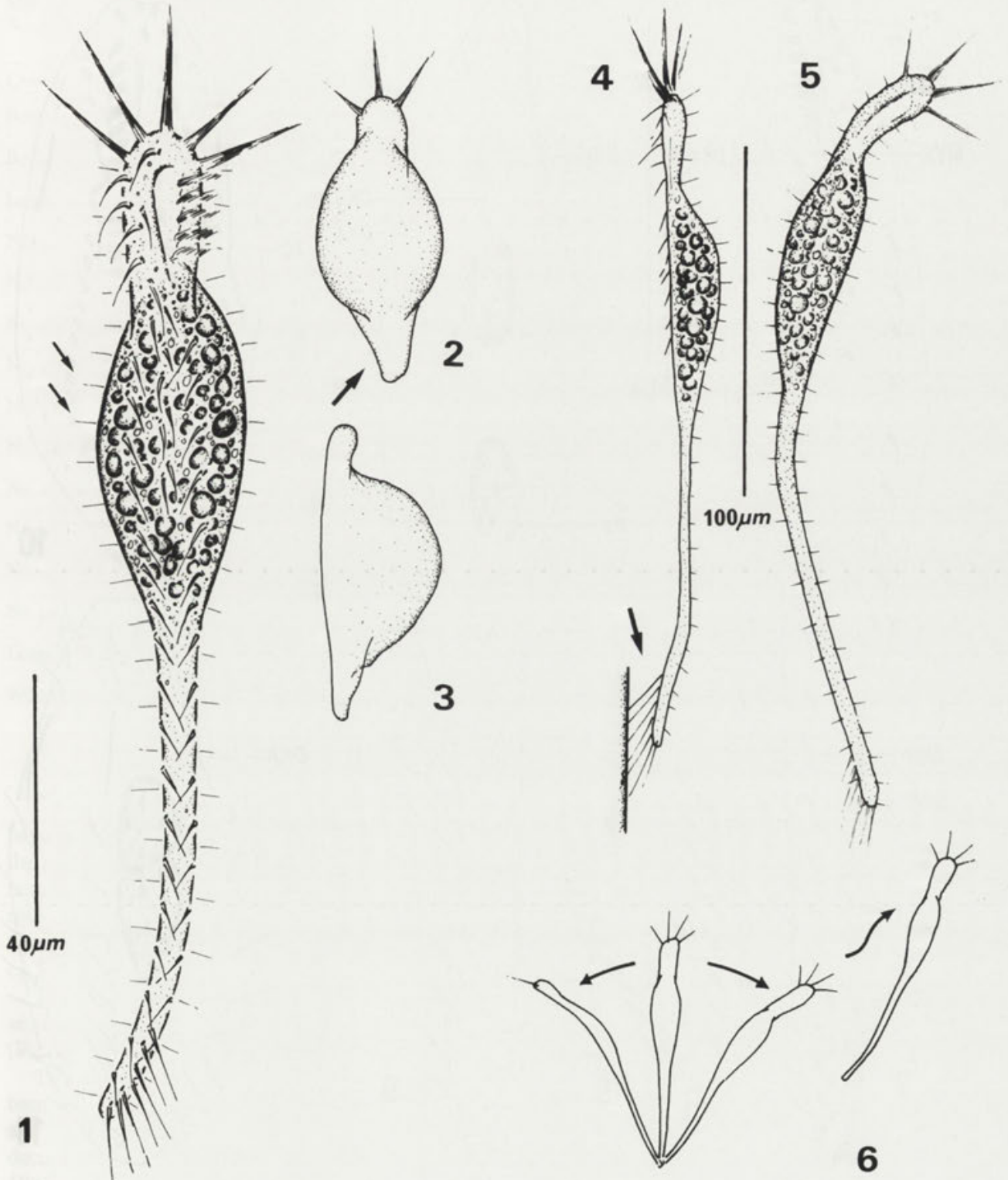
Cells *in vivo* normally about 140-200 x 20-30 µm, but active individuals at maximum extension can be up to 300µm long. Body slender and fragile when observed under stereomicroscope, highly contractile and evidently divided into three parts: head, trunk and tail. Head region about 1/5 to 1/8 of the whole length, narrow, colourless and dorso-ventrally flattened (Figs. 1, 4). Trunk elongated, 1/3 to 1/5 of total length; ventral side flat and straight, dorsal side highly convex (Fig. 4). Stalk-like tail very thin, long, hyaline and highly retractile and, when fully extended about twice as long as in normal state. 3-5 (usually 4 or, 5) highly developed membranelles (ca 20 µm long) forming a crown-shape at the anterior end of the cell (Figs. 1, 4, 5). Dorsal bristles (cilia) very conspicuous, spine- or needle-like and readily observed (Fig. 1).

Pellicle thin, without subpellicular granules. Cytoplasm colourless, although within the trunk portion always full of large (3-8 µm), colourless globules making the nuclear apparatus difficult to observe *in vivo*.

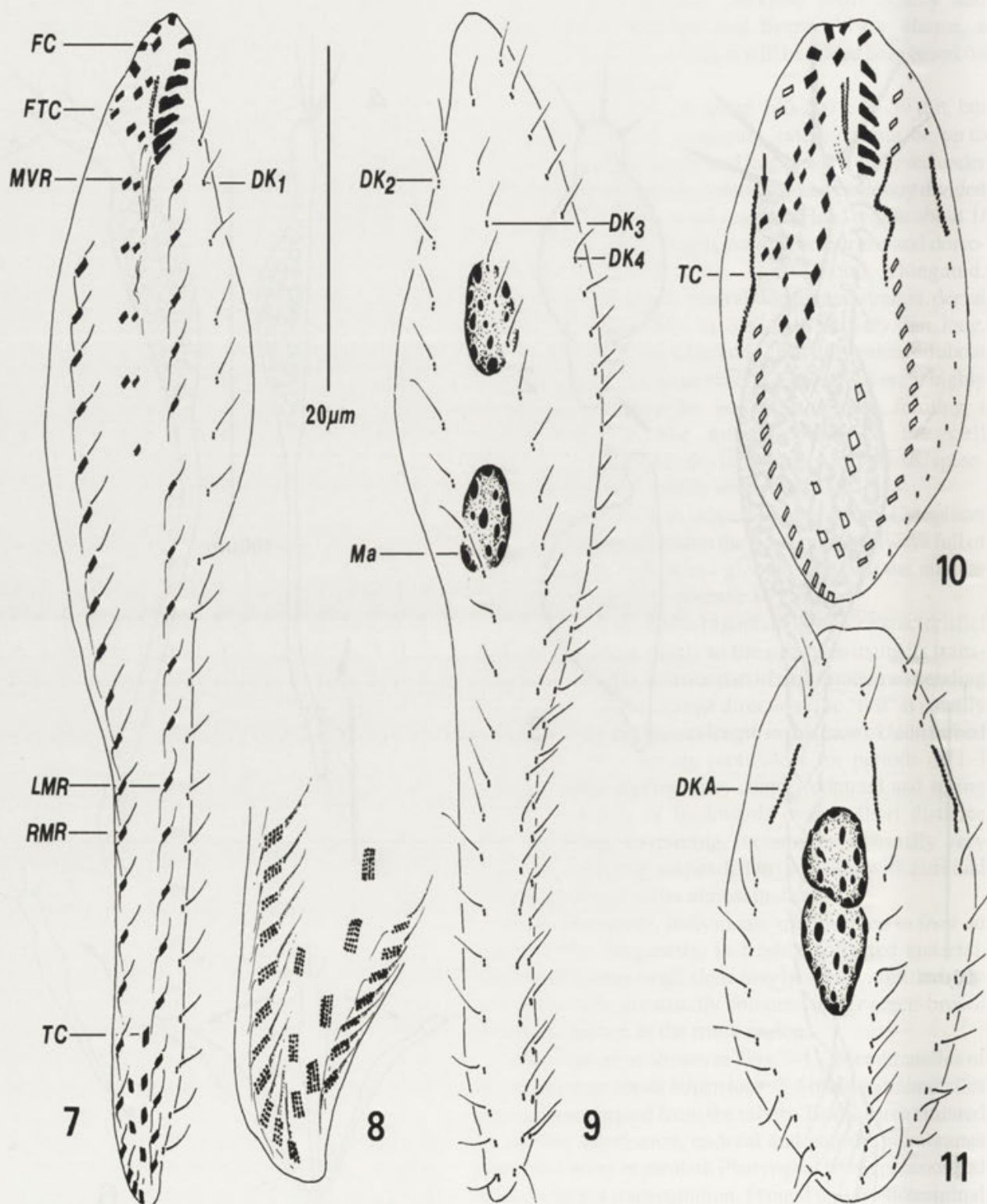
The behaviour of this organism is very characteristic: it usually attaches firmly to the substrate using its transverse cirri with the anterior part of cell sometimes bending from side to side to change direction (the "tail" is usually extended to the maximum length in this case). Undisturbed individuals may remain motionless for periods of 1-3 minutes. After stirring, they usually contract and spring rapidly forwards or backwards over a short distance (Fig. 6). When swimming, locomotion is usually very slow, the cell being suspended in the water with cirri and other ciliary organelles almost motionless.

In the laboratory, individuals are observed to feed on bacteria. But frequently, in freshly collected material, diatoms and other small algae may be seen within the body and so the cells are usually coloured either green-brown or yellow-brown in the trunk region.

Infraciliature as shown in Figs. 7-11. Membranelles of the adoral zone about 10µm long, 3-4 distal membranelles distinctly separated from the others. Buccal area situated in shallow depression, endoral and paroral membranes short, and lying in parallel. Pharyngeal fibres pronounced after protargol impregnation. Frontal and frontoterminal cirri (FC, FTC) typical of the genus. Midventral row (MVR) usually with 5 pairs of cirri, extending about half the length of the trunk. Transverse cirri (TC) arranged in a U-shape near the posterior end of the cell. Each cirrus slightly enlarged, ca 20 µm long, projecting distinctly



Figs. 1-6. Morphology of *Uroleptus retractilis* from observations of cells *in vivo*. 1 - ventral view of a "normal" organism, arrows marking the dorsal bristles; 2-3 - dorsal and lateral views of contracted individuals, arrow demonstrating the almost disappeared "tail"; 4-5 - lateral and dorsal view of highly relaxed forms, arrow showing the transverse cirri attached to the substrate; 6 - diagram illustrating typical movement



Figs. 7-11. Infraciliature of *Uroleptus retractilis* after protargol impregnation. 7-9 - ventral and dorsal view; 8 - showing the posterior part of the cell; 10-11 - ventral and dorsal view of a physiological reorganizer, arrow in Fig. 10 showing the fronto-terminal cirri which start to move anteriorly. Abbreviations: DK1-4 - dorsal kinety 1-4, DKA - anlagen of dorsal kineties, FC - frontal cirri, FTC - fronto-terminal cirri, LMR - left marginal row, Ma - macronucleus, MVR - midventral row, RMR - right marginal row, TC - transverse cirri

Table 1. Biometric characterization of *Uroleptus retractilis* (1st line) and *Epiclintes ambiguus* (2nd line) based on protargol-stained specimens. Min - minimum, Max - maximum, n - sample size, SD - standard deviation, SE - standard error of mean, CV - coefficient of variation in %, X - arithmetic mean, measurements in μm

Character	Min	Max	X	SD	SE	CV	n
Body length*	30	71	41.5	13.81	4.37	33.3	10
	120	162	142.7	16.7	5.55	11.7	9
Body width*	19	28	23.8	2.90	0.92	12.2	10
	54	72	61.0	5.70	1.90	9.3	9
Length of cytostome*	8	12	10.0	1.25	0.39	12.5	10
	35	48	41.8	3.93	1.31	9.4	9
No. of fronto-terminal cirri	2	3	2.1	0.29	0.08	13.9	12
	-	-	-	-	-	-	-
No. of membranelles	10	12	11.1	0.71	0.24	6.3	9
	48	61	54.4	4.34	1.54	8.0	8
No. of frontal cirri	1	3	-	-	-	-	5
	1	1	1	0	0	0	9
No. of cirrus-pairs in mid-ventral rows	5	6	5.6	0.54	0.20	9.6	7
	-	-	-	-	-	-	-
No. left marginal cirri	18	23	20.0	1.83	0.58	9.1	10
	49	56	53.1	2.67	1.01	5.1	7
No. right marginal cirri	18	24	20.5	1.96	0.62	9.6	10
	63	75	66.1	4.41	1.67	6.7	7
No. of ventral rows	-	-	-	-	-	-	-
	12	13	12.4	0.52	0.18	4.2	8
No. of transverse cirri	5	8	6.7	0.95	0.30	14.2	10
	24	29	26.1	1.95	0.74	7.5	7
No. of dorsal kineties	4	4	4	0	0	0	11
	3	3	3	0	0	0	9
No. of macronuclei	2	2	2	0	0	0	16
	109	123	-	-	-	-	2
Length of macronucleus	7	10	8.5	1.07	0.38	12.6	8
	5	7	-	-	-	-	-
Width of macronucleus	4	8	5.2	1.30	0.43	24.9	9
	3	5	-	-	-	-	-

* Data based on contracted cells

beyond the posterior border. Marginal cirri ca 10 μm long; the right marginal row (RMR) more or less L-shaped, terminating at the posterior end of the cell, the left marginal row (LMR) ending at about the level of the posterior transverse cirrus (Fig. 8). Four dorsal kineties (DK) with ca 5-8 μm long cilia (Figs. 7, 9).

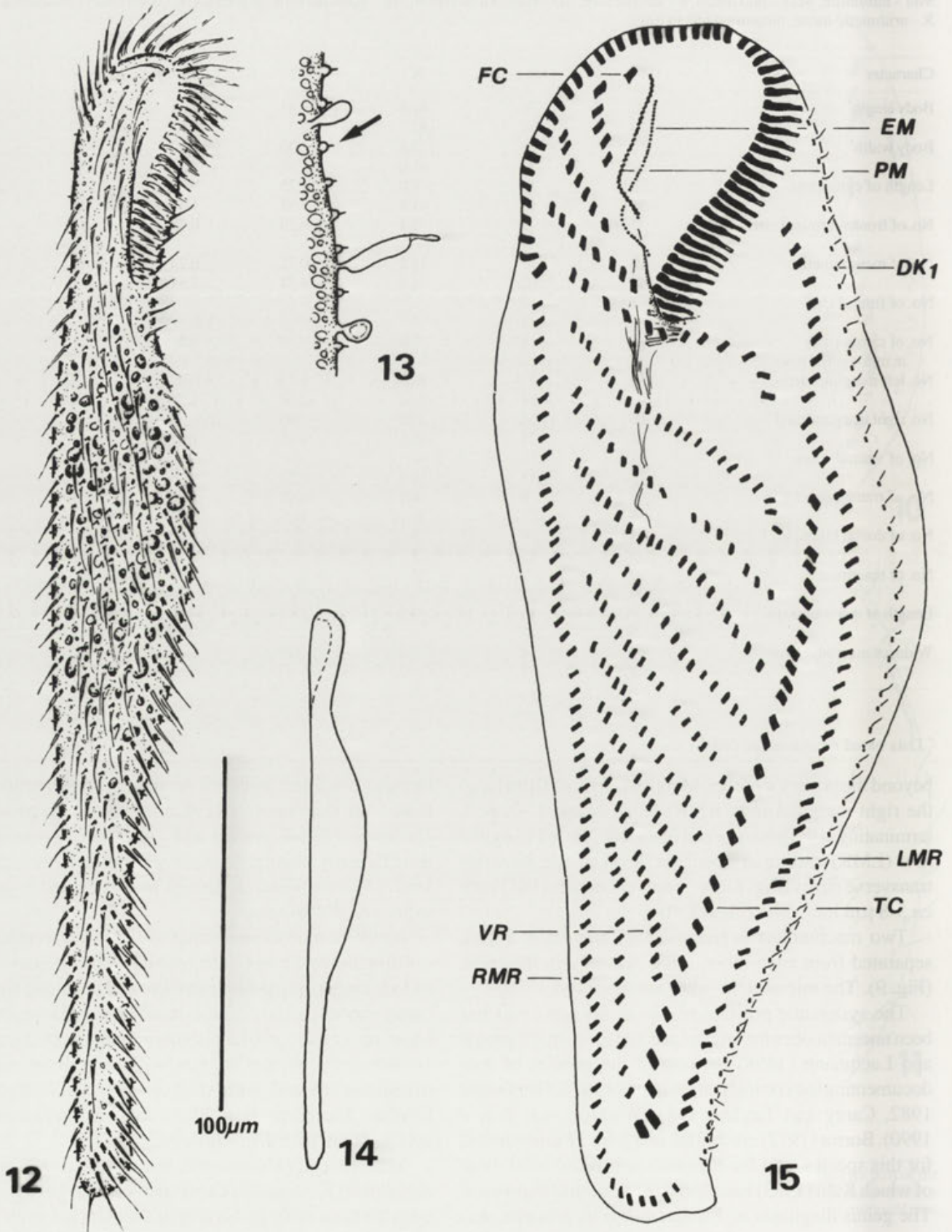
Two macronuclear segments (Ma) about 5 x 8 μm , separated from each other, lying centrally in the trunk (Fig. 9). The micronuclei were not observed.

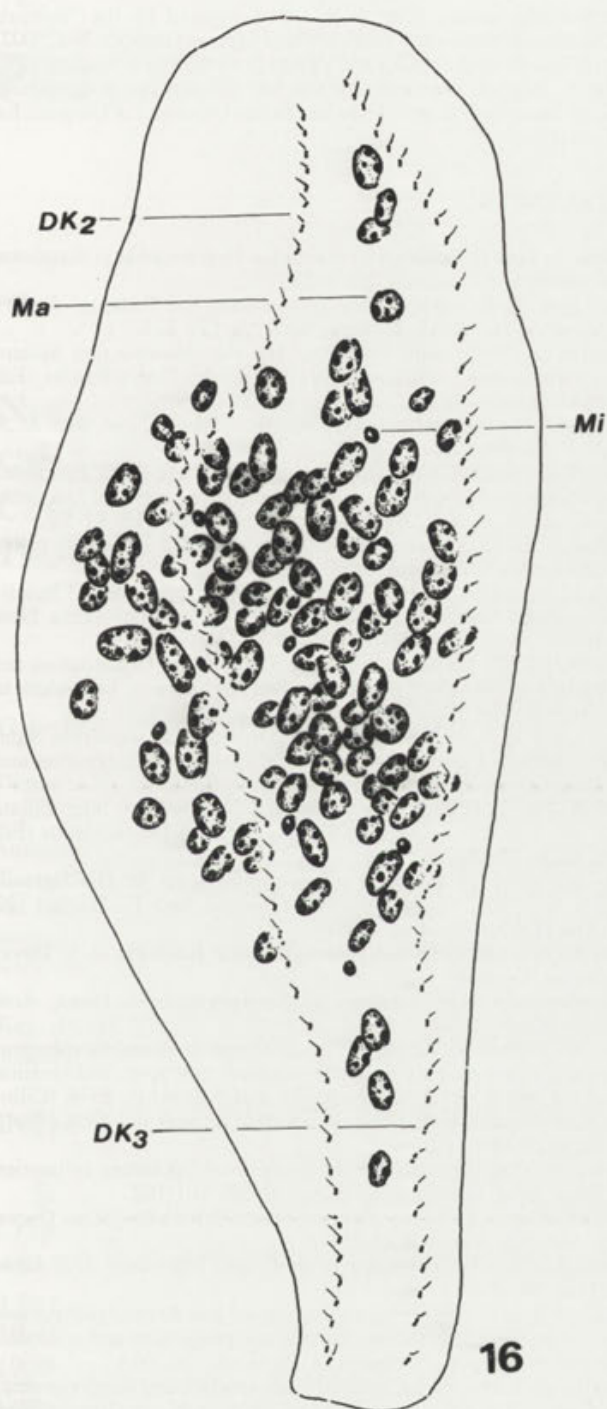
The systematic position of *Uroleptus retractilis* has been uncertain since the original account given by Claparède and Lachmann (1858) because of the paucity of data documenting the cortical pattern (Borror 1972, Hemberger 1982, Carey and Tatchell 1983, Wicklow and Borror 1990). Borror (1972) erected the new genus *Psammomitra* for this species, and for *P. brevicauda* Kahl, 1933, both of which Kahl (1933) had placed in the genus *Micromitra*. The genus diagnosis of *Psammomitra* is, however, ex-

tremely brief and includes no details of infraciliature. Based on Hemberger's (1982) improved diagnosis of *Uroleptus*, *Psammomitra* and *Uroleptus* appear to be insufficiently distinct for their separation at the generic level. *Psammomitra* is therefore considered a junior synonym of *Uroleptus*.

Furthermore, *Psammomitra* (= *Micromitra*) *brevicauda* is differentiated from *U. retractilis* only by the possession of four longer apical membranelles and in having significantly shorter caudal cirri and dorsal bristles. However, we have observed individuals among the population of *U. retractilis* from Qingdao with 3-5 longer apical membranelles and with short caudal cirri and dorsal bristles. Therefore, it is likely that *P. brevicauda* is synonymous with *U. retractilis*.

More recently *U. retractilis* was assigned to the genus *Epiclintes* (*E. radiosa*) (Carey and Tatchell 1983). However, the taxonomic problem of this species has never been





Figs. 12-16. Morphology and infraciliature of *Epiclintes ambiguus*, *in vivo* (12-14) and after protargol impregnation (15-16). 12 - ventral view of extended individual; 13 - part of pellicle showing the dorsal cilia within papillae (arrow), "extrusomes" and ectoplasmic granules; 14 - lateral view; 15-16 - ventral and dorsal view of infraciliature. Abbreviations: DK1-3 - dorsal kinety 1-3, EM - endoral membrane, FC - frontal cirrus, LMR - left marginal row, Ma - macronucleus, Mi - micronucleus, PM - paroral membrane, RMR - right marginal row, TC - transverse cirri, VR - ventral rows

resolved satisfactorily as stated in Carey and Tatchell's (1983) generic revision: "...further information is required on this interesting species before a definite decision can be taken regarding its validity". Fortunately many cells were obtained during the collections made for the present study enabling detailed morphological studies to be carried out. As a result of these investigations there is no doubt that this species should be placed in the genus *Uroleptus* Ehrenberg, 1831.

Carey and Tatchell (1983) discussed the confused nomenclature of "*Epiclintes radiosa* (Claparède and Lachmann, 1858)" and, based on their comparisons with the illustrations in Claparède and Lachmann (1858), they suggested changing the name from *Mitra retractilis* (Claparède and Lachmann, 1858) Kahl, 1932 to *Epiclintes radiosa* Calkins, 1902. We appreciate their careful comparisons, but have decided here to reject their new arrangement (the name *radiosa* should be a junior synonym) and regard only *retractilis* as a valid name.

Redescription of the morphology of *Epiclintes ambiguus* (Müller, 1786) Bütschli, 1889 (Figs. 12-16, Table 1)

Trichoda felis Müller, 1786

Oxytricha felis (Müller, 1786) Bory St Vincent, 1824

Oxytricha auricularis Claparède and Lachmann, 1858

Epiclintes auricularis (Müller, 1786) Stein, 1862

Epiclintes ambigua (Müller, 1786) Wallengren, 1900

Epiclintes felis (Müller, 1786) Carey and Tatchell, 1983

Compared with *Uroleptus retractilis*, this psammophilic and cephalized species has been carefully studied by many authors (Stein 1862, Kent 1880-82, Bütschli 1889, Wallengren 1900, Calkins 1902, Wicklow 1979, Carey and Tatchell 1983). Our observations are consistent with those of Bütschli (1889), Kahl (1932), Carey and Tatchell (1983) and Wicklow and Borror (1990), so a full redescription is unnecessary. We here underscore only some key characters and biometric data (Table 1).

As illustrated in Fig. 12, the body of this large hypotrich is flattened dorsoventrally about 1:2. Extended cells are divided into three distinct regions: an asymmetric, auriform anterior head connected *via* a thin neck to an elongate trunk which terminates in a markedly attenuated posterior tail (Fig. 12). Cells *in vivo* ranging from 250-400 μm long and 45-60 μm wide. Body strongly contractile (especially the tail region), sensitive to stimuli

but usually motionless on the substrate. Ectoplasm thin with numerous large (ca 2-3 µm), ovoid granules (Fig. 13). Sub-pellicular granules absent. Needle-like dorsal cilia located on the tips of cylindrical papillae (Fig. 13, arrow). Under the cover glass, specimens frequently observed with spherical, pyriform, or bar-shaped "extrusome-like" structures emerging from between the dorsal cilia (Fig. 13). Food vacuoles large, often full of diatoms and other algae in the trunk part, which usually give the body a green- or yellow-brownish colour.

Cells may remain motionless for long periods except for the activity of the membranelles. When moving rapidly forward the head may bend from side to side in a similar fashion to *Uroleptus retractilis*. When stimulated cells may reverse rapidly for a distance of about one body length.

Infraciliature as described by Carey and Tatchell (1983) and Wicklow and Borror (1990) (Figs. 15, 16). The anterior part of AZM bending markedly along the right margin and almost connected with the right marginal row. The dikinetid paroral membrane (PM) and monokinetid endoral membrane (EM) about parallel and *in vivo* hardly visible. A single, non-enlarged frontal cirrus is located to the right of the anterior end of undulating membranes. This cirrus is derived from the undulating-membrane-anlage and should more properly be called a buccal cirrus.

About 12-13 ventral rows of cirri (VR) running diagonally right to left; 3 rows situated within the frontal area (head region) and the rest occupy almost the whole ventral surface behind the buccal field (Fig. 15). Transverse cirri (TC) in a single row on the left side extending up to 3/5 of cell length. Two rows of marginal cirri beginning just behind the termination of the peristome field on both sides, passing down the lateral edges of the body and joining at the apex of the tail where the right row (RMR) overturns slightly to the left side whereas the left row (LMR) terminates adjacent to the posterior transverse cirrus (Fig. 15).

Three distinct longitudinal rows of single dorsal bristles, about 1 µm long, arising from the tips of cylindrical papillae (Fig. 13, arrow), which are probably unique in the order Hypotrichida (Carey and Tatchell 1983).

Numerous small macronuclei (Ma) ovoid or elongate, usually concentrated with the trunk region of the cell with several micronuclei (Mi) sparsely distributed among them (Fig. 16).

Acknowledgements. This work was supported by the "Science Foundation of Outstanding Youth of China", (project number: 39425002) awarded to the senior author and a grant from the Royal Society, U.K. to Dr A. Warren. We wish to thank Mr. Shi and Hu, postgraduate students from the College of Fisheries, Ocean University of Qingdao, for collecting material.

REFERENCES

- Borror A. (1972) Revision of the order Hypotrichida (Ciliophora, Protozoa). *J. Protozool.* **19**: 1-23
- Bullington W. E. (1940) Some ciliates from the Tortugas. *Papers Carnegie Inst. Wash. Tortugas Lab.* **32**: 179-221
- Bütschli O. (1887-1889) Protozoa, Abt. III. Infusoria und System der Radiolaria. In: *Klassen und Ordnung des Thiers-Reichs*, (Ed. H. G. Bronn). **1**: 1098-2023
- Calkins G. N. (1902) Marine Protozoa from Woods Hole. *Bull. U. S. Fish. Commn.* **21**: 413-468
- Carey P. G., Tatchell E. C. (1983) A revision of the genus *Epiclintes* (Ciliophora: Hypotrichida) including a redescription of *Epiclintes felis* comb. n. *Bull. Br. Mus. nat. Hist. (Zool.)* **45**: 41-54
- Claparède E., Lachmann J. (1858) Etude sur les infusoires et les rhizopodes. *Mém. inst. Gènevoise* **5**: 1-482
- Corliss J. O. (1979) *The Ciliated Protozoa. Characterization, Classification and Guide to the Literature*. 2 ed. Pergamon Press. New York
- Ehrenberg C. G. (1830) Beiträge zur Kenntnis der Organisation der Infusorien und ihrer geographischen Verbreitung, besonders in Siberien. *Abh. Akad. Wiss. DDR (Year 1832)*, 1-88
- Hemberger H. (1982) Revision der Ordnung Hypotrichida Stein (Ciliophora, Protozoa) an Hand von Protargolimprägung und Morphogenesedarstellungen. Diss. Univ. Bonn
- Kahl A. (1932) Urtiere oder Protozoa I. Wimpertiere oder Ciliata (Infusoria) III. Spirotricha. In: *Die Tierwelt Deutschlands* (Ed. F. Dahl) **25**: 399-650
- Kahl A. (1933) Ciliata Libera et Ectocommensalia. In: *Die Tierwelt der Nord und Ostsee* (Eds. G. Griempe and E. Wagler) **23 (Tiel II, c3)**: 29-146
- Kent W. S. (1880-1882) *A Manual of the Infusoria*. 1-3. David Bogue, London
- Quennerstedt A. (1867) Bidrage till Sveriges infusorie-fauna. *Acta Univ. Lund.* **2**: 41
- Song W., Wilbert N., Berger H. (1992) Morphology and morphogenesis of the soil ciliate *Bakuella edaphoni* nov. spec. and revision of the genus *Bakuella* Agamaliyev and Alekperov, 1976 (Ciliophora, Hypotrichida, Urostylidae). *Bull. Br. Mus. nat. Hist. (Zool.)* **58**: 133-148
- Stein F. R. (1862) Neue oder nicht genügend bekannten Infusorien Tiere. *Amtl. Ber. Dt. Naturf. Aerzte.* **37**: 161-162
- Strethill-Wright, T. (1862) Observations on British Protozoa. *Quart. J. Mic. Sci. New Ser.* **2**: 217-221
- Wallengren H. (1900) Studier öfver Ciliata Infusorier. *Acta Univ. Lund.* **36**: 1-54
- Wicklow B. J. (1979) *Epiclintes ambiguus* and *Kerona polyporum*: comparative ultrastructure, cortical morphogenesis and systematics of two hypotrich ciliates. *J. Protozool.* **26**: 16A
- Wicklow B. J., Borror A. C. (1990) Ultrastructure and morphogenesis of the marine Epiclinterid ciliate *Epiclintes ambiguus* (Epiclinteridae, n. fam.; Ciliophora). *Europ. J. Protistol.* **26**: 182-194
- Wilbert N. (1975) Eine verbesserte Technik der Protargolimprägung für Ciliaten. *Mikrokosmos* **64**: 171-179

Received on 18th July, 1995; accepted on 29th December, 1995

Notes on Flagellate Nomenclature. I. *Cryptaulaxoides* nom. n., a Zoological Substitute for *Cryptaulax* Skuja, 1948 (Protista *incertae sedis*) non *Cryptaulax* Tate, 1869 (Mollusca, Gastropoda) non *Cryptaulax* Cameron, 1906 (Insecta, Hymenoptera), with Remarks on Botanical Nomenclature

Gianfranco NOVARINO

Department of Zoology, The Natural History Museum, Cromwell Road, London, England

Summary. The new name *Cryptaulaxoides* is introduced to replace *Cryptaulax* Skuja, 1948 (non *Cryptaulax* Tate, 1869, non *Cryptaulax* Cameron, 1906), a name of a genus of heterotrophic flagellate protists, under Article 60 of the International Code of Zoological Nomenclature. All but one of the existing species of *Cryptaulax* Skuja are recombined in *Cryptaulaxoides*. If the genus is regarded as ambiregnal, under the International Code of Botanical Nomenclature it can bear the name *Cryptaulax* Skuja legitimately because the name is not pre-occupied by a homonym applied to a genus treated as a genus of plants. A "dual" (ICZN - ICBN) nomenclature of the genus and its species is presented.

Key words: Ambiregnal protists, *Cryptaulax* Skuja, 1948 non Tate, 1869 non Cameron, 1906, *Cryptaulaxoides* nom. n., flagellates, nomenclature.

INTRODUCTION

Skuja (1948) introduced the new generic name *Cryptaulax* to replace *Spiromonas* Skuja, 1939, a name which he himself had introduced a few years earlier for a new genus of heterotrophic flagellate protists (Skuja 1939). This was due to the fact that *Spiromonas* Skuja, 1939 had an earlier (senior) homonym in *Spiromonas* Perty, 1852. However, under the zoological nomenclature the name *Cryptaulax* Skuja, 1948 is pre-occupied by *Cryptaulax* Cameron, 1906, a name of a genus of parasitic wasps, which is itself pre-occupied by *Cryptaulax* Tate, 1869, a name of a genus of fossil gastropod

molluscs. Both the most junior homonym (*Cryptaulax* Skuja, 1948) and the most senior one (*Cryptaulax* Tate, 1869) have been used in the recent literature (Larsen and Patterson 1990, Vørs 1992, Novarino et al. 1994, Bandel 1994). This makes it difficult to argue a case for the conservation of the most junior homonym on the basis of more frequent use. Therefore, it is necessary to introduce a new name to replace *Cryptaulax* Skuja, 1948 under Art. 60 of the International Code of Zoological Nomenclature (ICZN) (Ride et al. 1985).

The genus for which Skuja coined the names *Spiromonas* Skuja, 1939 and then *Cryptaulax* Skuja, 1948 may be regarded as ambiregnal (Patterson 1986), that is, one whose nomenclature is governed both by the ICZN and the International Code of Botanical Nomenclature (ICBN: Greuter et al. 1994). In the author's view, this makes it necessary to specify the correct nomenclature under both Codes, as advocated by Patterson and Larsen (1991). This procedure

Address for correspondence: Gianfranco Novarino, Department of Zoology, The Natural History Museum, Cromwell Road, London SW75BD, England; Fax: [+44](0)171-938.8754; E-mail (INTERNET): gn@nhm.ac.uk

is in line with the current practice for various groups of ambiregnal protists (Larsen and Patterson 1990, Novarino and Lucas 1995), although its laboriousness has attracted some criticism (Corliss 1995). Unlike the case of the ICZN, it appears that the name *Cryptaulax* Skuja, 1948 can be used under the ICBN because it is not pre-occupied by a homonym applied to a genus treated as a genus of plants (ICBN, Art. 54.1).

NOMENCLATURE

Cryptaulaxoides Novarino nom. n. (ICZN)

Cryptaulax Skuja, 1948 (ICBN)

Gender of *Cryptaulaxoides* (ICZN) and *Cryptaulax* (ICBN): feminine

Etymology: from the Greek words *κρυπτος* (= *cryptos*, "hidden") and *αυλαξ* (= *aulax*, "furrow"), referring to the characteristic groove on the cell surface.

Synonyms of *Cryptaulaxoides* (ICZN): *Spiromonas* Skuja, 1939 (Skuja 1939, p. 99) non *Spiromonas* Perty, 1852 (Perty 1852, p. 171) non *Spiromonas* Skvortzow, 1957 (Skvortzow 1957, p. 190); *Cryptaulax* Skuja, 1948 pro parte (Skuja 1948, p. 363) non *Cryptaulax* Tate, 1869 (Tate 1869, p. 418) non *Cryptaulax* Cameron, 1906 (Cameron 1906, p. 150).

Synonyms of *Cryptaulax* (ICBN): *Spiromonas* Skuja, 1939 (Skuja 1939, p. 99) non *Spiromonas* Perty, 1852 (Perty 1852, p. 171) non *Spiromonas* Skvortzow, 1957 (Skvortzow 1957, p. 190).

A *bona fide* list of species of the genus is as follows:

Cryptaulaxoides akopos (Skuja, 1939) comb. n. (ICZN)

Basionym: *Spiromonas akopos* Skuja, 1939 (p. 99, pl. V, fig. 25).

Synonym: *Cryptaulax akopos* (Skuja, 1939) Skuja, 1948 (p. 363).

Equivalent name in botanical nomenclature: *Cryptaulax akopos* (Skuja, 1939) Skuja, 1948 (ICBN) (synonym: *Spiromonas akopos* Skuja, 1939, p. 99, pl. V, fig. 25).

This is the type species, designated by Skuja (1948, p. 363). It was further reported by Skuja (1956, p. 351).

Cryptaulaxoides conoidea (Skuja, 1956) comb. n. (ICZN)

Basionym: *Cryptaulax conoidea* Skuja, 1956 (p. 351, pl. LXI, figs 9-11).

Equivalent name in botanical nomenclature: *Cryptaulax conoidea* Skuja, 1956 (ICBN).

Cryptaulaxoides elegans (Larsen and Patterson, 1990) comb. n. (ICZN)

Basionym: *Cryptaulax elegans* Larsen and Patterson, 1990 (p. 905, figs 53c, 54a-d).

Equivalent name in botanical nomenclature: *Cryptaulax elegans* Larsen and Patterson, 1990 (ICBN).

Cryptaulax elegans Larsen and Patterson, 1990, was described without an accompanying Latin diagnosis, the authors considering that it was under the jurisdiction of the ICZN alone. However, if *Cryptaulax elegans* is considered as ambiregnal, it could be regarded as belonging to the algae (see below). In this case, the name *Cryptaulax elegans* need only satisfy the requirements of the ICZN for status equivalent to valid publication under the ICBN; it retains its original authorship and date even though the original publication lacked a Latin diagnosis (ICBN, Art. 45.5; the present case is analogous to Example 5).

Cryptaulaxoides formica (Skuja, 1948) comb. n. (ICZN)

Basionym: *Cryptaulax formica* Skuja, 1948 (p. 364, pl. XXXVIII, figs 33, 34).

Equivalent name in botanical nomenclature: *Cryptaulax formica* Skuja, 1948 (ICBN).

Cryptaulaxoides longiciliata (Skuja, 1948) comb. n. (ICZN)

Basionym: *Cryptaulax longiciliatus* [sic] Skuja, 1948 (p. 364, pl. XXXVIII, figs 31, 32).

Equivalent name in botanical nomenclature: *Cryptaulax longiciliatus* [sic] Skuja, 1948 (ICBN).

Cryptaulaxoides marina (Thronsen, 1969) comb. n. (ICZN)

Basionym: *Cryptaulax marina* Thronsen, 1969 (p. 168, figs 3a, b).

Equivalent name in botanical nomenclature: *Cryptaulax marina* Thronsen, 1969 (ICBN).

This species was further reported by Vørs (1992, p. 74, figs 21.1-4, 37a-d; 1993, p. 115, fig. 40B).

Cryptaulaxoides thiophila (Skuja, 1956) comb. n. (ICZN)

Basionym: *Cryptaulax thiophila* Skuja, 1956 (p. 352, pl. LXI, figs 12-15).

Equivalent name in botanical nomenclature: *Cryptaulax thiophila* Skuja, 1956 (ICBN).

This species is provisionally retained in the genus until further information on its taxonomic position will become available (see below).

***Cryptaulaxoides vulgaris* (Skuja, 1948) comb. n. (ICZN)**

Basionym: *Cryptaulax vulgaris* Skuja, 1948 (p. 363, pl. XXXVIII, figs 27, 28).

Equivalent name in botanical nomenclature: ***Cryptaulax vulgaris* Skuja, 1948 (ICBN).**

This species was further reported by Skuja (1956, p. 351) and Novarino et al. (1994, p. 31, figs 11-14, 19B).

One further species assigned to the genus (*Cryptaulax taeniata* Skuja, 1956, p. 351, pl. LXI, figs 6-8), was recombined as *Rhynchobodo taeniata* (Skuja, 1956) Vørs, 1992 (Vørs 1992, p. 47), the type-species of the genus *Rhynchobodo* Lackey, 1940 emend. Vørs, 1992. In agreement with Vørs (1992), this species is excluded from *Cryptaulaxoides/Cryptaulax* on taxonomic grounds (see below).

DISCUSSION

In spite of the fact that nomenclatural changes may be viewed as irritating (Crisp and Fogg 1988), changes are necessary when there is a conflict between existing names in current use. In order to avoid changes as a mere consequence of what is sometimes termed “antiquarian” nomenclatural research, the ICZN and ICBN allow for the possibility of proposing the conservation of a junior homonym if it has been used much more frequently than a senior homonym. In the case of the name *Cryptaulax* Skuja, 1948, this possibility cannot be envisaged under the ICZN. Cosmann (1913) included 15 species in the genus *Cryptaulax* Tate, 1869, and new species have been described in this genus as recently as in 1994 (Bandel 1994). Therefore, *Cryptaulax* Tate, 1869 cannot be considered as a forgotten name, as confirmed by Morris (Dr N. Morris, Dept. of Palaeontology, Natural History Museum, London: personal communication). It follows that under the ICZN (Art. 60) the name *Cryptaulax* Skuja, 1948 must be rejected and replaced. Since the name has no known available synonyms, it must be replaced by a new name (ICZN, Art. 60c). *Cryptaulaxoides* is chosen as the new name because it recalls the one it replaces. In accordance with the ICZN (Art. 67h) the type species of *Cryptaulaxoides* is the same as that of *Cryptaulax* Skuja, 1948.

Ambireginal issues are a further source of regrettable but hardly avoidable nomenclatural confusion. The genus *Cryptaulax* Skuja, 1948 was included in a catalogue of plant genera (Greuter et al. 1993) as a genus of cryptomonads, a group of ambireginal flagellates (Novarino and Lucas 1995). This reflected Skuja’s (1939) attribution of the genus to the botanical class Cryptophyceae, family Katablepharidaceae Skuja, 1939. Observations by Larsen and Patterson (1990) and Vørs (1992) have shown that the genus is not a genus of cryptomonads, suggesting that it could be removed from the jurisdiction of the ICBN altogether and placed under exclusive ICZN control. However, Vørs (1992) suggested that the genus could belong to the kinetoplastids. This has not been confirmed, and although the genus is currently considered as a genus of protists *incertae sedis*, the possibility that it belongs to the kinetoplastids might justify a future assignment not only to the zoological class Kinetoplastidea Honigberg, 1963, order Bodonida Hollande, 1952 (see Corliss 1994), but also to the botanical class Bodonophyceae Silva, 1980, a class of algae (Silva 1980). Therefore, as a precaution the genus should be considered as falling under the dual jurisdiction of the ICZN and ICBN, and the correct nomenclature under each Code should be presented, in agreement with the “non-partisan” approach of Patterson and Larsen (1991). Under the ICBN, the name *Cryptaulax* Skuja, 1948 can be used legitimately because it is not pre-occupied by a homonym applied to a genus treated as a genus of plants (ICBN, Art. 54.1). Thus the correct name of the genus under the ICBN (*Cryptaulax*) differs from that under the ICZN (*Cryptaulaxoides*), analogous to other genera of flagellates, most notably euglenids such as *Pernanema/Pseudoperanema* and *Dinema/Dinematomonas* (see Larsen and Patterson 1990).

The taxonomic concept of the genus *Cryptaulaxoides/Cryptaulax* adopted here follows that of Vørs (1992), who recombined *Cryptaulax taeniata* Skuja, 1956 as *Rhynchobodo taeniata* (Skuja, 1956) Vørs, 1992, thereby excluding that species from *Cryptaulaxoides/Cryptaulax*. Currently, differential criteria for admission to *Cryptaulaxoides/Cryptaulax* and *Rhynchobodo* Lackey, 1940 emend. Vørs, 1992 are as follows:

- Polykinetoplastid flagellates with extrusomes of the “latticetube” type; surface groove present or absent.....***Rhynchobodo***
- Extrusomes absent; groove always present***Cryptaulaxoides/Cryptaulax***

As underlined by Vørs (1992), unlike all other species of *Cryptaulaxoides/Cryptaulax* described by Skuja (1939, 1948, 1956) *Cryptaulax thiophila* Skuja, 1956 was described as possessing extrusomes. As such, that species does not belong with *Cryptaulaxoides/Cryptaulax* if the taxonomic criteria given here are followed. However, it is provisionally retained in the genus until the presence of extrusomes is confirmed.

Acknowledgements. Many thanks are due to Dr P. K. Tubbs (International Commission on Zoological Nomenclature, London), who made helpful comments and suggested the name *Cryptaulaxoides*; and Dr N. Morris (Natural History Museum, London), who provided useful information on the genus *Cryptaulax* Tate non Cameron non Skuja.

REFERENCES

- Bandel K. (1994) Comparison of Upper Triassic and Lower Jurassic gastropods from the Peruvian Andes (Pucara Group) and the Alps (Cassian Formation). *Palaeontographica, Abt. A: Palaeozoologie-Stratigraphie* **233**: 127-160
- Cameron P. (1906) Descriptions of new species of parasitic Hymenoptera, chiefly in the collection of the South African Museum, Cape Town. *Ann. S. Afr. Mus.* **5**: 17-186
- Corliss J. O. (1994) An interim utilitarian (user-friendly) hierarchical classification and characterization of the protist. *Acta Protozool.* **33**: 1-51
- Corliss J. O. (1995) The ambiregnal protists and the Codes of nomenclature: a brief review of the problem and of proposed solutions. *Bull. Zool. Nomencl.* **52**: 11-17
- Cosmann M. (1913) Contribution à la paléontologie française des terrains Jurassiques. III. Cerithiacea et Loxonematacea. *Mém. Soc. Géol. Fr. - Paléontologie* **46**: 1-264
- Crisp D. J., Fogg G. E. (1988) Taxonomic instability continues to irritate. *Nature* **335**: 120-121
- Greuter W., Barrie F. R., Burdet H. M., Chaloner W. G., Demoulin V., Hawksworth D. L., Jørgensen P. M., Nicolson D. H., Silva P. C., Trehane P., McNeill J. (1994) International Code of Botanical Nomenclature (Tokyo Code). Adopted by the Fifteenth International Botanical Congress, Yokohama, August-September 1993. Koeltz Scientific Books, Königstein
- Greuter W., Brummitt R. K., Farr E., Kilian N., Kirk P. M., Silva P. C. (1993) NCU -3. Names in current use for extant plant genera. Koeltz Scientific Books, Königstein
- Larsen J., Patterson D. J. (1990) Some flagellates (Protista) from tropical marine sediments. *J. Nat. Hist.* **24**: 801-937
- Novarino G., Lucas I. A. N. (1995) A zoological classification system of cryptomonads. *Acta Protozool.* **34**: 173-180
- Novarino G., Warren A., Kinner N. E., Harvey R. W. (1994) Protists from a sewage-contaminated aquifer on Cape Cod, Massachusetts. *Geomicrobiol. J.* **12**: 23-36
- Patterson D. J. (1986) Some problems of ambiregnal taxonomy and a possible solution. *Symp. Biol. Hung.* **33**: 87-93
- Patterson D. J., Larsen J. (1991) Nomenclatural problems with protists. In: Improving the stability of names: needs and opinions, (Ed. D. L. Hawksworth). *Regnum Vegetabile*, Koeltz Scientific Books, Königstein, **123**: 197-208
- Perty M. (1852) Zur Kenntniss kleinster Lebensformen nach Bau, Funktionen, Systematik, mit Spezialverzeichnis der in der Schweiz beobachtet. Verlag von Jent und Reinert, Bern
- Ride W. D. L., Sabrosky C. W., Bernardi G., Melville R. V., Corliss J. O., Forest J., Key K. H. L., Wright C. W. (1985) International Code of Zoological Nomenclature, Third Edition. Adopted by the XX General assembly of the International Union of Biological Sciences. International Trust for Zoological Nomenclature and University of California Press, London
- Silva P. C. (1980) Names of classes and families of living algae. *Regnum Vegetabile* **103**: 1-156
- Skuja H. (1939) Beitrag zur Algenflora Lettlands II. *Acta Hort. Bot. Univ. Latv.* **11/12**: 41-169
- Skuja H. (1948) Taxonomie des Phytoplanktons einiger Seen in Uppland, Schweden. *Symb. Bot. Upsal.* **9**: 1-399
- Skuja H. (1956) Taxonomische und biologische Studien über das Phytoplankton Schwedischer Binnengewässer. *Nova Acta R. Soc. Scient. Upsal., Ser IV* **16**: 1-404
- Skvortzow B. W. (1957) New and rare flagellatae from Manchuria, Eastern Asia. *Phil. J. Science* **86**: 139-202
- Tate R. (1869) Contributions to Jurassic palaeontology. 1. *Cryptaulax*, a new genus of Cerithiadae. *Ann. Mag. Nat. Hist., Series IV* **4**: 417-419
- Vørs N. (1992) Heterotrophic amoebae, flagellates and heliozoa from the Tvärminne area, Gulf of Finland. *Ophelia* **36**: 1-109
- Vørs N. (1993) Heterotrophic amoebae, flagellates and heliozoa from Arctic marine waters (North West Territories, Canada and West Greenland). *Polar Biol.* **13**: 113-126

Received on 25th September, 1995; accepted on 11th January, 1996

Nematopsis idella sp. n. and *Uradiophora cuenoti* Mercier: Two Cephaline Gregarines from Freshwater Prawns in Kerala

P K. PRASADAN and K P. JANARDANAN

Parasitology Laboratory, Department of Zoology, University of Calicut, Kerala, India

Summary. Two species of cephaline gregarines, *Nematopsis idella* sp. n. and *Uradiophora cuenoti* Mercier infecting the freshwater prawns, *Macrobrachium idella* and *Caridina* sp. respectively have been reported. *U. cuenoti* is reported for the first time from an Indian prawn.

Key words: *Caridina* sp., gregarines, *Macrobrachium idella*, prawns, *Nematopsis idella* sp. n., *Uradiophora cuenoti* Mercier.

Abbreviations: AAL - atrophied appendix length, AAW - atrophied appendix width, DL - deutomerite length, DW - deutomerite width, LA - length of association, PL - protomerite length, PW - protomerite width.

INTRODUCTION

Three species of *Nematopsis*, 4 species of *Caridohabitans* and a species *Cephalolobus* have been reported from Indian prawns (Setna and Bhatia 1934, Ball 1959, Sprague and Couch 1971, Janardanan and Ramachandran 1980, Shanavas et al. 1989, Prema and Janardanan 1990). Extensive survey of freshwater prawns of Kerala for their parasites revealed two species of cephaline gregarines belonging to the genera *Nematopsis* Schneider, 1892 and *Uradiophora* Mercier, 1912. Detailed studies proved that *Nematopsis* is new to science, and is designated *N. idella* sp. n. The other is identified and reported here as *Uradiophora cuenoti* described by Mercier (1912) from France.

MATERIALS AND METHODS

The freshwater prawns, *Macrobrachium idella* collected from a rivulet in Ramanattukara in Calicut district and *Caridina* sp. from rivulets in Thazhechovva, in Cannanore district, Ramanattukara in Calicut district and Olippuramkadavu in Malappuram district of Kerala, were brought alive to laboratory and examined for their gregarines. Sporadins and trophozoites recovered from the intestine and gametocysts from the rectum and faecal pellets were studied following the procedure outlined by Prema and Janardanan (1990). Descriptions are based on the measurements of a minimum of 20 specimens. Measurements are in micrometers (μm). Drawings were made with the help of a camera lucida.

RESULTS

Nematopsis idella sp. n. (Fig. 1)

Host: *Macrobrachium idella* (Heller)

Site: intestine.

Locality: Ramanattukara, Calicut district, Kerala (India).

Date of collection: July to December of 1986, 1987.

Address for correspondence: K. P. Janardanan, Department of Zoology, University of Calicut, Kerala - 673 635, India

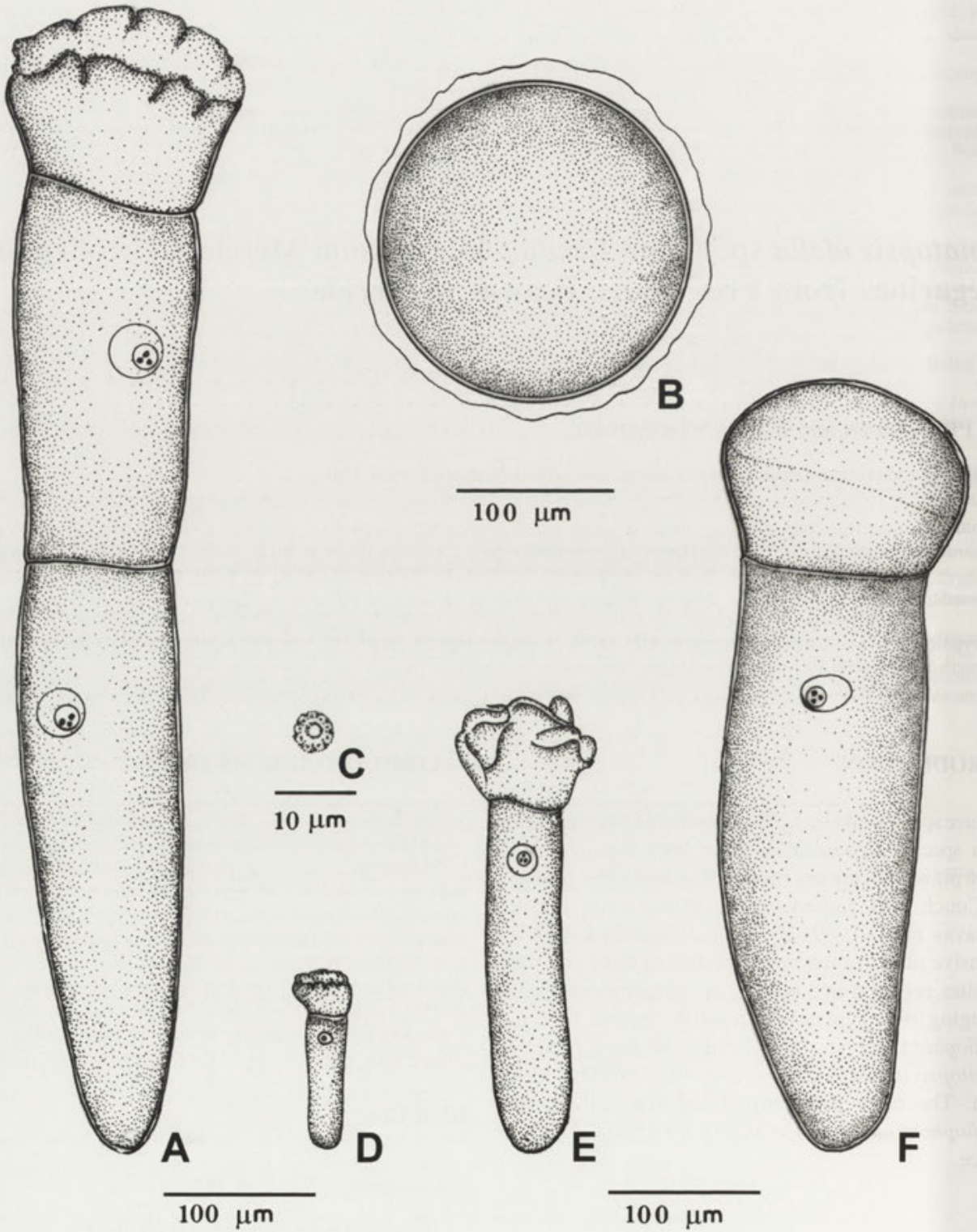


Fig. 1. *Nematopsis idella* sp. n. A - sporadin, B - gametocyst, C - gymnospor, D-F - trophozoites

Holotype: on slide No. G/N-4 kept in the parasite collections, Parasitology Laboratory, Department of Zoology, University of Calicut, Kerala (India).

Description

Sporadins (Fig. 1A) biassociative, linear, elongate, cylindrical, milky-white; protomerite flower-like, changes its shape frequently; epimerite absent in all stages of development.

Primites elongate, milky-white; protomerite flower-like, frequently assuming hemispherical shape; broader than deutomerite; epicyte thin, hyaline; endocyte granular. Septum slightly convex toward deutomerite; constriction at septum conspicuous. Deutomerite cylindrical; epicyte thin, uniformly thick; endocyte granular. Nucleus spherical; variable in position. Endosome single, round; extraendosome region clear. Nucleus in a 377.3 long primate measured 30.8 in diameter.

Satellites elongate, cylindrical, maximally wide just below the line of association and gradually tapers to end in a round caudad; protomerite not distinct. Epicyte uniformly thick; endocyte granular. Nucleus spherical; feebly visible in fresh satellites; endosome single, round; extraendosome region clear. Nucleus in a 400.4 long satellite measured 30.8 in diameter.

Measurements of sporadins (with mean in parentheses) are noted below:

LA = 577.5-777.7 (665.3)

Primites: DW = 80.8-127.1 (101.6); PL = 84.7-127.1 (103.9)

PW = 107.8-173.3 (135.6); TL = 269.5-377.3 (314.2)

Satellites: DW = 77-127.1 (96.3); TL = 308-400.4 (351.1)

Ratios: Primites:PL:TL = 1:3.01; PW:DW = 1:0.75

Gametocysts (Fig. 1B) spherical, rarely ovoid, milky-white, with a hyaline, 15.4-19.8 thick cyst wall. Line of association clear in early gametocysts. Spherical gametocysts measured 151.8-246.2 (187.8) in diameter.

Gymnospores (Fig. 1C) spherical, opaque, milky-white; uninucleated bodies arranged in the form of a rosette, around a central, hyaline cytoplasm. Fresh gymnospores measured 4.5 in diameter.

Biology: gametocysts recovered from the hindgut were in different stages of development. A few of them completed development and ruptured to liberate gymnospores in the rectal lumen. Further development of the gymnospores could not be observed, since molluscan host involved in the life-cycle is unknown.

The smallest observed trophozoite (Fig. 1D) measured 119.4 by 30.8 with 27 long protomerite and 92.4 long

deutomerite. Protomerite flower-like. Largest observed trophozoite (Fig. 1F) measured 532 by 146.3. The flower-like protomerites (Fig. 1E) of trophozoites change frequently to hemispherical shape (Fig. 1F).

Uradiophora cuenoti Mercier, 1912 (Fig. 2)

Host: *Caridina* sp.

Site: intestine.

Locality: Thazhechovva, Cannanore district; Olippuramkadavu, Malappuram district, Kerala (India).

Date of collection: July to November 1987, 1988, 1989.

Description

Sporadins (Fig. 2A) biassociative, linear, elongate, cylindrical milky-white; syzygy early. Tongue-shaped epimerite (Fig. 2C) observed on sporadins in syzygies up to a length of 333 (Fig. 2B). Length of association range from 329.2 to 568 (405.3).

Primites elongate, milky-white, cylindrical. Protomerite hemispherical to rectangular with thin striated epicyte; endocyte granular. Septum flat or slightly convex toward protomerite; constriction at septum conspicuous. Deutomerite elongate, cylindrical with almost uniform width throughout. Epicyte thin; endocyte granular. Nucleus ovoid, feebly visible in mature sporadins, variable in position; endosome single, spherical. Nucleus in a primate of 268.1 by 13.2 measured 9.9 by 7.4.

Satellites elongate, cylindrical milky-white. Protomerite rectangular to hemispherical. Deutomerite, nucleus and endosome similar to that of primate. Nucleus in a 160 long satellite measured 11.6 by 8.3.

An elongate, cylindrical, atrophied appendix present at the posterior end of satellite; its cytoplasm agranular, without any nucleus. The appendix measured 35.5-182.3 by 4.1-10.7 (64.4 by 6.2).

Measurements of sporadins (without epimerites) in micrometers (with mean in parentheses) are noted below:

LA = 329.2-568 (405.3)

Primites: DW = 7.4-13.2 (9.5); PL = 5.8-9.9 (7.1)
PW = 6.6-9.9 (8). TL = 153.5-268.1 (201.3)

Satellites: AAL = 35.5-182.3 (64.4); AAW = 4.1-10.7 (6.2); DW = 8.3-13.2 (9.9); PL = 3.3-7.4 (4.9); PW = 6.6-9.9 (7.6).

Ratios: Primites: PL:TL = 1:28.8; PW:DW = 1:1.2; Satellites: PL:TL = 1:43.1; PW:DW = 1:1.3

Gametocysts (Fig. 2D) spherical to ovoid; milky-white, with a thin hyaline cyst wall. Line of association clear in early gametocysts. Spherical gametocysts measured 29.7-52.8 (36.6) in diameter.

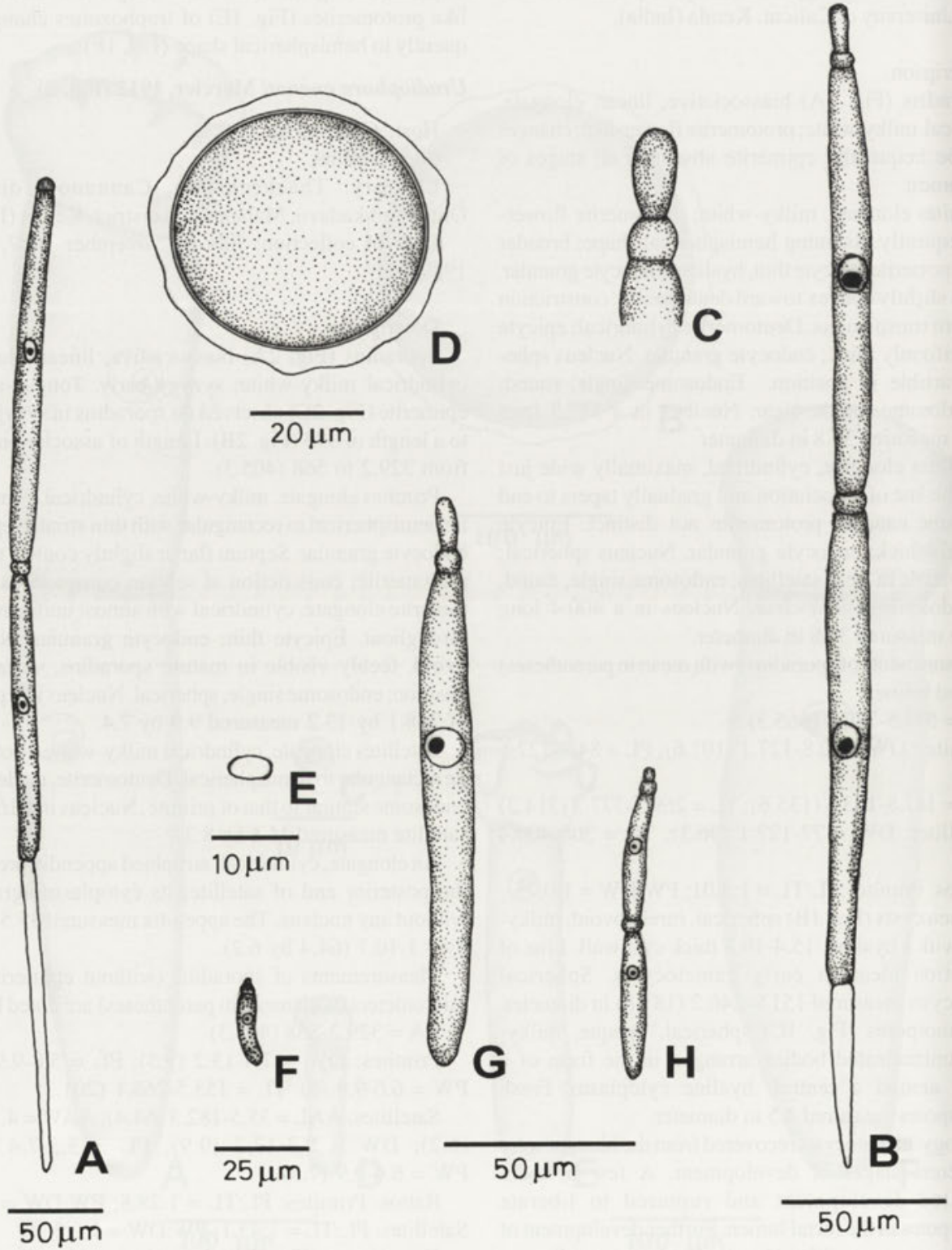


Fig. 2. *Uradiophora cuenoti* Mercier, 1912. A-B - sporadins, C - anterior part of Fig. 2B (enlarged), D - gametocyst, E - spore, F-H - trophozoites

Spores (Fig. 2E) elongate ovoid. Fresh spores measured 5.31-6 by 2.6 (5.5 by 2.6).

Biology: gametocysts recovered from the hindgut and faecal pellets were in different stages of development. Gametocysts maintained in moist chamber released the spores by simple rupture.

Smallest observed trophozoite (Fig. 2F) measured 24 long with a bud-like epimerite, hemispherical protomerite and elongate cylindrical deutomerite. The largest observed trophozoite (Fig. 2G) measured 165 long with a 15 long, tongue-shaped epimerite, 8 long, hemispherical protomerite and 142 long, cylindrical deutomerite.

Smallest observed association (Fig. 2H) measured 85.8 in length; small bud-like epimerite present. Its primate measured 41.3 and satellite 44.5 in length.

DISCUSSION

Nematopsis idella sp. n.

The gregarine recovered from *Macrobrachium idella* has trophozoites and sporadins which are comparable to that of the genus *Nematopsis*; its gametocyst formed gymnosporous. These characters are significant enough for inclusion of the gregarine under the genus, *Nematopsis*. The present gregarine differs from the known species of *Nematopsis* in morphology and morphometry. The flower-like protomerite of this gregarine makes it distinct from all other species. Besides, this is the first report of a cephaline gregarine from *M. idella*. The gregarine is, therefore, reported as a new species and named *Nematopsis idella* sp. n., after its host.

Uradiophora cuenoti Mercier

The gregarine under study has extracellular development, an elongate papilla like epimerite, cysts without sporoducts, subspherical spores which do not form chains and an atrophied appendix at the posterior part of satel-

lites. Based on these characters, the gregarine is assigned to the genus *Uradiophora*. This gregarine resembles *U. cuenoti* reported by Mercier (1912) from *Atyaephyra desmaresti* and *Neocardina denticulata* in France in its morphological characters. Hoshide (1969) also reported *U. cuenoti* from *N. denticulata* in Japan. But it shows some differences in morphometry, in the nature of the epimerite and in the shape of gametocysts and spores. These differences are not significant enough for the creation of a new species under the genus *Uradiophora*. The gregarine is therefore reported as *Uradiophora cuenoti* Mercier. This forms the first report of the genus from an Indian prawn.

Acknowledgements. The authors express their sincere thanks to the UGC, New Delhi for financial assistance in the form of a major research project (F. 3-79/86 SR II). One of the authors (P.K.P) is grateful to CSIR, New Delhi for financial support.

REFERENCES

- Ball G. H. (1959) Some gregarines from crustaceans taken near Bombay, India. *J. Protozool.* **6**: 8-13
- Hoshide K. (1969) Studies on gregarines from Japan. 1. *Cephaloidophora warekara* n. sp. and two other gregarines from crustaceans. *J. Fac. Sci., Hokkaido University* **17**: 6-16
- Janardanan K. P., Ramachandran P. (1980) Three new species of cephaline gregarines from marine prawns off the Arabian coast at Cannanore. *Arch. Protistenkd.* **123**: 471-478
- Mercier L. (1912) Monographie d' *Uradiophora cuenoti*. *Arch. Zool. Exper.* **10**: 177-202
- Prema S., Janardanan K. P. (1990) Two new species of cephaline gregarines (Apicomplexa: Sporozoa) from the marine prawn *Penaeus indicus* H. Milne Edwards. *Acta Protozool.* **29**: 365-373
- Setna B., Bhatia B. L. (1934) On some gregarines from the prawn, *Parapenaeopsis sculptilis* (Heller). *Parasitology* **26**: 34-43
- Shanavas K. R., Prasad P. K., Janardanan K. P. (1989) *Nematopsis rosenbergii* n. sp. (Apicomplexa: Cephalina) from the brackishwater prawn *Macrobrachium rosenbergii* (De Man). *Arch. Protistenkd.* **137**: 161-164
- Sprague V., Couch J. (1971) An annotated list of protozoan parasites, hyperparasites, and commensals of decapod Crustacea. *J. Protozool.* **18**: 526-537

Received on 27th April, 1995; accepted on 23rd October, 1995

Ionic Mechanisms Controlling Photophobic Responses in the Ciliate *Blepharisma japonicum*

Stanisław FABCZAK¹, Hanna FABCZAK¹, Mirosława WALERCZYK¹, Jerzy SIKORA¹, Bożena GROSZYŃSKA¹ and Pill-Soon SONG²

¹Nencki Institute of Experimental Biology, Department of Cell Biology, Warszawa, Poland, ²University of Nebraska, Department of Chemistry and Institute for Cellular and Molecular Photobiology, Lincoln, NE, USA

Summary. The resting, photoreceptor and action potentials in the ciliate *Blepharisma japonicum* were investigated by conventional microelectrode technique. During exposure to the control solution the membrane resting potentials of the ciliates ranged from -43 to -54 mV. Tenfold increase in the higher concentration of K⁺ in the medium depolarized the membrane potential by 54 mV, while a similar change in extracellular Ca²⁺ caused an alteration in membrane potential by about 14 mV. Changes in external K⁺ concentration did not affect essentially the peaks of receptor and action potentials appearing in response to a given light stimulus, whereas extracellular Ca²⁺ increased by one order of magnitude evoked shift of photoreceptor and the action potential peaks by about 16 mV and 27 mV, respectively. These data indicate that Ca ions take place either in generation of photoreceptor and action potentials in *Blepharisma* cells.

Key words: Action potentials, *Blepharisma japonicum*, Ca²⁺ ions, photoreceptor potentials, photosensory transduction.

INTRODUCTION

Illumination of pink-colored ciliates *Blepharisma japonicum* causes a modification of their motile behavior. This sensitivity to light is ascribed to an endogenous pigment, blepharismine, enclosed in small granules (photoreceptive units) and distributed over the entire cell body surface (Kraml and Marwan 1983, Matsuoka 1983a). When a dark adapted cell is subjected to a short light stimulus it displays a transient reversal of ciliary beating resulting in backward swimming. After the ciliary reversal terminate, the cell resumes again the forward movement, usually in a new direction (step-up photophobic response) (Matsuoka 1983b, Kraml and Marwan 1983,

Fabczak et al. 1993a). Electrophysiological experiments showed that the similar light stimuli elicit a transient depolarization of cell membrane in the ciliate, i.e. generation of photoreceptor potential, which can, in turn, trigger an action potential (Fabczak et al. 1993a). Like in other ciliates (Eckert et al. 1976, Macheimer and De Peyer 1977, Macheimer and Sugino 1989), an action potential leads to reversal of ciliary beating during the cell photophobic response (Fabczak et al. 1993a). Most of the studies devoted to photophobic responses in *Blepharisma* testified to the crucial role of Ca ions in this motile behavior (Passarelli et al. 1984, Fabczak et al. 1994), however, the ionic basis of the light dependent changes of membrane potential in these cells has not been elucidated.

The presented experiments were designed to examine the ionic specificity of the resting membrane potential, receptor and action potentials appearing in *Blepharisma japonicum* in response to light stimulation.

Address for correspondence: Stanisław Fabczak, Nencki Institute of Experimental Biology, Department of Cell Biology, ul. Pasteura 3 02-093 Warszawa, Poland; Fax: 48-22 225342; E-mail: sfabczak@nencki.gov.pl

MATERIALS AND METHODS

Cells and solutions

The stock of *Blepharisma japonicum* were cultured by standard methods (Fabczak et al. 1993a). The control medium included: 0.5 mM CaCl_2 , 1 mM MgSO_4 , 1 mM NaNO_3 , 0.1 mM KCl and 1 mM TRIS-HCl , pH 6.9-7.1. The test solutions with low concentrations of free Ca^{2+} were obtained by addition of appropriate amounts of Ca^{2+} to fixed 1 mM EGTA in Ca^{2+} -free control medium (Portzehl et al. 1964) and the resulting concentrations were verified by means of Ca^{2+} selective electrode (Kwik-TipTM-TIPCA, World Precision Inst., USA). The higher concentrations of Ca^{2+} and other ions were obtained by means of mixing stock solutions in such a way that the level of only one ion was changed while the levels of the remaining ions present in the control medium were unchanged. In experiments with changed concentrations of extracellular Cl^- ions in test solutions, chloride was replaced by nitrate or organic anion propionate and adjusted to a proper pH with HEPES.

Light stimulation

Cells suspended in test solution were illuminated from above with continuous or pulse light (flash) using a 150 W light projector (MLW 9403-0200, Germany) equipped with an electromagnetic programmable shutter (type 22-841, Ealing Electro-Optics, England). The light was delivered close to the chamber containing the cells with a fiber optic guide and its intensity was monitored with a calibrated silicon photodiode (VTA 9313, EG & Vactec, USA) linked to an oscilloscope or a digital voltmeter. Interference and neutral density optic filters were used to provide monochromatic light differing in intensity.

Intracellular recordings

The electrical measurements were made in an experimental chamber with temperature set at 12°C, mounted on a stage of stereoscopic microscope (Citoval Zeiss, Germany). The conventional glass microelectrodes were filled with 1 M potassium acetate adjusted to pH 7.0 with acetic acid. The microelectrode resistances selected for the recordings were in the range of 45 to 65 M Ω with tip potential of -8 to -12 mV. To start the recording session a chosen cell was sucked into the micropipette of suitable tip diameter and kept in the same position. After insertion of a microelectrode the cell was liberated by lowering the pressure in the holding micropipette. The microelectrode signals were fed to a high input impedance amplifier (MPA-6, Transidyne General Corp., USA) and displayed on a storage oscilloscope (type 5103N, Tektronix, USA) equipped with an oscilloscope camera (C-5, Tektronix, USA). The electrical traces presented in the figures were copied by a scanner from the original polaroid records.

RESULTS AND DISCUSSION

The resting membrane potentials measured in individual cells were found to be from -43 to -54 mV in control solution and were shifted to more positive values when external concentrations of potassium and, to a lesser extent, calcium ions were increased. Changes in concentration of other ions normally present in control solution

had little or no effect on the membrane potential (data not shown). Tenfold increase of extracellular K^+ depolarized the cell membrane in accordance with the Nernst equation by about 54 mV (Fig. 1). The cell membrane potential was less affected by shift of K^+ concentration below 2 mM, while almost independent of concentrations between 0.1 and 1 mM. Nonlinear concentration dependence of the resting potential is noticeable in *Blepharisma* cells on changes in concentration of external Ca^{2+} as well (Fig. 2). Increase of Ca^{2+} up to 1 mM influenced the membrane potential on a limited scale but the elevation beyond this level increasingly depolarized the cell membrane. Removal of Ca^{2+} from the cell surrounding by addition of EGTA to the control solution decreased slightly the membrane potential in relation to the potential of control cells. No membrane depolarization were induced in cells by increase of external Na^+ or Mg^{2+} . The curvilinear relationship between the resting potential and external K^+ or Ca^{2+} concentration is characteristic of some other ciliates as well. The ability of both K^+ and Ca^{2+} to permeate the cell membrane in its resting state was reported for related ciliates: *Stentor* (Wood 1982) that displays photophobic responses (Song et al. 1980, Fabczak et al. 1993b) similar to those of *Blepharisma* (Matsuoka 1983, Kraml and Marwan 1983, Fabczak et al. 1993a) and for ciliates lacking the sensitivity to light, like *Paramecia* (Naitoh et al. 1972, Satow et al. 1983) or *Stylonychia* (De Peyer and Machemer 1977).

When dark adapted *Blepharisma* is stimulated with light in the lower intensity range, depolarizing photoreceptor potentials are generated (Fabczak et al. 1993a). Distinct effects of changes in concentrations of K^+ or Ca^{2+} ions in the medium are illustrated in Figs 1 and 2. Effects of these alterations of ionic composition in external solution clearly indicated that only Ca^{2+} were the only cations which had an appreciable effect on the light-dependent responses in *Blepharisma*. Raising of the external Ca^{2+} concentration from 0.1 to 8 mM shifted peak of the receptor potential in response to a given light stimulus by 14 to 18 mV when Ca^{2+} was changed by order of magnitude. At Ca^{2+} concentrations lower than its level in the control solution the amplitude of the receptor potential was declined and in solutions containing 10^{-7} M of free Ca^{2+} or less there were no light dependent membrane responses (data not shown). The photoreceptor potential in *Blepharisma* does not show any dependence on increasing K^+ concentration in the medium. These results lead to the conclusion that Ca^{2+} of external solution normally defines the magnitude of

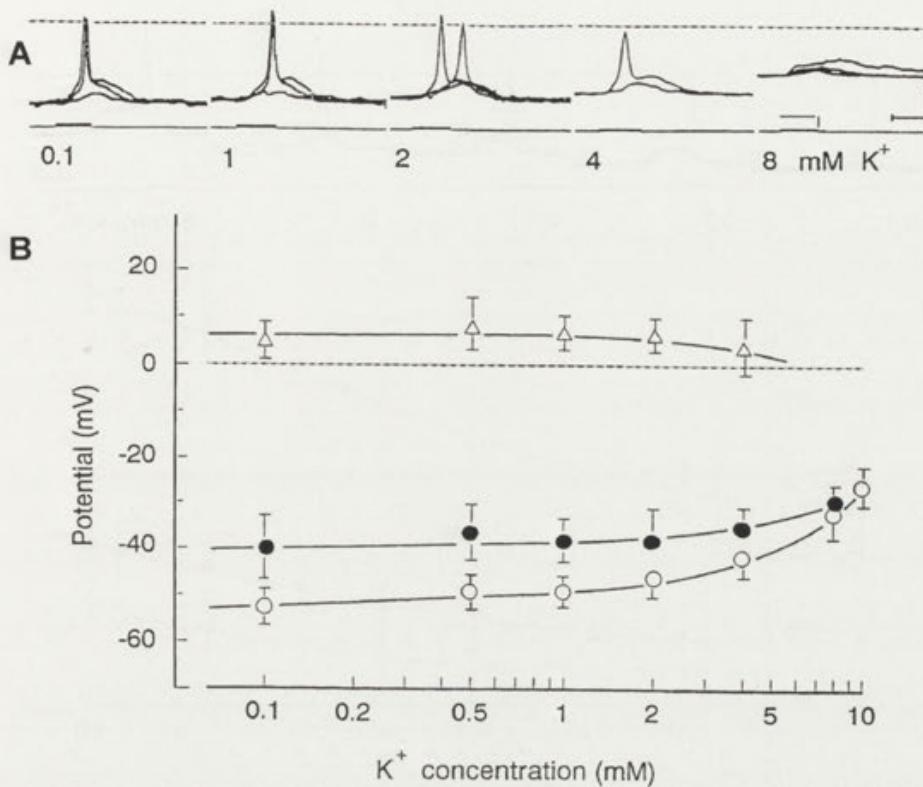


Fig. 1. Dependence of the resting, receptor and action potentials in *Blepharisma japonicum* upon potassium concentrations in external solution (pH 6.9, 12°C). (A) Sets of oscilloscope traces generated by the same cell in each of testing solutions showing resting, receptor and action potentials. Dashed line - 0 mV baseline; vertical bar - 20 mV and $6.5 \times 10^{-4} \text{ W cm}^{-2}$ (580 nm); horizontal bar - 15 s. (B) Resting potential (open circles), receptor (black circles) and action (triangles) potential peaks as a function of external K⁺ level. Each point represents the mean and standard deviation of data collected from 5 to 8 measurements. Action potentials were not observed at 8 mM and higher concentrations of K⁺ ions in test solution

the depolarizing photoreceptor potential. It seems that the mechanism of photoreceptor potential generation in *Blepharisma* depends, as commonly is observed in the eye photoreceptor cells of higher organisms (Yarfitz and Hurley 1994), on an increase in membrane conductance which selectively allows one ion to flow across the membrane and thereby elicits a receptor potential. Among other ciliates, similar depolarizing response of membrane to light stimulation have been recorded in *Paramecium bursaria* (Nakaoka et al. 1987). The light-dependent receptor potential in these cells are exclusively caused by a transient increase in membrane conductance to Ca ions.

Depolarizing receptor potential resulting of high intensity light stimuli in *Blepharisma* triggered in control solution an all-or-none action potential with a well defined threshold (Fabczak et al. 1993a). In view of the results from other ciliates, it seems reasonable to suppose that the action potential in *Blepharisma* is dependent on the external Ca²⁺ level. To check this assumption the action potentials were generated in two sets of experimental solutions in which the concentration of only one ion, Ca²⁺ or K⁺, was varied. As shown in Fig. 2, the peak of the

action potential was displaced linearly with the increase of external Ca²⁺, with a slope predicted by Nernst equation (27 mV/tenfold increase in Ca²⁺ concentration). Decrease of external free Ca²⁺ concentration below that of control solution depressed gradually the action potential amplitude. The action potentials could not be elicited in the cells suspended in free Ca²⁺ solutions below 10⁻⁶ M. The absence of action potentials at the extremely low level of external calcium ions explains the disappearance of photophobic responses in *Blepharisma* (Fabczak et al. 1994). The action potential was also appreciably depressed in solutions in which Ca²⁺ was replaced by Co²⁺. A subsequent incubation of the cells in control solution restored entirely the generation of the action potential in its regular shape. The changes in concentration of K⁺ between 0.1 and 4 mM had no effect on the recorded action potential peak, however, in the cells suspended in solutions containing K⁺ at 8 mM or higher concentration, light stimulation did not elicit any action potential. Possibly this could be the result of high depolarization of cell membrane which increased membrane permeability to K⁺ ions, leading to inactivation of

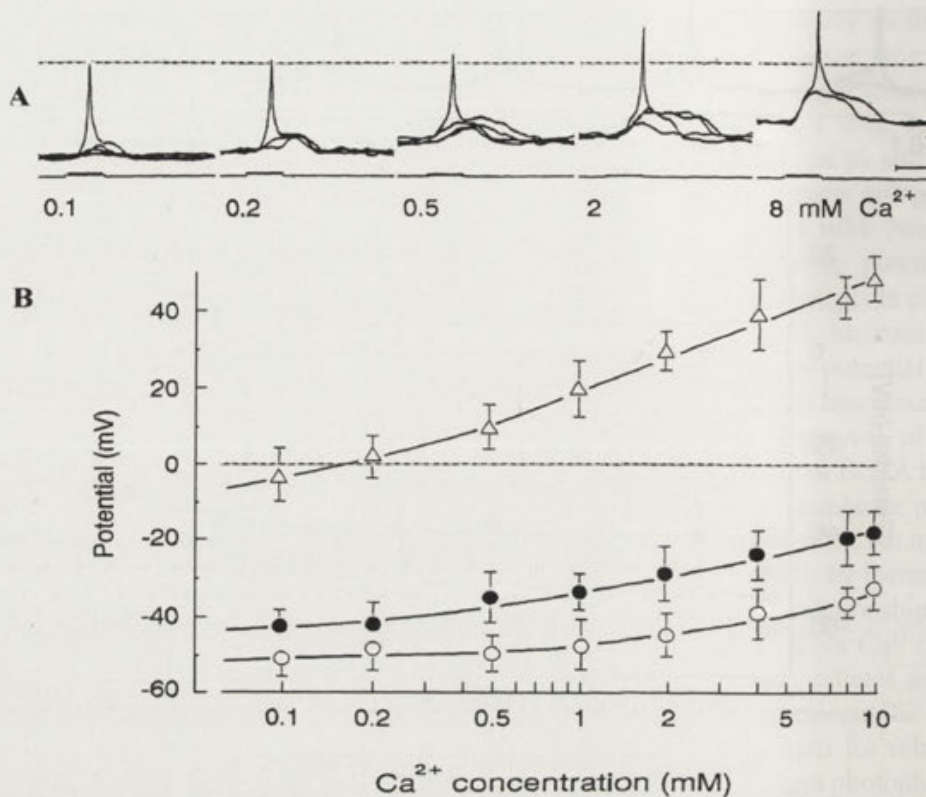


Fig. 2. Relationship between the resting, receptor and action potentials in *Blepharisma japonicum* and changes in external Ca^{2+} concentration. (A) Sets of intracellular recordings of resting, receptor and action potentials from the same cell in each of the testing solutions (pH 6.9, 12°C). Dashed line - 0 mV base line; vertical bar - 20 mV and $3 \times 10^{-4} \text{ W cm}^{-2}$ (580 nm); horizontal bar - 15 s. (B) Resting potential (open circles), receptor (black circles) and action (triangles) potential peaks as a function of extracellular Ca^{2+} ion concentrations. Each point shows the mean and standard deviation of data obtained from 5 to 12 measurements

the mechanism responsible for generation of the action potential. Removal from the medium: Na^+ , Mg^{2+} or Cl^- ions had no significant effect on the peak of the action potential. These results substantiate the view that the action potentials in *Blepharisma* are produced by Ca^{2+} ions. The similar Ca^{2+} -dependent action potentials evoked by photic stimulation have been also observed in related ciliate *Stentor coeruleus* (Wood 1982, Fabczak et al. 1993b). It appears likely that in *Blepharisma* cells the membrane depolarization causes activation of voltage-dependent Ca^{2+} channels located in the ciliary membrane, as in *Paramecium* or *Stylonychia* (Ogura and Takahashi 1976, Dunlap 1977), resulting in transient increases of free Ca^{2+} within the cilia, and the generation of action potential (Pernberg and Machemer 1995). These Ca^{2+} concentration changes in the cilia may, in turn, induce the transient ciliary reversal which is the initial step in the development of *Blepharisma* photophobic responses. In a variety of other ciliates it is well documented that the increase in the intraciliary Ca^{2+} concentration elicits the reversal in the ciliary beat, and hence the reversal in the direction of swimming (Eckert et al. 1976, Machemer and Sugino 1989).

The obtained results evidence that either voltage-sensitive conductance for action potential and the sensory conductance for photoreceptor potential use Ca^{2+} as their major current carrier. At the present moment it is not clear where the sensory conductance in *Blepharisma* is localized. From the ionic studies of phototransduction in the other ciliate *Paramecium bursaria* it appears that the light-dependent Ca^{2+} conductance in these photosensitive cells is located on the somatic rather than ciliary membrane (Nakaoka et al. 1987). This suggestion results from the fact that removal of the cilia in these organisms led to disappearance of an action potential because the voltage-sensitive Ca^{2+} channels in ciliates are known to be present exclusively in the ciliary membrane (Dunlap 1977, Machemer and Ogura 1979), while in deciliated cells photostimulation still induced the regular Ca^{2+} -dependent depolarizing receptor potentials.

Acknowledgements. This work was supported in part by Grant from State Committee for Scientific Research (KBN-6-P203-046-04), statutory Grant to the Nencki Institute from the State Committee for Scientific Research, the U.S. Army Research Office Grant (DAAH04-94-G-0346) and the National Institute of Health Grant (NS 15426).

REFERENCES

- De Peyer J.E., Macheimer H. (1977) Membrane excitability in *Stylonychia*: Properties of the two-peak regenerative Ca-response. *J. Comp. Physiol.* **121**: 255-266
- Dunlap K. (1977) Localization of calcium channels in *Paramecium caudatum*. *J. Physiol.* **271**: 119-134
- Eckert R., Naitoh Y., Macheimer H. (1976) Calcium in the bioelectric and motor functions of *Paramecium*. *Proc. Soc. Exp. Biol.* **30**: 233-255
- Fabczak S., Fabczak H., Song P.-S. (1993a) Photosensory transduction in ciliates. III. The temporal relation between membrane potentials and photomotile responses in *Blepharisma japonicum*. *Photochem. Photobiol.* **57**: 872-876
- Fabczak S., Fabczak H., Tao N., Song P.-S. (1993b) Photosensory transduction in ciliates. I. An analysis of light-induced electrical and motile responses in *Stentor coeruleus*. *Photochem. Photobiol.* **57**: 696-701
- Fabczak S., Fabczak H., Song, P.-S. (1994) Ca²⁺ ions mediate the photophobic response in *Blepharisma* and *Stentor*. *Acta Protozool.* **33**: 93-100
- Kraml M., Marwan W. (1983) Photomovement responses in the heterotrichous ciliate *Blepharisma japonicum*. *Photochem. Photobiol.* **37**: 313-320
- Macheimer H., De Peyer J. E. (1977) Swimming sensory cells: Electrical membrane parameters, receptor properties and motor control in ciliated protozoa. *Verh. Dtsch. Zool. Ges. Erlangen*, 86-110
- Macheimer H., Ogura A. (1979) Ionic conductances of membranes in ciliated and deciliated *Paramecium*. *J. Physiol. Lond.* **296**: 49-60
- Macheimer H., Sugino (1989) Electrophysiological control of ciliary beating: a basis of motile behavior in ciliated protozoa. *Comp. Biochem. Physiol.* **94A**: 365-374
- Matsuoka T. (1983a) Distribution of photoreceptors inducing ciliary reversal and swimming acceleration in *Blepharisma japonicum*. *J. Exp. Zool.* **225**: 337-340
- Matsuoka T. (1983b) Negative phototaxis in *Blepharisma japonicum*. *J. Protozool.* **30**: 409-414
- Mogami Y., Pernberg J., Macheimer, H. (1990) Messenger role of calcium in ciliary electromotor coupling: A reassessment. *Cell Calcium* **11**: 665-673
- Naitoh Y., Eckert R., Friedman K. (1972) A regenerative calcium response in *Paramecium*. *J. Exp. Biol.* **56**: 667-681
- Nakaoka Y., Kinugawa K., Kurotani T. (1987) Ca²⁺-dependent photoreceptor potential in *Paramecium bursaria*. *J. Exp. Biol.* **131**: 107-115
- Ogura A., Takahashi K. (1976) Artificial deciliation causes loss of calcium-dependent responses in *Paramecium*. *Nature* **264**: 170-172
- Passarelli V., Lenci F., Colombetti G., Barone E., Nobili R. (1984) The possible role of H⁺ and Ca²⁺ in photobehavior of *Blepharisma japonicum*. In: Blue Light Effect in Biological Systems (Ed. H. Senger), Springer Verlag, Berlin, Heidelberg, 480-483
- Pernberg J., Macheimer H. (1995) Fluorometric measurement of the intracellular free Ca²⁺ concentration in the ciliate *Didinium nasutum* using Fura-2. *Cell Calcium* **18**: 484-494
- Portzehl H., Caldwell P.C., Ruegg, J.C. (1964) The dependence of contraction and relaxation of muscle fibers from the crab *Maio squinado* on the internal concentration of free calcium ion. *Biochim. Biophys. Acta* **790**: 581-591
- Satow Y., Murphy A., Kung C. (1983) The ionic basis of the depolarizing mechanoreceptor potential of *Paramecium tetraurelia*. *J. Exp. Biol.* **103**: 253-264
- Song P.-S., Hader D.-P., Poff K. L. (1980) Step-up photophobic response in the ciliate *Stentor coeruleus*. *Arch. Microbiol.* **126**: 181-186
- Wood D.C. (1982) Membrane permeabilities determining resting, action and mechanoreceptor potentials in *Stentor coeruleus*. *J. Comp. Physiol.* **146**: 537-550
- Yarfitz S., Hurley J. B. (1994) Transduction mechanisms of vertebrate and invertebrate photoreceptors. *J. Biol. Chem.* **269**: 14329-14332

Received on 24th June, 1996; accepted on 4th July, 1996

InsP₃-modulated Photophobic Responses in *Blepharisma*

Hanna FABCZAK, Mirosława WALERCZYK, Stanisław FABCZAK and Bożena GROSZYŃSKA

Department of Cell Biology, Nencki Institute of Experimental Biology, Warszawa, Poland

Summary. Cells of *Blepharisma japonicum* are characterized by a light avoiding reaction, the step-up photophobic response. Microscope video-recording and behavioral analysis showed that photosensitivity of these cells is greatly reduced when they were incubated in solutions containing such agents as neomycin, an inhibitor of phospholipase C, heparin, a inhibitor of inositol receptors and Li⁺ ions, potent inhibitor of monophosphoinositol phosphatase, which are known to modify the cell inositol lipid pathway. All of these substances caused a decrease of the number of cells reacting to light stimulation with photophobic responses, and latency of the cell responses were appreciably extended. The observed inhibitory effects in all tested cases were dependent on both the time of cell incubation and doses of neomycin, heparin or Li⁺ ions used. The obtained behavioral results allow to suggest that in protozoan *Blepharisma* there exists possibly InsP₃ pathway which seems to be one of the mechanisms of signal transduction.

Key words: *Blepharisma*, ciliate, inositol 1,4,5-trisphosphate, photosensory transduction, step-up photophobic response.

INTRODUCTION

The ciliates *Blepharisma japonicum* exhibit a distinct sensitivity to light, due to their endogenous pigment, blepharismine, which are enclosed in small granules (photoreceptive units) and distributed regularly over the cell body (Giese 1981, Kraml and Marwan 1983). In dark adapted cells short light stimuli elicit a step-up photophobic response which consists of a delayed stop of movement and transient ciliary reversal followed by renewed forward swimming in a randomly changed direction (Kraml and Marwan 1983, Matsuoka 1983, Fabczak H. et al. 1993, Fabczak S. et al. 1993). From the bioelectrical recordings it is evident that light initiates

a sensory transduction chain causing generation of a delayed membrane photoreceptor potential which triggers, in turn, an action potential (Fabczak S. et al. 1993). This action potential is followed by, typical for other ciliates, reversal of ciliary beating observed during the photophobic response in *Blepharisma*. The dependence of phobic responses and photoreceptor and action potentials in these organisms on the presence of Ca²⁺ ions in external solution testifies the participation of Ca²⁺ in generation of both these potentials (Fabczak S. et al. 1994, 1996).

The detailed molecular mechanism of the phototransduction process in *Blepharisma* remains unknown. Some recent data suggest that the phototransduction in these ciliates involves cyclic GMP nucleotide as a second messenger which may affect a cGMP-activated ion channels on the plasma membrane (Ishida et al. 1989, Fabczak H. et al. 1993). It has been reported that, in photoreceptor or olfactory receptor cells of some in-

Address for correspondence: Hanna Fabczak, Nencki Institute of Experimental Biology, Department of Cell Biology, ul. Pasteura 3, 02-093 Warszawa, Poland; Fax: 48-22 225342; E-mail: hannafab@nencki.gov.pl

vertebrates, at least two independent signal transduction pathways can exist within the same cell and, in addition to cGMP, inositol lipid could serve as a second messenger (Rayer et al. 1990, Minke and Selinger 1992, Hatt and Ache 1994).

Therefore to check whether there in *Blepharisma* ciliates, in addition to the cGMP involving pathway, another light transduction pathway exists, we have analyzed the occurrence of photophobic response in the cells pretreated with an InsP_3 cascade disturbing agents.

MATERIALS AND METHODS

Stock cultures of the ciliate *Blepharisma japonicum* were maintained as previously described (Fabczak S. et al. 1993). Prior to the experiments, the cells were transferred to a fresh culture medium and kept in the dark for about 1 h. Subsequently the dark adapted cells were placed in an experimental chamber filled with a solution containing the tested substance. The measurements were performed usually after 10 or 30 min of incubation at room temperature ($21 \pm 2^\circ\text{C}$). The particular solutions containing neomycin, heparin or Li^+ ions (Sigma) were prepared using fresh culture medium.

The latency of photophobic responses and number of photoresponding cells were estimated using microscopy video recording described elsewhere (Fabczak S. et al. 1994). To estimate the degree of photosensitivity of the cells, two parameters were used: (i) the number of cells reacting to the given light stimulus, and (ii) the latency of the photophobic response. The intensity of the light stimulus was selected in such a way that, 50% of the cells in the control conditions showed this level of responses. The effects of solutions containing neomycin, heparin or Li^+ ions on the cell photoresponses were expressed as the changes of percentage of the cells responding to a given stimulus and as alteration of latency of the photophobic response.

RESULTS AND DISCUSSION

Blepharisma japonicum, when suspended in a solution containing neomycin, an inhibitor of phospholipase C (Schibeci and Schacht 1977, Downes and Michell 1981), are less sensitive to light than the control cells. This is evidenced both by reduction of the number of cells responding to the light stimulus, and prolongation of latency of the photophobic response (Fig. 1). Treatment with $1 \mu\text{M}$ neomycin for 15 min resulted in an almost 50% decrease in the number of responding cells (Fig. 1A), and a twofold prolongation of the latency (Fig. 1B) as compared with control cells. When concentration of neomycin in external solution was raised to $10 \mu\text{M}$, the cells after 15 min of incubation showed no photophobic response. In medium containing Li^+ ions, which are known to be an inhibitor of monophosphoinositol phosphatase (Takimoto et al. 1985), the photophobic re-

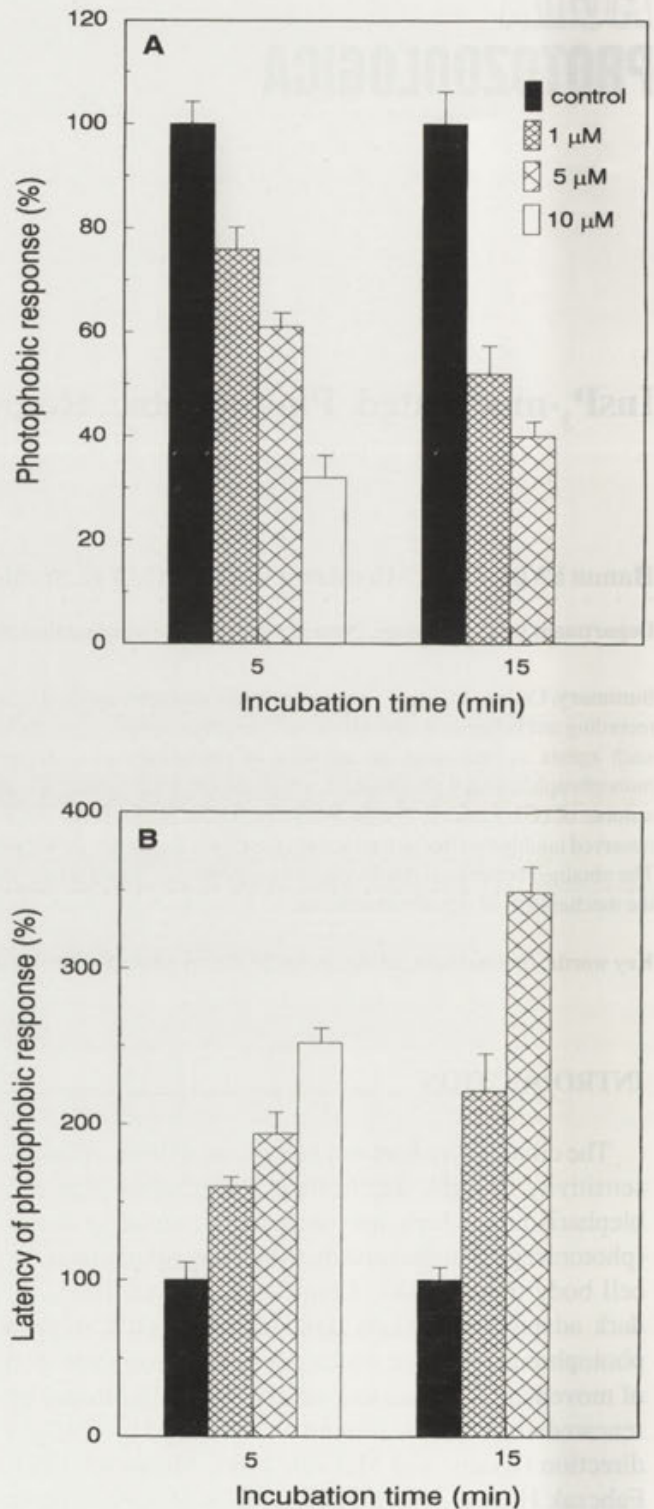


Fig. 1. Influence of neomycin on (A) photophobic responses and (B) response latency of *Blepharisma japonicum* to standard light stimulus of $5 \times 10^4 \text{ Wcm}^{-2}$. The control values showed in this and following Figures are taken as 100%. Each bar shows the mean and standard deviation of data obtained from 5 measurements on cell samples containing 20-30 organisms for photophobic response measurements (A) and 25 cells for relative latency measurements (B)

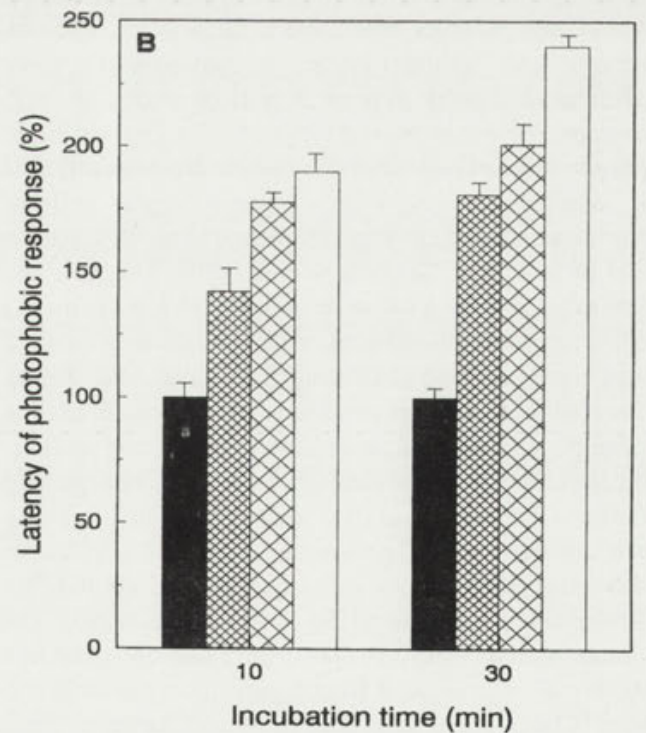
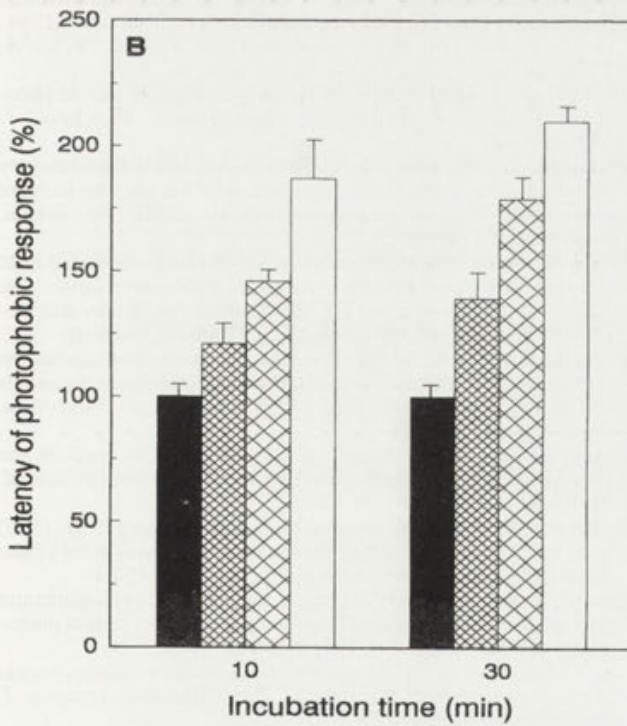
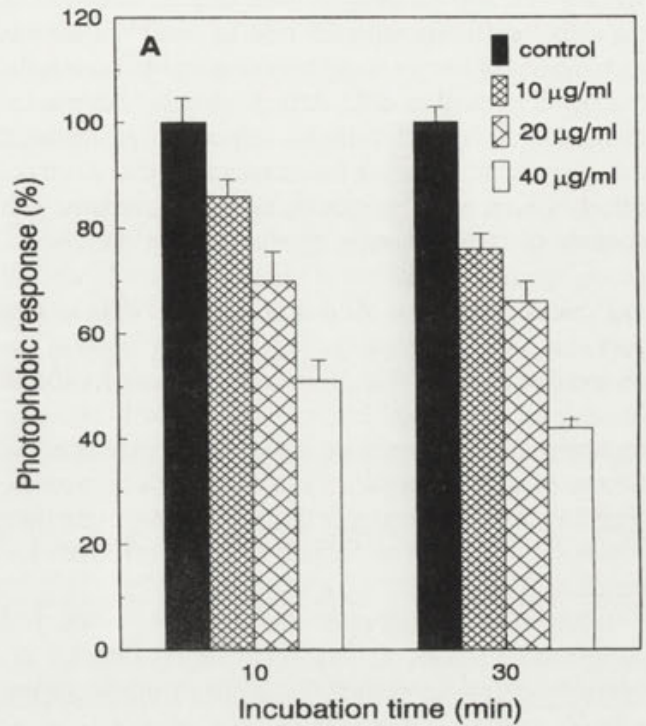
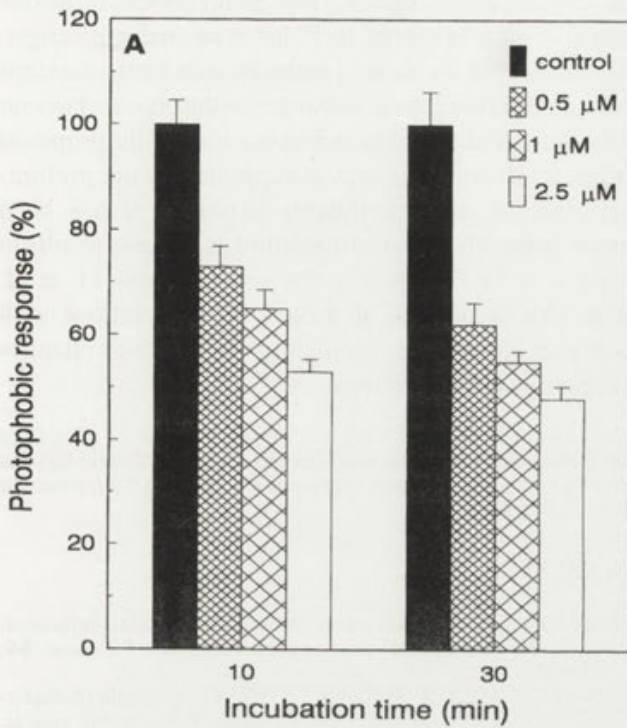


Fig. 2. Effect of external lithium ions on (A) photophobic responses and (B) response latency of *Blepharisma japonicum* to the same standard light stimulus as in Fig. 1. Each bar represents the mean and standard deviation of data obtained from 4 measurements on about 40 - 50 cells in (A) and 30 cells in (B)

Fig. 3. Dependence of (A) photophobic response and (B) response latency of *Blepharisma japonicum* to light stimulation ($5 \times 10^{-4} \text{ Wcm}^2$) on heparin. Each bar means the mean and standard deviation of data from measurements on 4 samples with 25 - 40 cells in (A) and on 20 cells in (B)

sponses were also markedly inhibited (Fig. 2). Incubation of the cells for 10 min with 0.5 mM Li⁺ caused a distinct prolongation of latency of cell responses and decrease in the number of responding cells. At higher level of external Li⁺ (5 mM i 10 mM) the photophobic responses were inhibited to higher extent; moreover, the character and the velocity of cell movement were significantly altered as compared with controls (data not shown). Similarly as in the case of neomycin and Li⁺, addition of heparin, a potent blocker of InsP₃ binding receptors (Supattapone et al. 1988), caused both time and concentration dependent inhibition of the photophobic response (Fig. 3). The cell incubation for 10 min in solutions containing 10 µg/ml, 20 µg/ml or 40 mg/ml of heparin resulted in a decrease in the number of responding *Blepharisma* cells by about 15%, 30% and 50% respectively (Fig. 3A). Also the latency of the cell response to the light stimulus was distinctly prolonged as the level of heparin was increased (Fig. 3B).

It has been demonstrated that InsP₃, the product of phosphatidylinositol 4,5-bisphosphate (PtdIns 4,5 P₂) hydrolysis by phospholipase C, can play, in photoreceptor cells of some invertebrates, the role of second messenger in the phototransduction process (Rayer et al. 1990, Minke and Selinger 1992). Such factors as neomycin, heparin and lithium ions are known to cause large disturbances in this process at various stages of InsP₃ cascade, present in several types of cells. Decreasing of phospholipase C activity by neomycin has been reported to suppress the responses of photoreceptor cells of *Hermisenda* and *Limulus* (Frank and Fein 1991, Faddis and Brown 1993, Sakakibara et al. 1994, Striggow and Bohnensack 1994, Contzen et al. 1995). A low sensitivity of the receptor cells of *Hermisenda* to light was observed also in the presence of Li⁺ ions (Sakakibara et al. 1994). The role of lithium ions consisted in this case by inhibiting monophosphoinositol phosphatase activity and decreasing the cellular pool of inositol, the primary substrate for PtdIns(4,5)P₂ synthesis (Berridge 1987). The inhibitory effect of heparin on the responses induced by light were showed in photoreceptor cells of *Limulus* (Frank and Fein 1991, Faddis and Brown 1993, Contzen et al. 1995). The similar action of heparin was clearly demonstrated in a variety of cells isolated from brain, smooth muscle and liver (Chadwick et al. 1990, Joseph and Samanta 1993, Mayrleitner et al. 1995).

The demonstrated results of the behavioral experiments on *Blepharisma* ciliates provide convincing evidence that all three compounds used, neomycin, heparin and Li⁺ ions inhibit strongly the light induced ciliary responses. Thus, it seems highly probable that, these

ciliate an unicellular organism possess the phototransduction system which involves InsP₃ as a second messenger. Disturbances of the inositol pathway at its particular steps are related to the observed changes in the photobehaviour of the cells. The presence in *Blepharisma* of the proposed phototransduction pathway is supported by our preliminary data of the experiments in which it has been demonstrated that photostimulation of the cells results in changes of InsP₃ levels in the cell (Fabczak H. et al. 1996). An incubation of these cells in solutions with neomycin inhibited or completely blocked these changes at higher its concentrations.

Acknowledgements. This work was supported in part by grant from State Committee for Scientific Research (KBN-6-P203-046-04) and statutory Grant to the Nencki Institute from the State Committee for Scientific Research.

REFERENCES

- Berridge M. J. (1987) Inositol triphosphate and diacylglycerol: two interacting second messengers. *Ann. Rev. Biochem.* **56**: 159-193
- Chadwick C. C., Saito A., Fleischer S. (1990) Isolation and characterization of the inositol triphosphate receptor from smooth muscle. *Proc. Natl. Acad. Sci. USA* **87**: 2132-2136
- Contzen K., Richter K.-H., Nagy K. (1995) Selective inhibition of the phospholipase C pathway blocks one light-activated current component in *Limulus* photoreceptor. *J. Comp. Physiol. A*, **177**: 601-610
- Downes C. P., Michell R. H. (1981) The polyphosphoinositide phosphodiesterase of erythrocyte membranes. *Biochem. J.* **198**: 133-140
- Fabczak H., Tao N., Fabczak S., Song P.-S. (1993) Photosensory transduction in ciliates. IV. Modulation of the photomovement response of *Blepharisma japonicum* by cGMP. *Photochem. Photobiol.* **57**: 889-892
- Fabczak H., Walerczyk M., Fabczak S. (1996) InsP₃-mediated light signal transduction in the protozoan ciliate *Blepharisma japonicum*. Abstr. Int. Conference on UV/Blue Light: Perception and Responses in Plants and Microorganisms, Marburg, Germany
- Fabczak S., Fabczak H., Song P.-S. (1993) Photosensory transduction in ciliates. III. The temporal relation between membrane potentials and photomobile responses in *Blepharisma japonicum*. *Photochem. Photobiol.* **57**: 872-876
- Fabczak S., Fabczak H., Song P.-S. (1994) Ca²⁺ ions mediate the photophobic response in *Blepharisma* and *Stentor*. *Acta Protozool.* **33**: 93-100
- Fabczak S., Fabczak H., Walerczyk M., Sikora J., Song P.-S. (1996) Ionic mechanisms controlling photophobic responses in the ciliate *Blepharisma japonicum*. *Acta Protozool.* **35**: 245-249
- Faddis M. N., Brown J. E. (1993) Intracellular injection of heparin and polyamines. Effect on phototransduction in *Limulus* ventral photoreceptor. *J. Gen. Physiol.* **101**: 909-931
- Frank T. M., Fein A. (1991) The role of the inositol phosphate cascade in visual excitation of invertebrate microvillar photoreceptor. *J. Gen. Physiol.* **97**: 697-723
- Giese A. C. (1981) The photobiology of *Blepharisma*. *Photochem. Photobiol. Rev.* **6**: 139-180
- Hatt H., Ache B. W. (1994) Cyclic nucleotide- and inositol phosphategated ion channels in lobster olfactory receptor neurones. *Proc. Natl. Acad. Sci. USA* **91**: 6264-62-68
- Ishida M., Shigenaka Y., Taneda K. (1989) Studies of the mechanism of cell elongation in *Blepharisma japonicum*. I. A physiological mechanism: How light stimulation evokes cell elongation. *Eur. J. Protistol.* **25**: 182-186

- Joseph S. K., Samanta S. (1993) Detergent solubility of the inositol triphosphate receptor in rat brain membranes. *J. Biol. Chem.* **268**: 6477-6486
- Kraml M., Marwan W. (1983) Photomovement responses of the heterotrichous ciliate *Blepharisma japonicum*. *Photochem. Photobiol.* **37**: 313-319
- Matsuoka T. (1983). Distribution of photoreceptors inducing ciliary reversal and swimming acceleration in *Blepharisma japonicum*. *J. Exp. Zool.* **225**: 337-340
- Mayrleitner M., Schafer R., Fleischer S. (1995) IP₃ receptor purified from liver plasma membrane is an (1,4,5)IP₃ activated and (1,3,4,5)IP₃ inhibited calcium permeable ion channel. *Cell Calcium* **17**: 141-153
- Minke B., Selinger Z. (1992) The inositol-lipid pathway is necessary for light excitation in fly photoreceptors. In: Sensory Transduction (Ed. Corey D. P., Roper S. D.) Rockefeller Univ. Press, New York, 201-217
- Rayer B., Naynert M., Stieve H. (1990): Phototransduction: Different mechanisms in vertebrates and invertebrates. *J. Photochem. Photobiol. B.* **7**: 107-148
- Sakakibara M., Alkon D. A., Kouchi T., Inoue H., Yoshioka T. (1994) Induction of photoresponse by the hydrolysis of polyphosphoinositides in the *Hermissenda* type B photoreceptor. *Biochem. Biophys. Res. Commun.* **202**: 299-306
- Schibeci A., Schacht J. (1977) Action of neomycin on the metabolism of polyphosphoinositides in the guinea pig kidney. *Biochem. Pharmacol.* **26**: 1769-1774
- Strigow F., Bohnsack R. (1994) Inositol 1,4,5-triphosphate activates receptor-mediated calcium entry by two different pathways in hepatocytes. *Eur. J. Biochem.* **222**: 229-234
- Supattapone S., Worley P. F., Baraban J. M., Snyder S. H. (1988) Solubilization, purification and characterization of an inositol triphosphate receptor. *J. Biol. Chem.* **263**: 1530-1534
- Takimoto K., Okada M., Matsuda Y., Nakagawa H. (1985) Purification and properties of *myo*-inositol-1-phosphatase. *J. Biochem.* **98**: 363-370

Received on 5th July, 1996; accepted on 10th July, 1996.

INSTRUCTIONS FOR AUTHORS

ACTA PROTOZOLOGICA publishes original papers embodying the results of experimental or theoretical research in all fields of protistology with the exception of faunistic notices of local character and purely clinical reports. Short (rapid) communications are acceptable but also long review articles. The papers should be as concise as possible, be written in English. Submission of a manuscript to ACTA PROTOZOLOGICA implies that it has not been submitted for publication elsewhere and that it contains unpublished, new information. There are no page charges except colour illustration. Names and addresses of suggested reviewers will be appreciated. In case of any question please do not hesitate to contact Editor. Authors should submit papers to:

Miss Małgorzata Woronowicz
Managing Editor of ACTA PROTOZOLOGICA
Nencki Institute of Experimental Biology,
ul. Pasteura 3
02-093 Warszawa, Poland
Fax:48- 22 225342

Organization of Manuscripts

Submissions

Please enclose three copies of the text, one set of original of line drawings (without lettering!) and three sets of copies with lettering, four sets of photographs (one without lettering). In case of photographs arranged in the form of plate, please submit one set of original photographs unmounted and without lettering, and three sets of plates with lettering.

The ACTA PROTOZOLOGICA prefers to use the author's word-processor disks (3.5" and 5.25" format IBM or IBM compatible, and Macintosh 6 or 7 system on 3.5" 1.44 MB disk only) of the manuscripts instead of rekeying articles. If available, please send a copy of the disk with your manuscript. Preferable programs are Word or Wordperfect for Windows and DOS Wordperfect 5.1. Disks will be returned with galley proof of accepted article at the same time. Please observe the following instructions:

1. Label the disk with your name: the word processor/computer used, e.g. IBM; the printer used, e.g. Laserwriter; the name of the program, e.g. Word for Windows or Wordperfect 5.1.
2. Send the manuscript as a single file; do not split it into smaller files.
3. Give the file a name which is no longer than 8 characters.
4. If necessary, use only italic, bold, underline, subscript and superscript. Multiple font, style or ruler changes, or graphics inserted the text, reduce the usefulness of the disc.
5. Do not right-justify and use of hyphen at the end of line.
6. Avoid the use of footnotes.
7. Distinguish the numerals 0 and 1 from the letters O and I.

Text (three copies)

The text must be typewritten, doublespaced, with numbered pages. The manuscript should be organized into Summary, Key words, Abbreviations used, Introduction, Materials and Methods, Results, Discussion, Acknowledgments, References, Tables and Figure Legends. The Title Page should include the full title of the article, first name(s) in full and surname(s) of author(s), the address(es) where the work was carried out, page heading of up to 40 characters. The present address for correspondence, Fax, and E-mail should also be given.

Indexed in Chemical Abstracts Service, Current Contents (Agriculture, Biology and Environmental Sciences), LIBREX-AGEN, Protozoological Abstracts. POLISH SCIENTIFIC JOURNALS CONTENTS - AGRIC. & BIOL. SCI. data base is available in INTERNET under URL (UNIFORM RESOURCE LOCATOR) address: <http://saturn.ci.uw.edu.pl/psjc/> or <http://ciuw.warman.org.pl/alf/psjc/> any WWW browser; in graphical operating systems: MS Windows, Mac OS, X Windows - mosaic and Netscape programs and OS/2 - Web Explorer program; in text operating systems: DOS, UNIX, VM - Lynx and www programs.

Each table must be on a separate page. Figure legends must be in a single series at the end of the manuscript. References must be listed alphabetically, abbreviated according to the World List of Scientific Periodicals, 4th ed. (1963). Nomenclature of genera and species names must agree with the International Code of Zoological Nomenclature, third edition, London (1985) or International Code of Botanical Nomenclature, adopted by XIV International Botanical Congress, Berlin, 1987. SI units are preferred.

Examples for bibliographic arrangement of references:

Journals:

Häder D-P., Reinecke E. (1991) Phototactic and polarotactic responses of the photosynthetic flagellate, *Euglena gracilis*. *Acta Protozool.* **30**: 13-18

Books:

Wichterman R. (1986) The Biology of Paramecium. 2 ed. Plenum Press, New York

Article's from books:

Allen R. D. (1988) Cytology. In: Paramecium, (Ed. H.-D. Görtz). Springer-Verlag, Berlin, Heidelberg, 4-40
Zeuthen E., Rasmussen L. (1972) Synchronized cell division in protozoa. In: Research in Protozoology, (Ed. T. T. Chen). Pergamon Press, Oxford, **4**: 9-145

Illustrations

All line drawings and photographs should be labeled, with the first author's name written on the back. The figures should be numbered in the text as arabic numerals (e.g. Fig. 1). Illustrations must fit within either one column (86 x 231 mm) or the full width and length of the page (177 x 231 mm). Figures and legends should fit on the same page. Lettering will be inserted by the printers and should be indicated on a tracing-paper overlay or a duplicate copy.

Line drawings (three copies + one copy without lettering)

Line drawings should preferably be drawn about twice in size, suitable for reproduction in the form of well-defined line drawings and should have a white background. Avoid fine stippling or shading. Computer printouts of laser printer quality may be accepted, however *.TIF, *.PCX, *.BMP graphic formats on disk are preferred.

Photographs (three copies + one copy without lettering)

Photographs at final size should be sharp, with a glossy finish, bromide prints. Photographs grouped as plates (in size not exceeding 177 x 231 mm **including legend**) must be trimmed at right angles accurately mounted and with edges touching and mounted on firm board. The engraver will then cut a fine line of separation between figures. Magnification should be indicated. Colour illustration on transparent positive media (slides 60 x 45mm, 60 x 60mm or transparency) are preferred.

Proof sheets and offprints

Authors will receive one set of page proofs for correction and are asked to return these to the Editor within 48-hours. Fifty reprints will be furnished free of charge. Orders for additional reprints have to be submitted with the proofs.

ORIGINAL ARTICLES

- W. Kłopocka and P. Pomorski:** Cytoplasmic calcium transients in *Amoeba proteus* during induction of pinocytotic and non-pinocytotic rosettes 169
- R. Marangoni, L. Gobbi, F. Verni, G. Albertini and G. Colombetti:** Pigment granules and hypericin-like fluo-rescence in the marine ciliate *Fabrea salina* 177
- K. Golińska:** Modifications of cortical pattern in a ciliate, *Dileptus margaritifer* under the influence of elevated external potassium concentration. 183
- N. Ricci, A. Morelli and F. Verni:** The predation of *Litonotus* on *Euplotes*: a two step cell-cell recognition process. 201
- P. Madoni:** Sludge biotic index for the evaluation of the activated-sludge plant performance: the allocation of the ciliate *Acineria uncinata* to its correct functional group 209
- H. Zimmermann:** Interactions between planktonic protozoans and metazoans after the spring bloom of phytoplankton in a eutrophic lake, the Belauer See, in the Bornhöveder Seenkette, North Germany 215
- M. Svobodová:** A *Sarcocystis* species from goshawk (*Accipiter gentilis*) with Great tit (*Parus major*) as intermediate host. 223
- W. Song and A. Warren:** A redescription of the marine ciliates *Uroleptus retractilis* (Claparède and Lachmann, 1858) comb. n. and *Epiclintes ambiguus* (Müller, 1786) Bütschli, 1889 (Ciliophora, Hypotrichida). 227
- G. Novarino:** Notes on flagellate nomenclature. I. *Cryptaulaxoides* nom. n., a zoological substitute for *Cryptaulax* Skuja, 1948 (*Protista incertae sedis*) non *Cryptaulax* Tate, 1869 (Mollusca, Gastropoda) non *Cryptaulax* Cameron, 1906 (Insecta, Hymenoptera), with remarks on botanical nomenclature. 235
- P. K. Prasad and K. P. Janardanan:** *Nematopsis idella* sp. n. and *Uradiophora cuenoti* Mercier: two cephaline gregarines from freshwater prawns in Kerala 239

SHORT COMMUNICATIONS

- S. Fabczak, H. Fabczak, M. Walerczyk, J. Sikora, B. Groszyńska and P.-S. Song:** Ionic mechanisms controlling photophobic responses in the ciliate *Blepharisma japonicum*. 245
- H. Fabczak, M. Walerczyk, S. Fabczak and B. Groszyńska:** InsP₃-modulated photophobic responses in *Blepharisma*. 251